CHAPTER ONE

INTRODUCTION

1.1 Background

The phytoplankton is the prime essential primary producer in the oceanic food chain, playing an essential part in the chemical cycles as well as the energy circulation. There are a very much diversified population of tiny photosynthesizing microalgae and cyanobacteria that serve as a connection to a few activities that take place in the atmosphere and the ocean (Petrou, 2016). Through the photosynthetic activity, marine phytoplankton can take up carbon dioxide from the surrounding surface waters (Li et al., 2018). In the method of extracting carbon from the atmosphere, a portion of this carbon eventually finds its way into the ocean's depths (Smayda, 1970). The quickly sinking phytoplankton is the main element of carbon transfer from surface layers, whereas slow-moving phytoplankton export a small amount of carbon to the water (Boyd and Newton, 1999). Globally phytoplankton is responsible for sequestering 50% of carbon by primary production and removing 50 GT of anthropogenic carbon per year (Baumert and Petzoldt, 2008).

A carbon flux refers to the amount of carbon exchanged between carbon stocks over a specified time. In simple terms, it is the movement of carbon between lands, oceans, the atmosphere, and living things (Mélières and Maréchal, 2015). Carbon dioxide (CO_2) has been recognized as one of the most important factors contributing to climatic changes. It is regarded as one of the significant obstacles facing humanity in the twenty-first century (Lam et al., 2012). While the CO_2 that is released into the atmosphere from human-caused activities like deforestation and the combustion of fossil fuels for energy production is quickly dissolved at the surface of the sea and causing a decrease in the pH of the water and creating ocean acidification. The CO_2 that is left in the atmosphere raises average global temperatures and leads to a rise in the thermal stratification of the ocean. It is believed that the concentration of CO_2 in the air was around 270 parts per million before industrialization, but it has since climbed to over 400 parts per million (Hader et al., 2014), and according to the "Business as Usual" scenario for CO_2 emissions, it is projected that the level would hit 800–1000 ppm by the end of the 20th century (Li et al., 2012). In recent

times, the global climate change-related summit “Paris Climate Accords” identified sustainable ocean carbon sink as a key concern for mitigating global climate change because by this process approximately 25% of global carbon sank in the ocean between 1850 to 2019 (Friedlingstein et al., 2020).

Ocean ecosystems are a large area for the sink of atmospheric CO_2 and take up a similar amount of CO_2 that is comparable to that taken up by land ecosystems. At the present time, ocean ecosystems are responsible for the transfer of about one-third of the anthropogenic CO_2 emissions from the atmosphere (Hader et al., 2014; Li et al., 2012). The coastal ocean creates a highly dynamic land-ocean interface where biogeochemical processes regulate and modify carbon components from both the open sea and the land surface, thereby affecting air-sea CO_2 transfers and exporting of carbon to the seafloor (Bauer et al., 2013; Cai 2011; Lacroix et al., 2021). The coastal ocean, despite its relatively low surface area, is home to a wide variety of ecosystems and contains a wealth of spatial, economic, and biological resources. These factors allow the coastal ocean to offer essential ecosystem services that are beneficial for human civilization. The anthropogenic CO_2 absorption is one of the major significant services that is supplied by the coastal ecosystem and its related shore ecosystem (Cooley et al., 2009).

The overall transport of CO_2 from the atmosphere to the seas and eventually to the deep ocean is mostly a direct result of the interaction between the biological pump and solubility (Hulse et al., 2017). Both organic and inorganic carbon is fixed by primary producers (phytoplankton) in the euphotic zone are transferred by the biological carbon pump, which is an important natural process and a key element of the earth's carbon cycle that controls atmospheric CO_2 levels. This transmission occurs from the euphotic zone to the inner of the ocean and then from there to the underlying sediments (Hulse et al., 2017; Chisholm, 1995). The biological carbon pump performs a major crucial role in the net transfer of carbon dioxide from the atmosphere to the seas and then to the sediments; atmospheric carbon dioxide is kept at a substantially lower level than it would be if the biological carbon pump did not present (Basu and Mackey, 2018).

In the euphotic zone, the biological pump receives inputs of particulate organic carbon (POC) and dissolved organic carbon (DOC) from phytoplanktonic carbon fixation by autotrophs as well as the generation of heterotrophic bacterial products. This POC delivery to the top portion ocean is consequently changed and shortened by a broad range of grazing actions, which convert the majority of the phytoplankton and microbial carbon into heterogeneous droplets, which eventually end up out of the surface ocean after a residence time of days to weeks (Boyd and Stevens, 2002). This flow of POCs in subterranean waters is further reduced as a result of further modifications of these settling particles brought about by heterotrophic bacteria and grazers (Steinberg et al., 2008). This sinking particle flux will be attenuated by several mechanisms, yet a tiny but considerable percentage of this carbon transfer will be stored in the deep ocean. This proportion will be a few percent of the surface signature (Boyd and Trull, 2007). If the ocean did not include a biological pump, which moves around 11 Gt C yr^{-1} into the bottom of the ocean, then atmospheric CO_2 concentration would be approximately 400 ppm greater than they are at the current time (Sanders et al., 2014; Boyd, 2015).

The main objective of this study is to highlight the seasonal variation of carbon flux and correlate it with the other component physicochemical factors. This study also, determines the carbon exchange rate in the northeastern coastal system of the Bay of Bengal.

1.2 Statement of the problem

Along its southern boundary, Bangladesh possesses significant marine and coastal resources. The coastal region of Bangladesh is often regarded as one of the extremely productive areas in the world. This is mainly because of both its geographical location and climatic condition. The coastal ecosystem of Bangladesh is wealthy in both enormous water regions and biological variety. The effect of the mangrove forests is one of the distinctive characteristics of the coastal region. These forests are home to a large variety of fishes and other aquatic creatures that are valuable from a business perspective. The blue economy is a crucial strategy for achieving long-term sustainability in Bangladesh. Without confusion, issues relating to the sea, such as the increase in global commerce, the use of underwater mineral wealth for long-term energy independence, the sensible management of marine fisheries, and the restoration of the marine environment

and biodiversity, will establish Bangladesh's potential economic development and growth (MoFA, 2014). Currently, 90% of the nation's commerce is carried out by sea (Alam, 2014). The Bay of Bengal fisheries stock and other inorganic materials have a significant economic impact on the country. It can be achievable if resource supervision is guided by the principles of the protection of the oceans, which contain ocean biodiversity, ecosystem maintenance, and nourishing environmental activities. Our coastal area is likely to be one of the world's most vulnerable areas in the event of climate change. Global warming is the major reason for Sea level rise (SLR) and temperature rise, and it is caused by the increase in greenhouse gas concentrations in the earth's atmosphere. Climate change and greenhouse gases are projected to impact almost every aspect of socioeconomic life in Bangladesh (Ali, 1999).

On the other hand, increases in ocean CO_2 concentration make ocean acidification. Excessive CO_2 concentration decreases the ocean's pH level and makes the water acidic. Acidic water disrupted the life cycle of all aquatic creatures. Especially for shellfish, the higher CO_2 concentration disrupted the shell formation of crustaceans. To protect our fisheries sector and coastal area, it is clearly an important matter to know about greenhouse gases, especially CO_2 concentration and carbon flux status of coastal water.

There are some studies that measure the seasonal distribution of phytoplankton in south-eastern coast of Bangladesh (Mehedi Iqbal et al., 2017), nutrients effects on phytoplankton distribution in the Bay of Bengal (Paul et al., 2008), phytoplankton variation with nutrient availability in Karnafully estuary (Ahmad, 2019a). A study also conducted in the north Indian Ocean for carbon flux estimation (Gauns et al., 2003). But, there is no study on carbon flux and its seasonal absorption in the northeastern Bay of Bengal. Assessing the carbon fluxes can be a mitigation process for climate change and help to determine the effect on fisheries sector. It gives an idea of how much carbon is exchanged between our northeastern ocean systems and helps develop new policies and laws related to carbon flux to protect our fisheries sector and coastal areas.

1.3 Significance of the study

The total maritime area of Bangladesh is approximately 118,813 km^2 (Hussain et al., 2018). Bangladesh is one of the most vulnerable countries to the negative effects of manmade climate change and global warming. Even though Bangladesh produces less than 0.1% of the world's greenhouse gases, they are one of the most affected nations. A one-meter sea level rise will completely drown 18% of Bangladesh's entire land area (Minar et al., 2013). Increases in CO_2 concentration make ocean acidification and affect our shellfish fisheries. So it is important to know about the status of greenhouse gases (CO_2) that affect our coastal climate condition with their mitigation mechanism. This research is the baseline research which helps to estimate carbon flux in the northeastern Bay of Bengal. This study shows the rate of carbon flux in our northeastern oceanic system. This study also estimated the sinking rate of phytoplankton and the density of phytoplankton along the coastal belt of Bangladesh.

1.4 Objectives

The objectives of this research include:

1. Perceiving seasonal variation of carbon flux and
2. Understanding the variation of carbon flux with phytoplankton sinking rate and nutrient availability along the northeastern Bay of Bengal.

CHAPTER TWO
REVIEW OF LITERATURE

Increasing global carbon has been a threat in recent years. Many relevant studies are being conducted around the world to get a concept about how much carbon is emitted and how much is being absorbed by different sources, either in the food web. Most studies show that the earth is going into a vulnerable condition and atmospheric carbon is the primary reason for anxiousness. So, the contribution of photosynthesis by plants or oceanic phytoplankton in absorbing this massive amount of carbon from the atmosphere can't be denied. Approximately half of the world's photosynthesis is performed by marine phytoplankton, which fixes around 50 Gt of carbon yearly (Basu and Mackey, 2018). The mechanisms leading to the transport of sinking particles, mainly phytoplankton, control how much carbon is sequestrated into the deep ocean through the biological pump. To accurately predict future levels of CO_2 in the atmosphere, it is important to understand how the biological carbon pump responds to climate change (Passow and Carlson, 2012). Due to the growing CO_2 levels in the atmosphere, the oceans will undergo significant changes.

Ocean sequestration of atmospheric carbon dioxide is becoming increasingly regarded as a key climate mitigation strategy to achieve the Paris Agreement's 1.5–2.0°C temperature rise goal (Aricò et al., 2021; Pörtner et al., 2019). Because it soaks up 37% of fossil fuel CO_2 emissions or 25% of the total emissions caused by fossil fuel burning and land use change between 1850 and 2019, the sustained oceanic carbon sink is vital for attaining this target (Friedlingstein et al., 2020).

The biological carbon pump is an important determining factor in the seas that play a role in the dispersion of carbon, as a result, additionally, it is one of the key elements that control the air-sea CO_2 interchange and plays a role in the sea surface pressure (Bishop, 2009). It is made up of phytoplankton cells, as well as the predators that feed on them and the bacteria that break down their detritus. It engages a crucial role in the circulation of carbon across the world, because it transports carbon from the air to the deep of the ocean, where it can be kept for many years (Chisholm, 1995).

Photosynthesis through phytoplankton lowers the partial pressure of carbon dioxide found in the upper ocean, hence creating a steeper CO_2 gradient that facilitates CO_2 absorption from the atmosphere (Falkowski et al., 2000). In addition to this, it contributes to the production of particulate organic carbon (POC) in the pelagic layer of the upper ocean zone (0 to 200m).

The POC is broken down into fecal fragments, biological aggregates (marine snow), and different forms, those are transferred to the mesopelagic zone (200 to 1000m) and hadal zone (>1000m depth) through sinking and perpendicular transportation by zooplankton and fish. These zones are located deeper in the ocean (Turner, 2015). Despite the fact that photosynthesis produces both dissolved and particles of organic carbon (DOC and POC, respectively), only POC contributes to efficient carbon export to the ocean depths, whereas the DOC element in surface waters is mostly recycled by bacteria. This is because POC is more movable than DOC in the water column (Kim et al., 2011). On the other hand, a more biologically resistant DOC component that is produced in the euphotic zone accounts for 15%–20% of the net community production and is not quickly mineralized by microorganisms. Instead, it consists of a physiologically labile DOC near the ocean surface (Hansell et al., 2009). This medium-labile DOC is then transported to the deeper ocean, which represents a strong element of the biological carbon pump (Carlson et al., 1994). Production of DOC and its export are both more effective in the oligotrophic subtropical seas than occur in other oceanographic zones (Roshan and DeVries, 2017).

Phytoplankton sinking rate fluctuations in the southern Benguela upwelling system (Pitcher et.al., 1989) is the studies that assessed the phytoplankton sinking rate using the SETCOL technique and the carbon flux from organic compounds. The duration of the Settling checks had an effect on the phytoplankton sinking rate. The chlorophyll sinking rate ranged from 0 m day^{-1} to 0.91m day^{-1}, but it had a weak correlation with the phytoplankton carbon sinking rate; the range varied from 0 m day^{-1} to 0.78 m day^{-1}. There was no strong correlation found between the carbon sinking rate and the environmental factors. However, they were significantly correlated with taxonomic characteristics of the assemblages that were controlled by the climate condition. Estimates of phytoplankton carbon flux were determined from both SETCOL observations and sediment trap

recoveries. Carbon flux determined by SETCOL experiments ranged from 26 and 186 mg C $m^{-2}d^{-1}$, which was higher than the carbon flux estimated from the analysis of the material extracted from the sediment traps (70-120 mg C $m^{-2}d^{-1}$).

Various factors affected the carbon flux in the estuary and the Open Ocean. Examples include zooplankton grazing, sedimentation, and lysis (Turner, 2002). In addition, the fluctuation in geographical and temporal of different physiological, biochemical, and biological processes, the assessment of sedimentation, and other loss processes, such as zooplankton feeding and lysis, all have an impact on the carbon flux (Guo et al., 2016). Estuaries have a mix of organic and inorganic carbon sources which come from land components transported by fresh river water (which has no salinity), marine materials brought by shelf sea water (which has a salinity of 30 or more) and materials that can only be found in estuaries. Also, physiological and biogeochemical processes control the source of organic carbon. Physiological resuspension, bioturbation, and fluidized mud layers also help move organic carbon to the open ocean (Bauer et al., 2013).

Many research studies on carbon flux are being undertaken across the globe. A comparison of carbon flux estimations in the northern part of the Indian Ocean's Arabian Sea and the Bay of Bengal by Gauns et al. (2003). This study revealed carbon flux which is regulated by season change. During the southwest and northeast monsoon seasons, the Arabian Sea and the Bay of Bengal exhibit greater fluxes. The influence of strong winds in creating mixing and upwelling in the summer and evaporative cooling and convection in the winter is highlighted by higher downward fluxes coupled with a deep mixed layer and high production in the Arabian Sea throughout the summer and winter. As a result of the inability of limited air in the Bay of Bengal to disrupt the stratification, the region remains unproductive during the whole year. The Arabian Sea contains a much higher level of total living carbon, whereas the Bay of Bengal has a much lower concentration of living carbon. During the southwest and northeast monsoon seasons, both areas see higher fluxes. The runoff delivers billions of tons of fluvial materials. Stratification limits the underlying nutrient flow into the surface waters, thus decreasing the Bay of Bengal's primary production. The Bay of Bengal contains significantly lower total living carbon than the Arabian Sea. The value carbon flux found in 100m was in spring inter-monsoon 1.8 mg C

m^{-3} d^{-1}, the northeast monsoon (winter) 1.9 mg C m^{-3} d^{-1}, and the southwest monsoon (summer) 2.5 mg C m^{-3} d^{-1}.

Another research was carried out at the Changjiang estuary, which is located on the Yangtze River (Guo et al., 2016). The study measured the phytoplankton sinking rate and carbon flux during two cruises in the spring and summer of 2011. A homogeneous sample method SETCOL was used to find out the phytoplankton sinking rate. The spring phytoplankton population was dominated by dinoflagellates, whereas the summer phytoplankton population was dominated by diatoms. Additionally, two different species, *Prorocentrum dentatum* and *Skeletonema dorhnii,* were responsible for the algal blooms that were observed at the survey location during the spring and summer cruises, respectively. The phytoplankton cells which sink quickly are the ones that are believed to be the most important contributors to the carbon export from the surface layers, while the phytoplankton cells that sink slowly contribute very little to the carbon export in the water column. The physiological status of phytoplankton cells, as well as their varied types of motility, cellular shape, and density, all have a role in determining the phytoplankton sinking rate. In addition, water nutrient content, irradiance, medium viscosity, and sometimes water turbulence influence the sinking rate and carbon flux. Carbon flux was estimated at the sample station using phytoplankton carbon biomass and phytoplankton sinking rate.

There is no study related to the phytoplankton sinking rate and carbon flux in the northeastern Bay of Bengal. But many studies were conducted mainly on phytoplankton community Physico-chemical parameters associated with the phytoplankton composition along the coast of the Bay of Bengal. The phytoplankton composition measured (Al et al., 2019) showed that, a total of 42 phytoplankton species, including 13 common and 13 dominant species, were discovered in the northern Bay of Bengal. These species were divided into eight divisions, including Ochrophyta (20.41%), Bacillariophyta (17.01%), Ciliophora (16.36%), Cyanobacteria (14.39), Myzozoa (12.45%), Miozoa (10.24%), Chlorophyta (7.21%), and Haptophyta (1.94%) The maximum species richness (2.32) and diversity (3.07) were discovered during the winter. The monsoon season produced the

lowest species (1.03 and 2.03, respectively). The post-monsoon season had the highest density (27,736 cells/l), while the monsoon season had the lowest density (6524 cells/l). Islam et al. (2018) conducted a study in the South Eastern Coastal Waters of the Bay of Bengal that measured Seasonal Variation of Physico-Chemical parameters. Various water quality parameters. The water salinity was recorded highest in the pre-monsoon season (33.21±3.61), and the minimum was recorded in the monsoon season (9.6±9.44). Water pH was found maximum in the pre-monsoon season (8.24±0.09) and the minimum was recorded in the monsoon season (7.5±0.24). Electric conductivity and TDS maximum values were found in the pre-monsoon season and minimum in the monsoon season (EC 49.22 to 18.09 mS/cm) and (TDS 30.5 to 8.32 g/l).

After reviewing all relevant articles from both at home and abroad, it is obvious that, while many studies on phytoplankton sinking rates and carbon fluxing have been undertaken in foreign countries, such research is still not being conducted in Bangladesh. During this research, the key concentration was on carbon flux and its associated relevant factors such as Physico-chemical parameters, phytoplankton density, and phytoplankton sinking rate in two specific stations (Cox's Bazar and Kutubdia). This research covered the northeastern coast of the Bay of Bengal. This research is pioneering research to measure the carbon flux on the northeastern coast of the Bay of Bengal. This research will help to measure the carbon flux in other parts of the Bay of Bengal.

CHAPTER THREE

MATERIALS AND METHODS

3.1 Research boundary

The Bay of Bengal, an extension of the Indian Ocean is 2090 km long, 1600 km wide, and has an average depth of more than 2600 m. Its surface area is roughly 2,172,000 sq.km. The Andaman and Nicobar Islands split it from the Andaman Sea, its eastern arm, which is bordered on the west by Sri Lanka and India, the north by Bangladesh, and the east by Myanmar and Thailand (Islam, 2003). The Bay of Bengal has a great impact on this surrounding country. In Bangladesh's prospects, the coastal area covers 47,201 km^2, that's nearly 32% of the country, and connects 19 districts (Ahmad, 2019b). Some northeastern coastal areas include Cox's Bazar, Teknaf, Patenga, Saint Martin's Island, Sonadia Island, Moheskhali, Nijhum Island, etc. These coastal areas are the most productive zone, including various ecological and economical systems, and also the victims of climate change.

This research was conducted at two important northeastern coastal areas, Sonarpara (Cox's Bazar) and Kutubdia Island. Samples were collected from these two sampling locations during the high tide period following the full moon phase. Various parameters were considered for selecting these specific two stations, such as water parameters, anthropogenic exposure, transportation, tidal condition, weather condition, etc.

This study specified two transects from each station as transects point-1 (T1) (21.275424N, 92.037620E) and transect point-2 (T2) (21.286309N, 92.035125E) in Sonarpara (Cox's Bazar) station and Transect point-3 (T3) (21.758975N, 91.858832E) and Transect point-4 (T4) (21.751535N, 91.851531E) in the Kutubdia offshore region (Fig. 1).

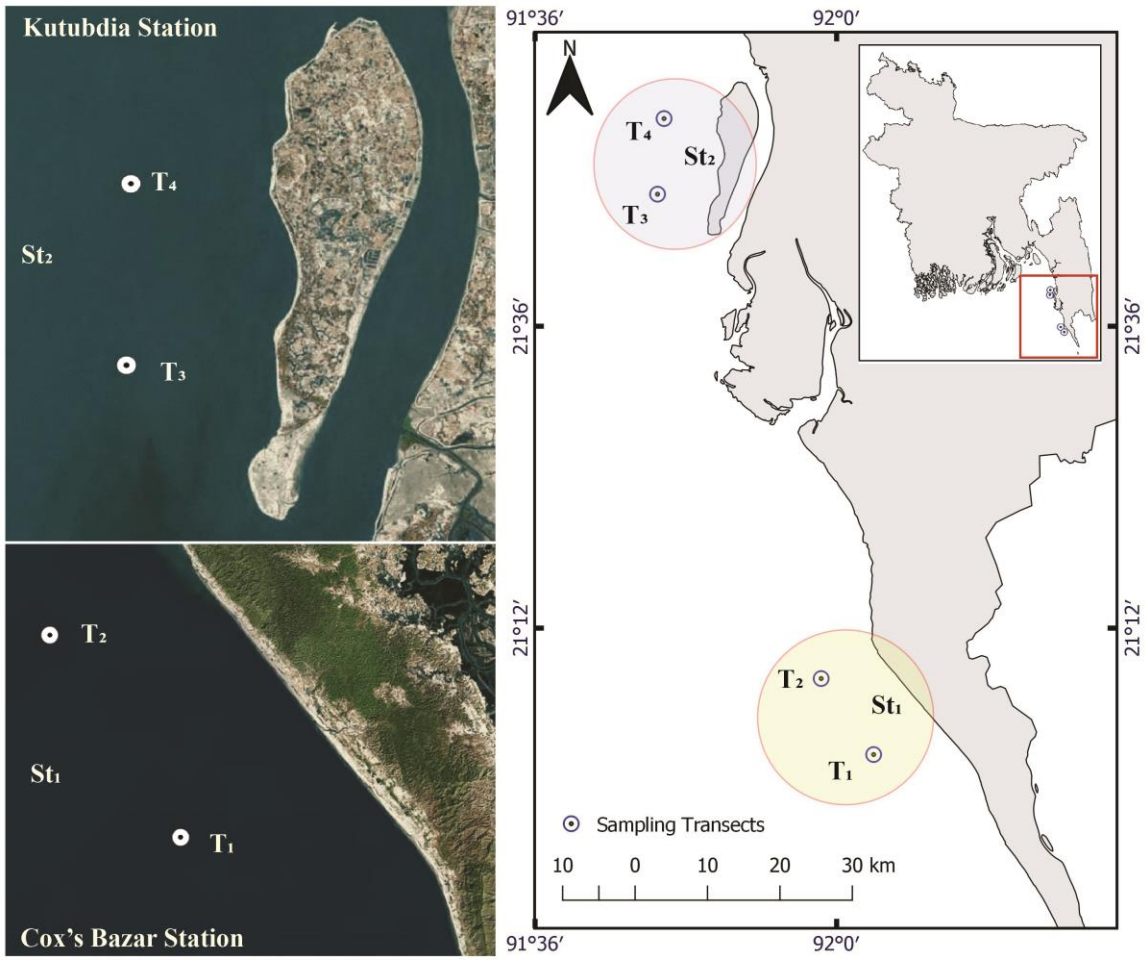

Figure 1: The Geographical location of Sonarpara (Cox's Bazar) and Kutubdia.

3.2 Sampling frequencies

The water sample was collected from two different stations. In these two stations, four transect points were selected. The water and phytoplankton sample was collected from approximately 1-2 km far away from the coastline for each station. The water samples were collected in four distinct seasons, the winter season (December - February), the pre-monsoon (March - May), the monsoon (June - September), and the Post-monsoon (October - November). In each season, a single sample was collected from each station.

3.3 Analysis of coastal and oceanic productivity

3.3.1 Water sample collection for SETCOL

This research determined the vertically depth-wise sinking rate of phytoplankton. After measurement of chlorophyll-*a*, we calculated the depth-wise sinking rate. For depth-wise

sinking rate determination, water had to collect from 3 depths (0m or surface, 5m, and 10m) on a specific station. Water was collected from a vertical water sampler (Wildco FL-32097). For water collection, on a specific station, two different transect points were selected. Maintain 1 to 1.5km distance among transect points for getting a proper result and escaping similarity. At each transect point, 5L of water samples were collected from the surface, 5m depths, and 10m depth. For proper sinking of the vertical water sampler, a heavy stone was bound to the sampler. After collection water was kept in a black water bottle for escaping photosynthesis and as soon as possible back into the laboratory and the water was filtrated within two hours. Some physical water parameters like pH, water salinity, water temperature, and water dissolved oxygen content were measured immediately after the collection of water on the boat (Fig. 2).

1. Release water sampler 2. Collection water from sampler 3. Stored the sample in plastic bottle

Figure 2: The sequence of water sample collection for SETCOL bottle

3.3.2 SETCOL procedure

SETCOL is a reliable and technologically simple method for measuring phytoplankton sinking rates. SETCOL stands for Settling Column. It was made according to (Bienfang, 1981). It is a cylinder-like structure made of PVC and a mouth opening covered by a transparent circular plate (Fig. 3). The diameter of the mouth is 2.5cm and the height is 0.6 meters (60 cm). Each cylinder has 3 chambers of different volume like 100ml (upper), 1000ml (middle) and 100ml (bottom). For each depth, water sample settling 3 SETCOL bottles are needed, and a total of 9 bottles are needed for three depths of a particular station.

For two stations total of 18 bottles are needed. Three bottles are fixed with a strong iron or wood structure.

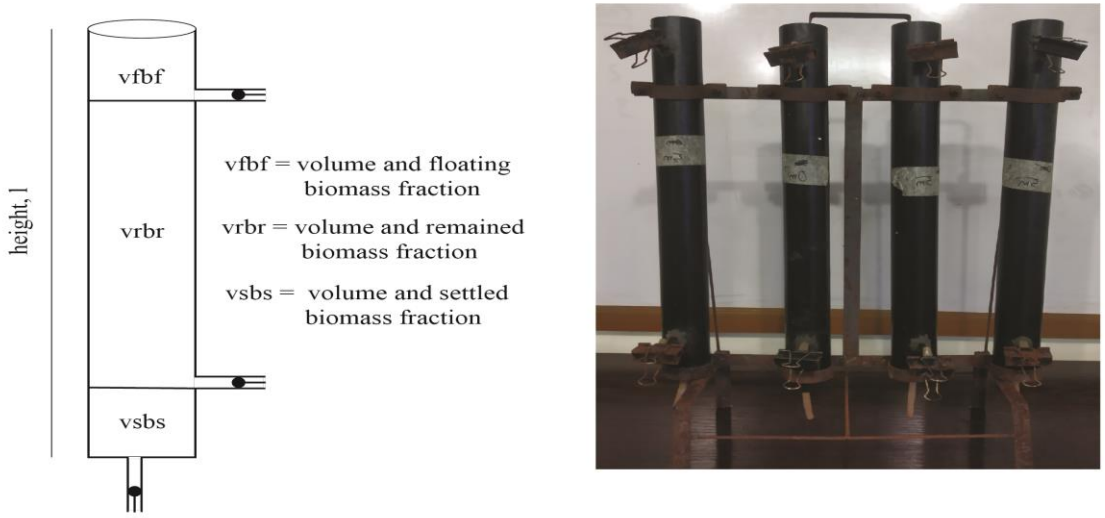

Figure 3: SETCOL bottle and different layer of bottle.

3.3.3 Chlorophyll- *a* measurement

It is also a key component of phytoplankton sinking rate measurement. But in this research, Chlorophyll-*a* was estimated following an established SETCOL method (Bienfang, 1981). A long procedure was followed, which was slightly different from the conventional chlorophyll -a measurement. At first, the water samples were collected with a vertical water sampler (Wildco FL-32097) from the station and were immediately taken to the laboratory as soon as possible. After that SETCOL bottles were filled with the sample water of 3 depths and kept for around 2 hours for settling. For each depth, three setcol bottles were used. Three depths (0, 5, and 10m) in a transects need a total of nine setcol bottles. In two transects of a station, a total of eighteen bottles were used. Each setcol bottle had three different chambers (100ml, 1000ml, and 100ml), and eighteen bottles of two transects consisted a total of 54 water samples. After that, the following steps (Fig. 4) were followed:

1) Using a vacuum pump (Rocker 300 Oil-Free Vacuum Filtration Unit), water samples were filtered by using glass microfiber filter paper (Whatman Glass MicroFiber Filters GF/C, 47mm Diameter). For each bottle, three volumes of water were filtrated (100 ml, 1000 ml, and 100 ml).

2) Then the filtered paper with sample residue was taken into 10 ml of 90% acetone solution (90ml acetone with 10ml distilled water) and kept overnight.
3) Using a glass rod, the filtered membrane with the sample was thoroughly mixed with acetone.
4) Then the centrifugation (Hermle Z 326K) was carried out for 2.30 minutes at 3500 RPM.
5) Compared to blank acetone, the supernatant contents (extract) were taken into cuvettes. The extract absorbance was estimated at 664nm, 647nm, 630nm, and 750 nm in a spectrophotometer (Nano Drop spectrophotometer, NanoPlus).
6) According to the equation (Jeffrey and Humphrey, 1975), the final chlorophyll-*a* concentration was determined.

Chlorophyll-*a*

$$= (11.85 * (E664 - E750) - 1.54 * (E647 - E750) - 0.08 * (E630 - E750)) * Ve/L * Vf$$

Where,

L = Cuvette light-path measured in centimeters.

Ve = The extraction volume in milliliter

Vf = Filtered water volume in liter.

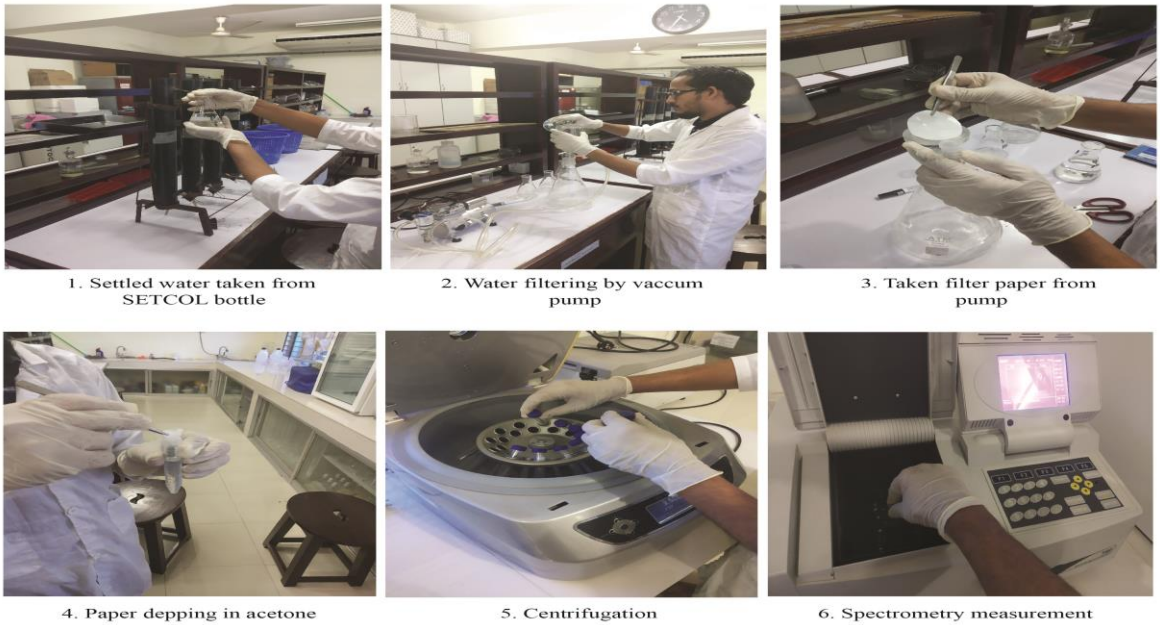

Figure 4: The sequence of Chlorophyll-*a* measurement.

3.3.4 Phytoplankton sinking rate measurement

Phytoplankton sinking rates of particulate matter were determined by using a homogeneous sample method called SETCOL (Guo et al., 2016). To determine the phytoplankton sinking rate, the total average Chlorophyll *a* of 3 SETCOL bottle (Bt) was calculated first. Then measured the settled average volume in 3 bottles (Bs). The sinking rate per hour was then calculated using the formula below, which was then multiplied by 24 hours to get the sinking rate each day.

Phytoplankton sinking rate: $\boldsymbol{\psi} = (\frac{\boldsymbol{Bs}}{\boldsymbol{Bt}}) \times \frac{\boldsymbol{L}}{\boldsymbol{t}}$

$$\boldsymbol{\psi} = \frac{\boldsymbol{Vsbs - Vs(bo,o + bo,t)/2}}{\boldsymbol{Vt(bo,o + bo,t)/2}} \times (\frac{\boldsymbol{l}}{\boldsymbol{t}})$$

Where,

ψ = Sinking rate

Bs = Total biomass settled during the trial time

Bt = Total biomass within SETCOL volume

Vs = The volume of settled region

bs = Biomass concentration in Vs at the end trial

bo,o = The whole sample concentration at the start of the trial

bo,t = The whole sample concentration at the end of the trail

Vt = Total volume of the sample in SETCOL

l = Height of sinking column (0.6m)

t = Duration of trial (2 hour)

3.3.5 Phytoplankton sample collection and analysis

Phytoplankton sample was collected from three different depths (0m or surface, 5m, and 10m) in each transect point. At each depth, a total of 5L water sample was collected. For collecting water from different depths, a heavy stone was bonded with the water sampler (Wildco FL-32097) for proper sinking. After the water was collected, it was filtered through a hand-made 45µm-mesh net and stored in a 250ml bottle with 10% buffered formalin (Fig. 5).

1. Water sample filtration by plankton net

2. Collect phytoplankton sample

3. Stored sample into plastic bottle

Figure 5: The sequence of phytoplankton sample filtration and collection

3.3.6 Qualitative and quantitative estimations of phytoplankton

Qualitative and quantitative analysis done in Oceanography laboratory (CVASU) by using a fluorescence research microscope with a camera (Feinoptic RB 50 + F 10). Following steps were followed for analysis (Fig. 6):

1) Using a Sedgwick-Rafter Counting Cell (Graticules Optics- S50, UK) for estimation of plankton that holds 1000 cubic millimeters of liquid 1-millimeter-deep over an area of 50×20 millimeter and the base is divided into 1-millimeter squares.
2) To fill the Sedgewick-Rafter chamber, the coverslip was placed on the top of the chamber, but an oblique angle, so that the chamber was only partially covered.

3) A pipette was used to measure 1 ml of well-mixed sample and fill the chamber, and then the coverslip was to be nudged gently so that it covered the chamber completely. The cell was left for 15 minutes undisturbed to allow plankton to settle. After settling the sample, the phytoplankton cell started counting.
4) Counting was done with the 10X magnification of a fluorescence research microscope with a camera (Feinoptic RB 50 + F 10).
5) The plankton in 10 randomly selected cells was identified up to the family level and counted under a microscope. The plankton was also observed under a microscope to study the major plankton classes.
6) Qualitative estimation of phytoplankton was used to find the major groups of phytoplankton. This was done by identifying and classifying phytoplankton.
7) The plankton cell density was calculated using the (Striling, 1985) formula:

$$N = \frac{(A \times 1000 \times C)}{(V \times F \times L)}$$

Where,

N = Number of plankton cells or units per liter of the original water

A = Total number of plankton counted.

C = Volume of final concentrate of the sample in ml.

V = Volume of a field in cubic mm (mm.

F = Number Of fields counted.

L = Volume of original water in liter.

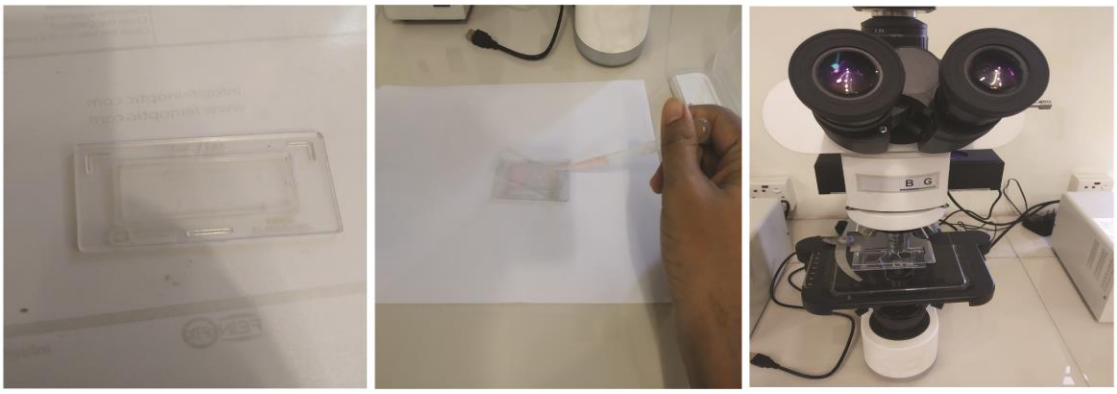

1. Sedgwick- rafter cell

2. Take sample in the cell

3. Cell placed in under microscope

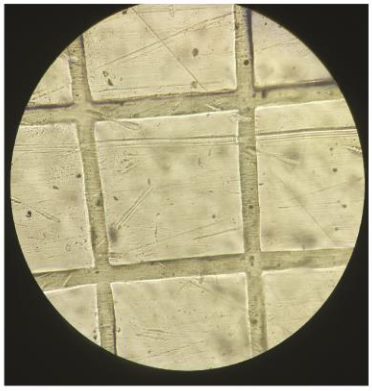

4. Counting and identification

Figure 6: The Sequence of phytoplankton counting and identification.

3.3.7 Total carbon estimation in each cell and a specific depth

Phytoplankton cell carbon was estimated according to (Guo et al., 2016). For cell carbon estimation, firstly need to measure the cell biovolume. The diameter, length, and width of phytoplankton cells were measured with a fluorescence research microscope with a camera (Feinoptic RB 50 + F 10) so that the cell biovolume could be found. Before measurement, the microscope was calibrated with a calibration slide (Fig. 7). The following process was followed

Process of calibration

1) A calibration slide with a known distance (here used a 10 mm scale with 100 division (1 division = 0.1mm) was placed in under the microscope.
2) The objective in the microscope was set up at 10X magnification.
3) Then opened the proview software and selected the camera from the camera list.

4) Zoomed in 100% and maxed up the resolution.
5) Then selected the calibrate option, and set the magnification to 100X (10X objectives * 10X eyepiece).
6) Then selected the measuring unit into Micrometer (µm)
7) Clicked the endpoint and selected the H-style.
8) Placed the right H-line on the farthest last hash line, counted from the left red H-line to the other, and added the total.
9) After added up the total between the red H-lines, input the number into the Actual Length (in here, it is 400µm).
10) Then pressed ok and start the measurement.

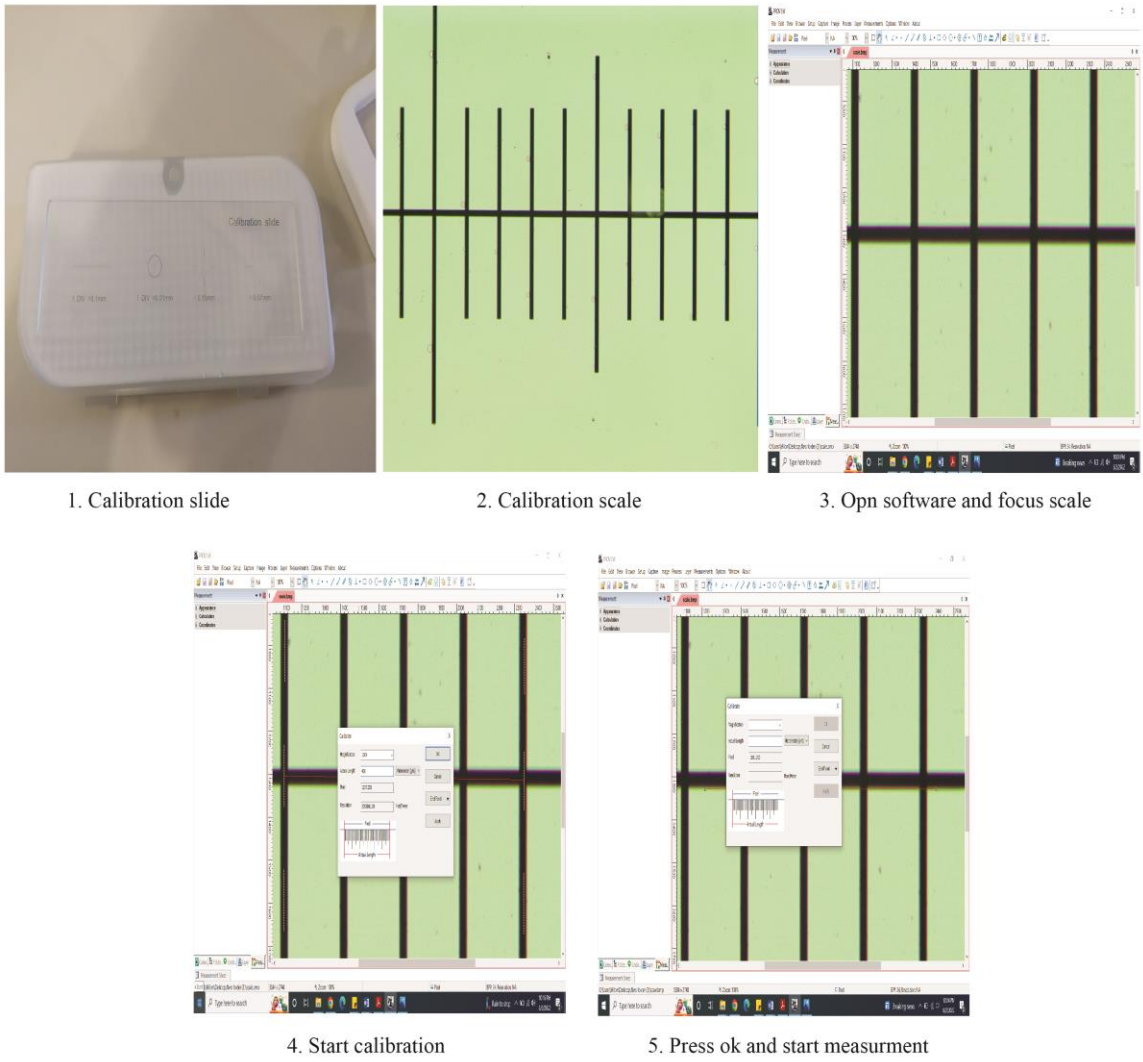

Figure 7: The sequence of microscope calibration for biovolume measurements.

After that cell volume was calculated geometrically **(**Olenina, 2006; Napiórkowska-Krzebietke and Kobos, 2006).

Then the carbon/cell was calculated using the volume of each plankton. Two formulas were used, one for diatoms and another for other algae (Guo et al., 2016).

1. $Log_{10} C = 0.76 \times Log_{10} V - 0.352$ for diatom
2. $Log_{10} C = 0.94 \times Log_{10} V - 0.60$ for other algae

Here,

- C is the carbon content of each species in pg C/cell
- V is the cell Biovolume of each species in μm^3

3.3.8 Carbon flux determination

Carbon content in each cell further multiplied with total cells found in a depth of one specific phytoplankton. After calculating the total amount of carbon at a given depth, this formula was used to determine the carbon flux (Guo et al., 2016).

Carbon flux = Sinking rate × Total carbon of a specific depth

3.4 Nutrients components analysis

3.4.1 Nitrite-nitrogen (NO_2-N)

Nitrite-nitrogen (NO_2-N) was determined using the methods from (Bendschneider and Robinson, 1952).

Equipment:

Spectrophotometer (Nano Drop Spectrophotometer, Model- NanoPlus), funnel, conical flask, measuring cylinder, the filter paper (Double Rings Qualitative Filter Paper, 12.5cm Diameter)

Reagents:

i. Sulphanilamidepment

ii. N-(1-Napthal)- ethylene diamine dihydrochloride (NNED)

Methods:

1) The 50 ml water sample was filtered with filter paper.
2) 50 ml filtered sample was then stored in a conical flask.
3) 1 ml of Sulphanilamide was added and mixed.
4) It was added for 2-8 min. for reaction.
5) Then, 1ml of NNED was added and blended.
6) The extinction is estimated at 543 nm after 10 minutes but before 2hrs.

Calculation:

(µg at NO_2-N/L): Factor (19.84) X (Absorbance of the samples – Absorbance of the blank)

3.4.2 Phosphate-Phosphorus (PO_4-P)

Phosphate-Phosphorus (PO_4-P) was observed using the methods described (Murphy and Riley, 1962).

Equipment:

Spectrophotometer (Nano Drop Spectrophotometer, Model- NanoPlus), funnel, conical flask, measuring cylinder, filter paper (Double Rings Qualitative Filter Paper, 12.5cm Diameter).

Reagents:

i. Acid ammonium molybdate
ii. Stannous chloride.

Methods:

1) The 50 ml water sample was filtered with filter paper.
2) Then, 50 ml of the filtered sample was taken in a conical flask.
3) Added 2 ml of ammonium molybdate and shake.
4) Then added 5 drops of stannous chloride.
5) Finally, the absence of the developed color was measured at 690 nm.

Calculation:

(µg at PO_4-P/L): Factor (45.93) x (Absorbance of the sample − Absorbance of the blank)

3.4.3 Silicate-Silicon (SiO_3-Si)

Silicate-Silicon (SiO_3-Si) was observed using the methods described (Mullin and Riley, 1955).

Equipment:

Spectrophotometer (Nano Drop Spectrophotometer, Model- NanoPlus), funnel, a conical flask, measuring cylinder, filter paper (Double Rings Qualitative Filter Paper, 12.5cm Diameter).

Reagents:

i. 10% Acid ammonium molybdate
ii. 25% Sulphuric acid (v/v)

Methods:

1) The 50 ml water sample was filtered with filter paper.
2) Then, 50 ml of the filtered water sample was taken in a conical container.
3) 2 ml of ammonium molybdate added and shake.
4) Added 0.5 ml of Sulfuric Acid.
5) Finally, the absence of the developed color was measured at 460 nm.

Calculation:

(µg at SiO_3-Si /Kg)= Factor (5372.58) x (Absorbance of sample − Absorbance of blank).

3.4.4 Nitrate-nitrogen (NO_3-N)

The photometer (Photoflex STD; WTW, Germany) was used for the measurement of Nitrate-nitrogen (NO_3-N). Before using the photometer, set the program 314 and proceed with zero adjustments by distilled water. Then followed the procedure.

Methods:

1) Pipetted 1 ml of sample into a reaction cell and closed the cell with the screw cap.
2) Mixed the contents by carefully swaying the cell (10x).
3) Added the Vario Nitrate Chromotropic Powder pack and closed the cell with the screw cap.
4) Mixed the contents by carefully swaying the cell (10x). A small number of solids may remain undissolved.
5) It was allowed to react for 5 minutes.
6) Inserted the cell in the photometer cell shaft and started the measurement.

3.5 Analysis of Physico-chemical water quality parameters

The seasonal distinction of physical and biochemical parameters of the two stations was carefully measured by following standard procedures and using supporting devices.

3.5.1 Onsite analysis of hydro-meteorological parameters

I. Water temperature

Water temperature was measured using a standard mercury-filled centigrade thermometer ranging from 0^{o} C to 100^{o} C.

II. Water pH

The water pH value was determined using a digital pen pH meter (EcoSense pH 10A). The water pH meter was calibrated before every measurement.

III. Water salinity

The water salinity was determined using a handheld refractometer (Bellingham Salinity ATC Refractometer, UK). The refractometer was calibrated before every measurement.

IV. Water dissolved oxygen (DO)

The water dissolved oxygen was determined using a portable Do meter (EcoSense DO 200A). The DO meter was calibrated before every measurement.

V. Electro-conductivity, TDS, NaCl (%)

Electro-conductivity value was measured by using a digital electro-conductivity meter (Hanna edge HI-2030). In the meantime, the water TDS and Percentage of NaCl can be known by this Electro-conductivity meter.

VI. Turbidity measurement procedure

The water turbidity was measured by using the turbo meter (Turb 430T). Before using it, it was calibrated with distilled water.

Process of water turbidity determination

1. Firstly, calibrated the turbo-meter with distilled water.
2. Shake the sampled water and take it to a vacant cell.
3. Then, inserted the cell into the turbo meter.
4. Measured the result.

3.5.2 Laboratory analysis of hydro-meteorological parameters

I. Total Suspended Solids (TSS)

Using the filtration procedure, total suspended solids were measured by accepted procedures (APHA 1995). Using a filtration process, total suspended solids were measured per standards guides. The water samples were filtered through filter paper (Double Rings Qualitative Filter Paper 12.5cm) that were oven (Binder ED-115) dried at 105°C (>1 hour) and weighted to obtain the sum of suspended solids for total suspended solid determination (TSS).

Equipment:

Filter paper, Electrical Balance, Oven, Desiccator

Methods:

1. The filter paper was first dried in the oven and put in the Desiccator (at least 30 min at both stages). The oven-dried filter paper was then weighted.
2. 50 ml sample of water taken and filtered with filter paper.

3. After filtration, the filter paper was dried in the oven at 105ºC and put in a desiccator for 15 min.
4. Then the weight of the filter paper with the remaining solids was calculated.
5. Finally, the total suspended solids (TSS) of sample water were calculated.

Calculation:

$$TSS = \frac{\mathrm{B} - \mathrm{A}}{50} \times 1000$$

Where,

A = Weight of the oven-dried filter paper

B = Weight of the filter paper with reaming solid

4. Statistical data analysis

The water quality data for each station were analyzed on a seasonal basis. Each season a single sample was collected from each station. The findings were analyzed using Microsoft Excel 2013. Both water quality and plankton composition experimental results were analyzed using two-way ANOVA with SPSS version 26.0.0 and R-studio software. Pearson correlation and PCA analysis was done by R-studio software

CHAPTER FOUR

RESULTS

The water Physico-chemical parameters of the Cox's Bazar and Kutubdia stations were recorded over four seasons. These Physico-chemical parameters included water temperature, Salinity, NaCl%, pH, Dissolved oxygen (DO), Total Dissolved Solids (TDS), Water Electrical Conductivity (EC), Turbidity, Total Suspended Solids(TSS), Chlorophyll-*a* and nutrients included Silicate-silicate (SiO_3-Si), Phosphate-phosphorus (PO_4-P), Nitrite-Nitrogen (NO_2-N), Nitrate nitrogen (NO_3-N).

4.1 Ocean and coastal productivity

4.1.1 Chlorophyll-*a* (Chl-*a*)

The level of Chlorophyll-*a* fluctuated from 0.025 to 1.65 µg/l during the study period (Table-5). The maximum chlorophyll-*a* (1.65 µg/l) was in Cox's Bazar (St1) during the post-monsoon season (S4) at the transect-1 (T1) at 5m depth (D2), whereas lowest Chl-*a* (0.025 µg/l) was found in Cox's Bazar (St1) during the monsoon season (S3) at the transect-2 (T2), 10m depth (D3) (Fig. 8). During the post-monsoon season (S4), Chl-*a* had the highest average concentration (0.61 µg/l) (Fig. 8A), on the other hand, Cox's Bazar station (St1) (0.41 µg/l) had a higher Chl-*a* than the Kutubdia station (St2) (0.18 µg/l) (Fig. 8B). In case of transects, transect point-1 (T1) of Cox's Bazar contained a higher amount of Chl-*a* (0.5 µg/l) concentration than the other three transects (Fig. 8C), while 5m depth (D2) had the highest amount of Chl-*a* (0.4 µg/l) containing than 0m (D1) and 10m (D3) depths (Fig. 8D). A two-way ANOVA showed that variations in Chlorophyll-*a* among four seasons [$F(1, 3) = 10.341$, $p<0.05$] (Table-1), two stations [$F(1, 1) = 8.292$, $p<0.05$ (Table-2)] and four transects [$F(1, 3) = 3.05$, $p<0.05$ (Table-3)] were significant.

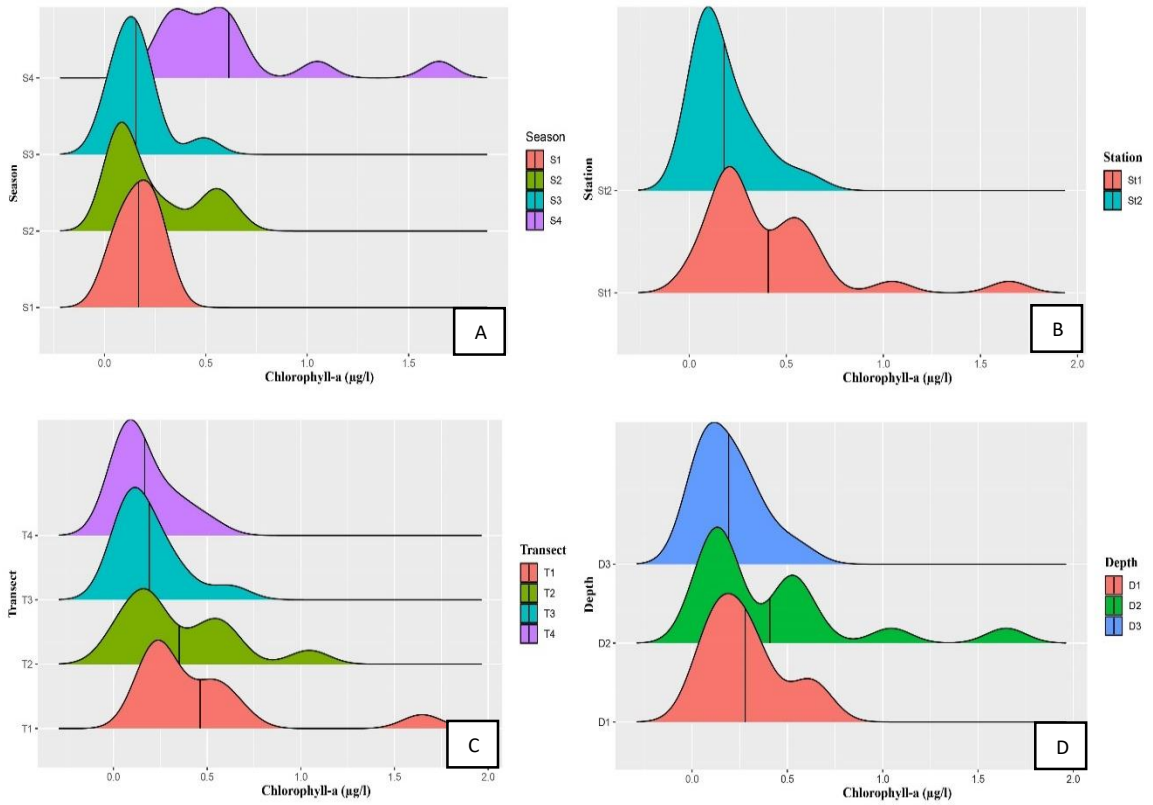

Figure 8: Chlorophyll-*a* fluctuation in northeastern BoB, A) Seasonal variation, B) Station-wise variation, C) Transect-wise variation, D) Depth-wise variation and black line indicate mean value.

4.1.2 Phytoplankton sinking rate (PSR)

Phytoplankton sinking rate (PSR) value varied from 0.04 to 1.86 m day^{-1} during the study period (Table-5). The maximum (1.86 m day^{-1}) PSR was found in the winter season (S1) at the Kutubdia station (St2) at transect point-4 (T4), 10m depth (D3), oppositely the lowest value (0.04 m day^{-1}) was observed in the monsoon (S3) of the Cox's Bazar station (St1) at transect point-2 (T2), 5m depth (D2) (Fig. 9). The winter season (S1) had the highest sinking rate (0.57 m day^{-1}) than the other three seasons (Fig. 9A), while the Kutubdia station (St2), had a higher PSR mean value (0.45 m day^{-1}) than the Cox's Bazar station (St1) (0.39 m day^{-1}) (Fig. 9B). On the other hand, transect-2 (T2) of Cox's Bazar and transect-4 (T4) of Kutubdia jointly consisted higher sinking rate (0.5 m day^{-}1) (Fig. 9C) whereas 10m depths (D3) had a higher PSR mean (0.6 m day^{-1}) than the other depths (Fig. 9D). A two-way ANOVA showed that variations in phytoplankton sinking rate among three depths [$F(1, 2) = 5.109$, $p<0.05$] (Table-4) were significant.

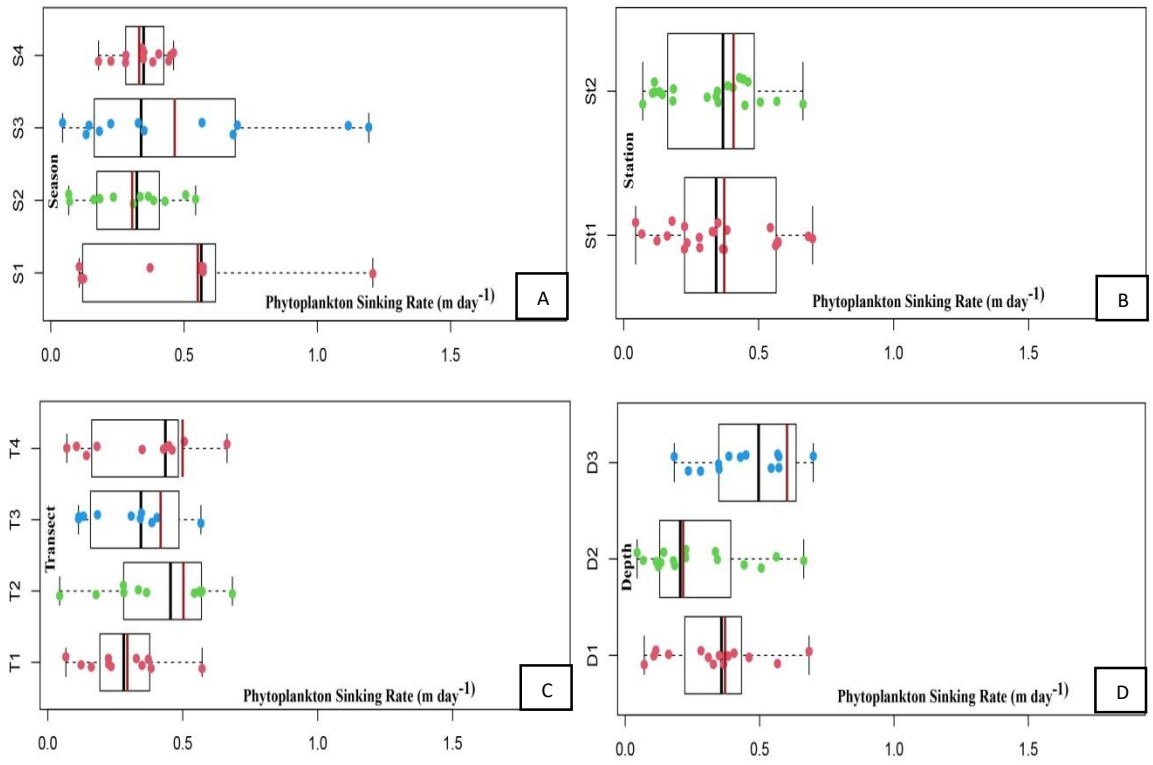

Figure 9: Phytoplankton sinking rate fluctuation in northeastern BoB, A) Seasonal variation, B) Station-wise variation, C) Transect-wise variation, D) Depth-wise variation and black line indicate median value and red line indicate the mean value.

4.1.3 Phytoplankton density (Pl. den)

The maximum phytoplankton density (8×10^4 cell/l) was observed in both the winter (S1) and pre-monsoon seasons (S2). In winter, it was in Cox's Bazar station (St1) at the transect-2 (T2), 10m depths (D3), and in the pre-monsoon season (St2), it was also in Cox's Bazar station (St1) at the transect-1 (T1) at 5m depths (D2). The minimum plankton in Kutubdia (St2) during pre-monsoon (S2) at the transect-4 (T4), 0m depths (D1). The highest average plankton density (5.9×10^4 cell/l) was observed in monsoon season (S3) than other three seasons (Fig. 10A), while Cox's Bazar station (St1) had a higher average of phytoplankton density (6×10^4 cell/l) than the Kutubdia (St2) station (4.8×10^4 cell/l) (Fig. 10B). In case of transects points, transect-2 (T2) of Cox's Bazar consisted of a higher average of phytoplankton than the other three transects (Fig. 10C), and the 5m depth (D2) had a higher plankton average (5.9×10^4 cell/l) than 0m (D1) and 10m (D3) (Fig. 10D). A two-way ANOVA showed that variations in phytoplankton density among two station [F (1, 1) =

9.61, $p<0.05$ (Table-2)] and four transects [$F(1, 3) = 0.024$, $p<0.05$] (Table-3) were significant.

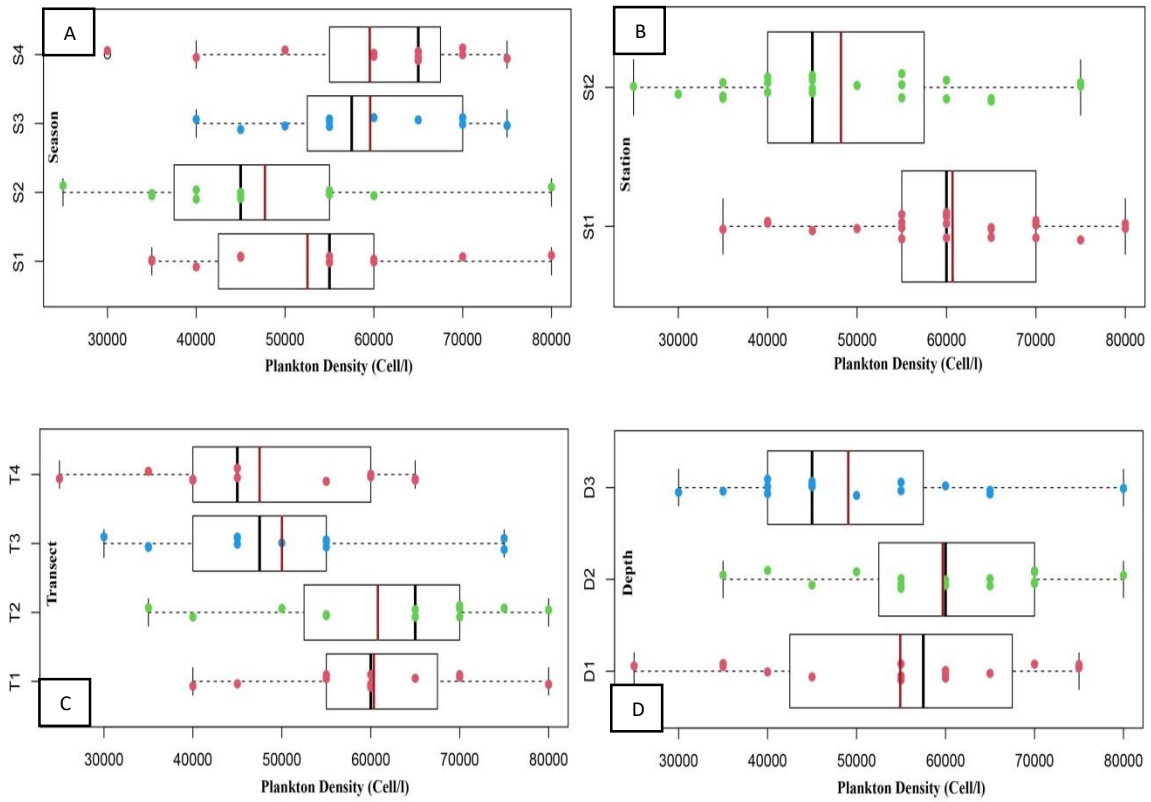

Figure 10: Phytoplankton density fluctuation in northeastern BoB, A) Seasonal variation, B) Station-wise variation, C) Transect-wise variation, D) Depth-wise variation and black line indicate median value and red line indicate the mean value.

4.1.4 Total carbon (TC)

Total carbon content ranged from 0.43 to 10.62 mg m^{-3} throughout the study (Table-5). The maximum value (10.62 mg m^{-3}) was observed in the pre-monsoon season (S2) of the Kutubdia station (St2) at transect point-2 (T2), 10m depth (D3). Oppositely lowest value (0.43 mg m^{-3}) was obtained in the post-monsoon season (S4) of the Cox's Bazar station (St1) at transect point-1 (T1), 5m depth (D2) (Fig. 11). In case of average TC, the monsoon season (S3) had more TC (5.48 mg m^{-3}) and it was decreased in the winter season (S1) (3.66 mg m^{-3}) (Fig. 11A). Kutubdia station (St2) contained higher TC (4.93 mg m^{-3}) while lower carbon found in the Cox's Bazar station (St1) (4.34 mg m^{-3}) (Fig. 11B). On the other hand in transects points, transect-4 (T4) of Kutubdia station had a higher mean TC (5.0 mg

m^{-3}) than other transects point (Fig. 11C) and 10m depth (D3) contained the highest TC (5.1 mg m^{-3}) (Fig. 11D). A two-way ANOVA showed that variation in total carbon among four seasons, two stations, four transects and three depths were not significant.

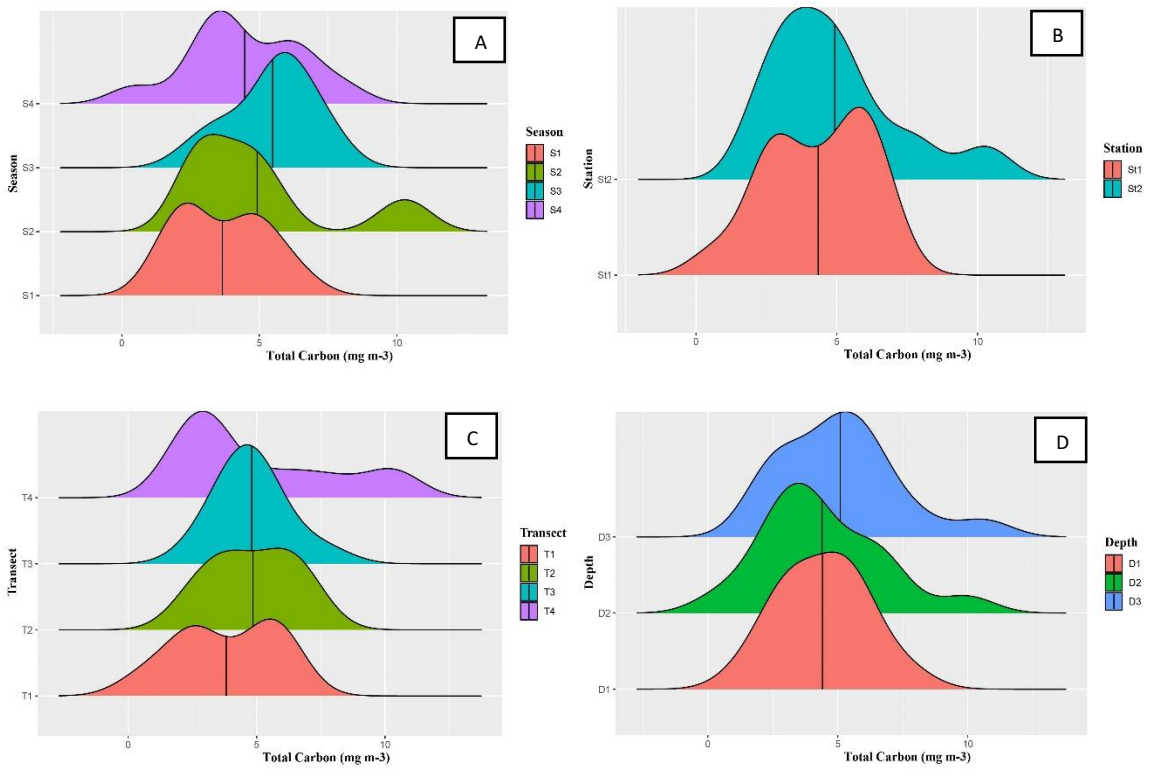

Figure 11: Total carbon content fluctuation in northeastern BoB, A) Seasonal variation, B) Station-wise variation, C) Transect-wise variation, D) Depth-wise variation and black line indicate mean value.

4.1.5 Carbon Flux (CF)

Throughout the study, carbon flux (CF) values ranged from 0.10 to 8.60 mg C m^{-2} day^{-1} (Table-5). Maximum CF (8.60 mg C m^{-2} day^{-1}) was found during the monsoon season (S3) of Kutubdia station (St2) at transect point-3 (T3), 0m depth (D1), whereas minimum CF (0.10 mg C m^{-2} day^{-1}) was observed in the post-monsoon season (S4) of Cox's Bazar (St1) at transect point-1 (T1), 5m depth (D2) (Fig. 12). Within the season, CF changed in a zigzag pattern. In the winter (S1) (2.03 mg C m^{-2} day^{-1}) to pre-monsoon (S2) (1.65 mg C m^{-2} day^{-1}), CF sharply decreased and then it increased in monsoon season (S3) (2.52 mg C m^{-2} day^{-1}). After monsoon season (S3) it was again decreased in post-monsoon season (S4) (1.56 mg C m^{-2} day^{-1}) (Fig. 12A).), on the other hand, Kutubdia (St2) had more CF value (2.21

mg C m^{-2} day^{-1}) than Cox's Bazar station (St1) (1.67 mg C m^{-2} day^{-1}) (Fig. 12B). In case of transects point, transect-3 (T3) of Kutubdia station (St2) consisted more CF (2.3 mg C m^{-2} day^{-1}) than others transects (Fig. 12C). A two-way ANOVA showed that variations in carbon flux among three depths [F (1, 2) = 3.811, $p<0.05$] were significant (Table-4). Higher CF (2.7 mg C m^{-2} day^{-1}) observed in the deep ocean (10m depth) (D3) and lower CF observed in 5m depth (Fig. 12D).

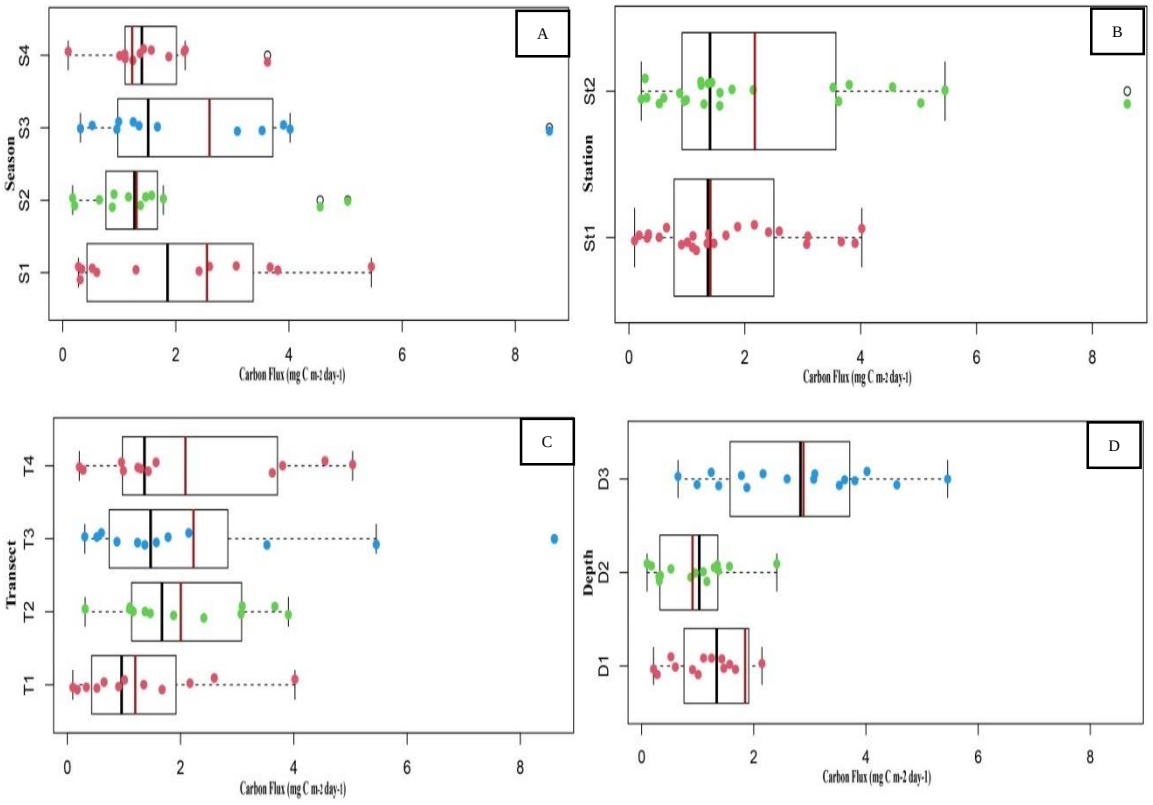

Figure 12: Carbon flux fluctuation in northeastern BoB, A) Seasonal variation, B) Station-wise variation, C) Transect-wise variation, D) Depth-wise variation and black line indicate median value and red line indicate the mean value.

4.2 Nutrients components availability

4.2.1 Nitrate Nitrogen (NO_3-N)

The highest concentration (9.2 µg/l) of Nitrate-nitrogen (NO_3-N) was in the Cox's Bazar station (St1) during winter season (S1) at the transect-2 (T2), 0m depth (D1) and the lowest concentration of NO_3-N (4.5 µg/l) was in Kutubdia station (St2) during the pre-monsoon season (S2) at transect-3 (T3), 10m depth (D3) (Fig. 13). In case of seasonal variation,

winter (S1) had the higher average concentration of NO_3-N (7.96 µg/l) then other seasons (Fig. 13A), while Cox's Bazar station (St1) consisted higher average of NO_3-N concentration (6.90 µg/l) than Kutubdia station (St2) (6.70 µg/l) (Fig. 13B). Whereas in transects point, transect-2 (T2) (7.0 µg/l) of Cox's Bazar consisted more NO_3-N concentration than other transect points (Fig. 13C) and over all surface water (D1) had the higher concentration of NO_3-N (6.9 µg/l) (Fig. 13D). A two-way ANOVA showed that variations in nitrate among four seasons [$F(1, 3) = 9.221$ $p<0.05$] (Table-1) were significant.

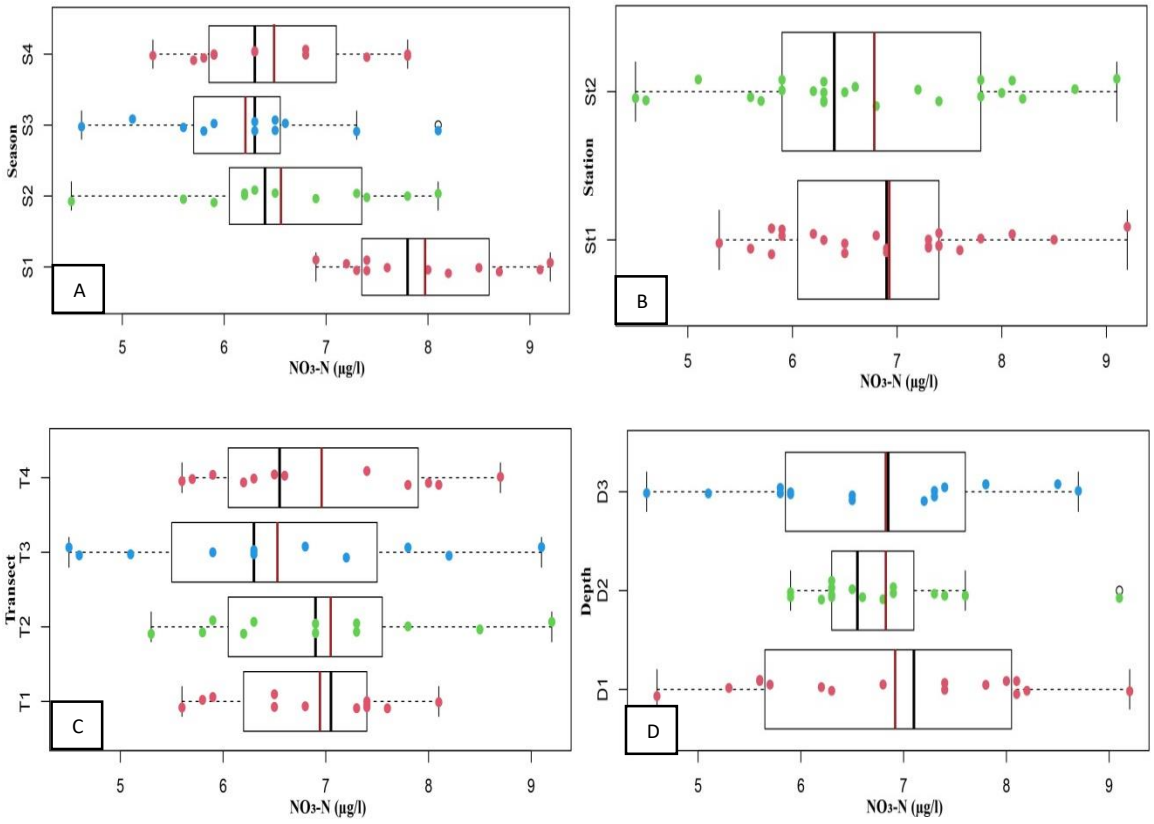

Figure 13: Nitrate nitrogen fluctuation in northeastern BoB, A) Seasonal variation, B) Station-wise variation, C) Transect-wise variation, D) Depth-wise variation and black line indicate median value and red line indicate the mean value.

4.2.2 Nitrite-Nitrogen (NO_2-N)

Nitrite-Nitrogen (NO_2-N) concentration ranged from 0.01 µg/l to 2.23 µg/l throughout the study (Table-5). NO_2-N concentration maximum (2.23 µg/l) was observed in Cox's Bazar station (St1), during winter season (S1) at transect-1 (T1), 5m depth (D2), while minimum

concentration (0.01 µg/l) was observed in the pre-monsoon season (S2) of Cox's Bazar station (St1), transect-1 (T1), 5m depth (D2) (Fig. 14). The average concentration of NO_2-N decreased from winter (S1) (1.08 µg/l) to pre-monsoon (S2) (0.05 µg/l) and then increased in monsoon (S3) and post-monsoon season (S4) (Fig. 14A), whereas Kutubdia station (St2) had the higher NO_2-N content (0.56 µg/l) then Cox's Bazar station (St1) (0.48 µg/l) (Fig. 14B). In case of transects point, transect-1 (T1) of Cox's Bazar and transect-3 (T3) of Kutubdia had similar amount (0.6 µg/l) of NO_2-N concentration (Fig. 14C), while D2 (5m depth) consisted higher concentration (0.6 µg/l) of NO_2-N (Fig. 14D). A two-way ANOVA showed that variations in nitrite among four seasons [$F(1, 3) = 25.055$, $p<0.05$] (Table-1) were significant.

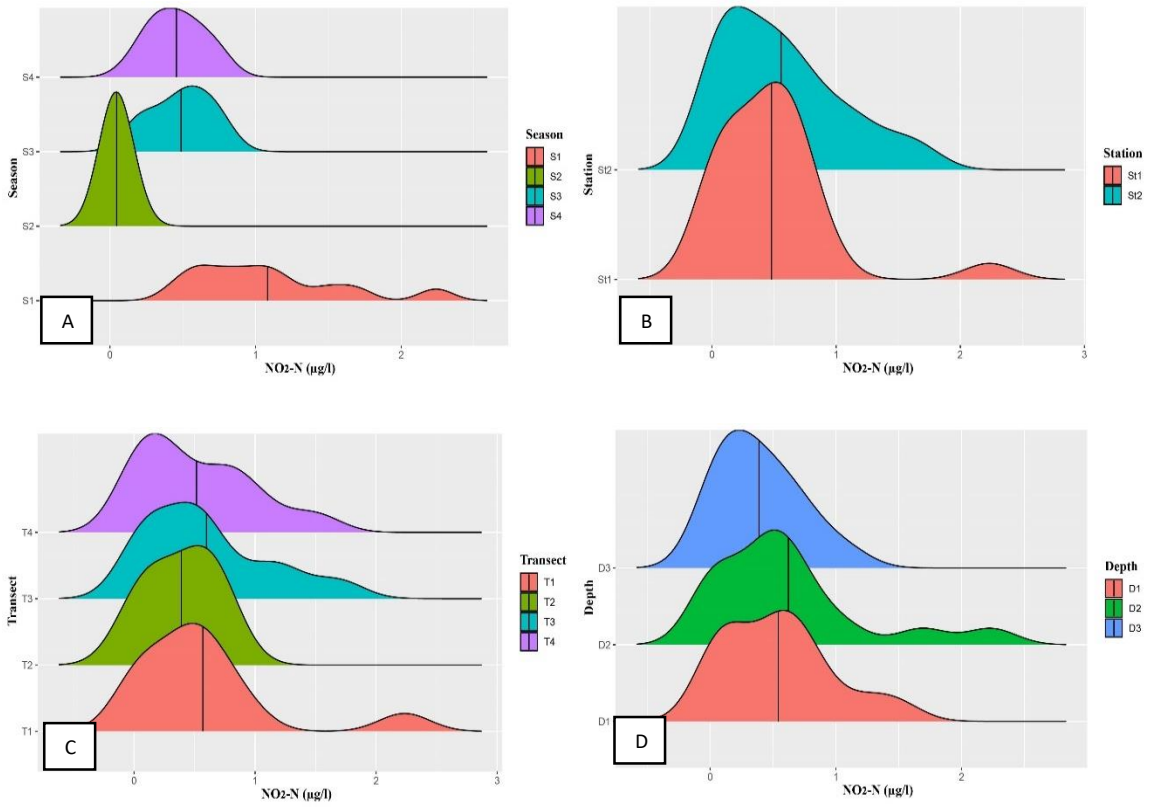

Figure 14: Nitrite-Nitrogen (NO_2-N) fluctuation in northeastern BoB, A) Seasonal variation, B) Station-wise variation, C) Transect-wise variation, D) Depth-wise variation and black line indicate mean value.

4.2.3 Phosphate-Phosphorus (PO_4-P)

The highest concentration (2.63 µg/l) of phosphate-phosphorus (PO_4-P) was in the Kutubdia station (St2) during winter season (S1) at the transect-4 (T4) at 5m depth (D2) and

the lowest concentration (0.03 µg/l) of PO_4-P was in Kutubdia (St2) during the pre-monsoon season (S2) at transect-3 (T3) at 5m depth (D2) (Fig. 15). The winter season (S1) was the higher average (1.31 µg/l) of PO_4-P then other seasons (Fig. 15A), where Kutubdia station (St2) was the more PO_4-P concentration (0.74 µg/l) rather than Cox's Bazar station (St1) (0.21 µg/l) (Fig. 15B). On the other hand in transects points, transect-3 (T3) and transect-4 (T4) of Kutubdia had the more average value (0.7 µg/l) than Cox's Bazar's transect (0.2 µg/l) (Fig. 15C), whereas PO_4-P concentration decreased from surface (D1) (0.49 µg/l) to deep (D3) water (0.46 µg/l) (Fig. 15D). A two-way ANOVA showed that variations in phosphate among four seasons [$F(1, 3) = 10.558$, $p<0.05$] (Table-1), two stations [$F(1, 1) = 6.129$, $p<0.05$ (Table-2)] were significant.

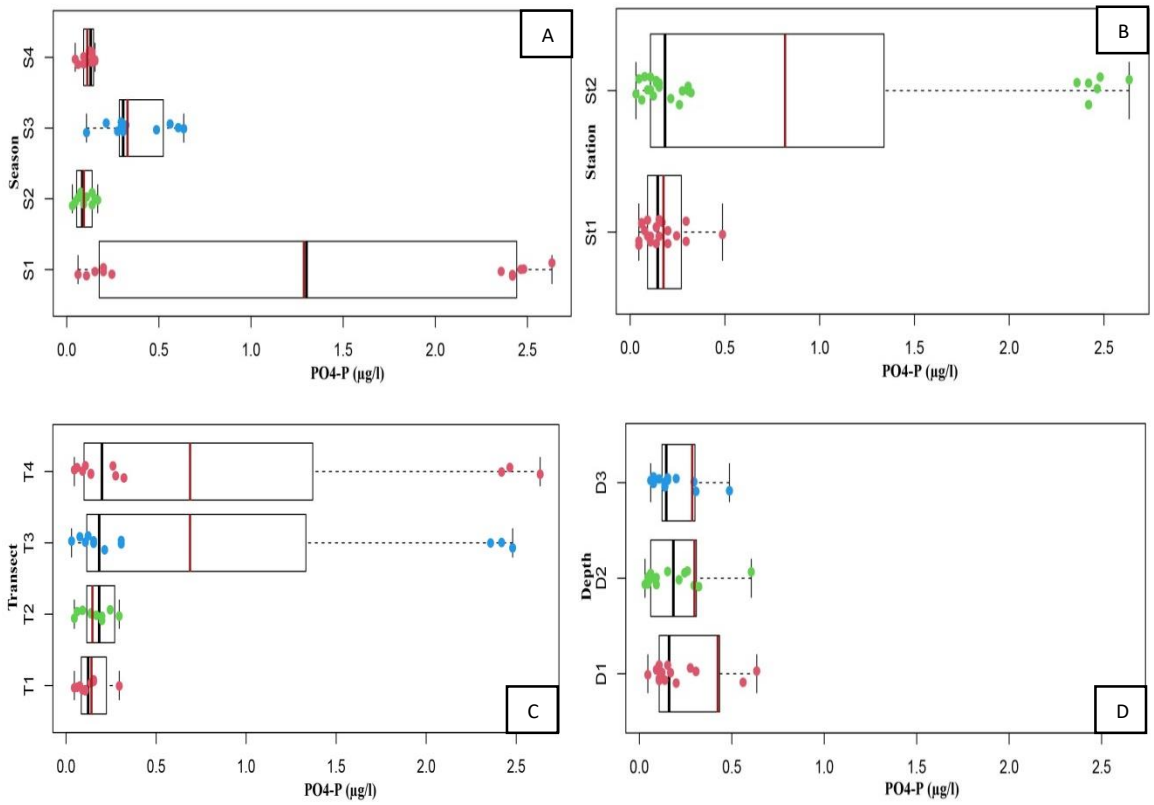

Figure 15: Phosphate-phosphorus a fluctuation in northeastern BoB, A) Seasonal variation, B) Station-wise variation, C) Transect-wise variation, D) Depth-wise variation and black line indicate median value and red line indicate the mean value.

4.2.4 Silicate-Silicate (SiO_3-Si)

Throughout the study, the highest (365.34 µg/l) silicate-silicate (SiO_3-Si) concentration was in the Kutubdia station (St2) during the winter season (S1) at transect- 4 (T4), 10m depth (D3), oppositely lowest value (5.37 µg/l) of SiO_3-Si was in at the same point in the post-monsoon season (S4) (Fig. 16). The winter season (S1) had the higher average concentration (200.29 µg/l) of SiO_3-Si then other seasons (Fig. 16A), whereas Kutubdia station (St2) contained more concentration of SiO_3-Si nutrient (107.53 µg/l) than Cox's Bazar station (St1) (38.14 µg/l) (Fig. 16B). In case of transect points, transect point-4 (T4) of Kutubdia included of more SiO_3-Si concentration (112.8 µg/l) than other transect (Fig. 16C). On the other hand, SiO_3-Si concentration decreased from surface (D1) (75 µg/l) to deep (D3) (68.8 µg/l) ocean (Fig. 16D). A two-way ANOVA showed that variations in Silicate among four seasons [F (1, 3) = 15.498, $p<0.05$] (Table-1), two stations [F (1, 1) = 5.479, $p<0.05$ (Table-2)] were significant.

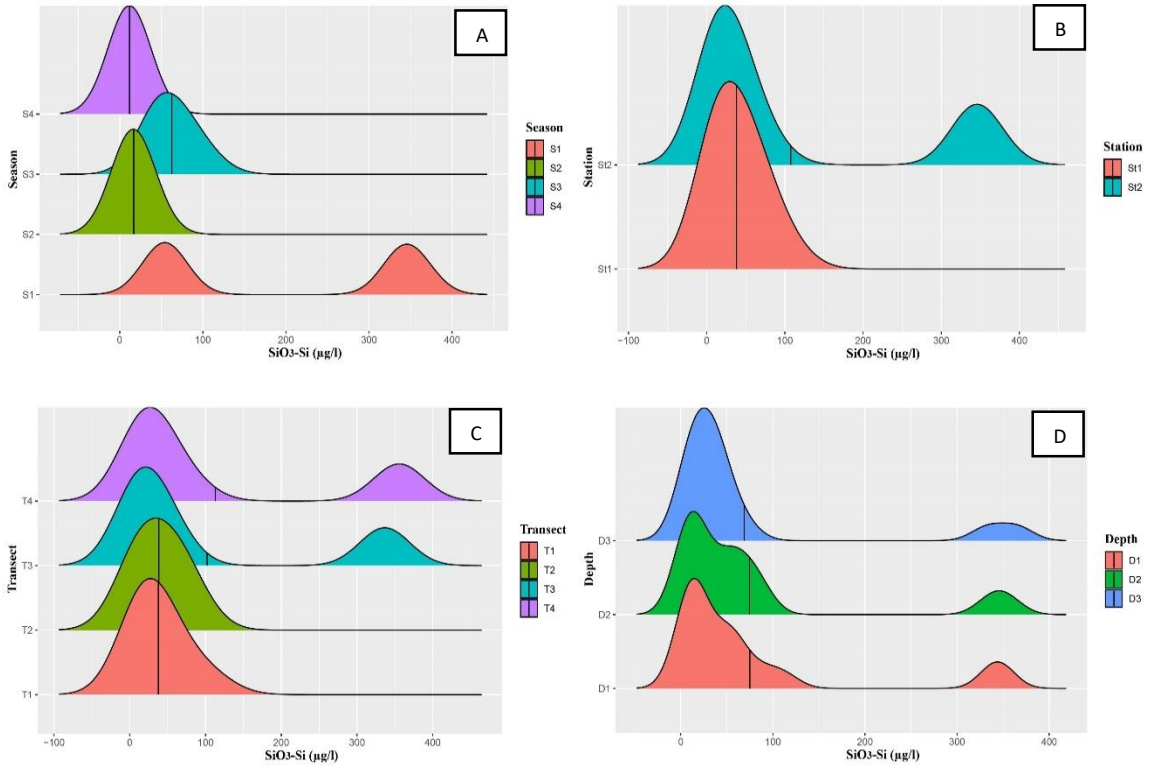

Figure 16: Silicate-silicate (SiO_3-Si) fluctuation in northeastern BoB, A) Seasonal variation, B) Station-wise variation, C) Transect-wise variation, D) Depth-wise variation and black line indicate mean value.

4.3 Water physicochemical parameters

4.3.1 Water temperature

The water temperature of the study area varied between 23.6 to 33.5ºC (Table-5). It was found to be the highest (33.5°C) throughout the monsoon season (S3) at transect-3 (T3), 5m depth (D2) of Kutubdia station (St2). The lowest value (23.6°C) was noted from the post-monsoon (S4) at transect-1 (T1), 5m depth (D2) of Cox's Bazar (St1) (Fig. 17). The seasonal average temperature was higher in monsoon (S3) (30.80°C) followed by than decreased to (25.67°C) in the post-monsoon season (S4) (Fig. 17A). The average water temperature was higher at Kutubdia station (St2) (28.92°C) rather than at Cox's Bazar station (St1) (28.30°C) (Fig. 17B). In case of transect wise variation, Kutubdia transect-3 (T3) represented higher temperature (29.1°C) level than Cox's Bazar station transect points (28.3°C) (Fig. 17C), while 10m depth (D3) (28.8°C) warmer than other depths (Fig. 17D). A two-way ANOVA showed that variations in temperature among four seasons [F (1, 3) = 57.967, p<0.05] (Table-1) were significant.

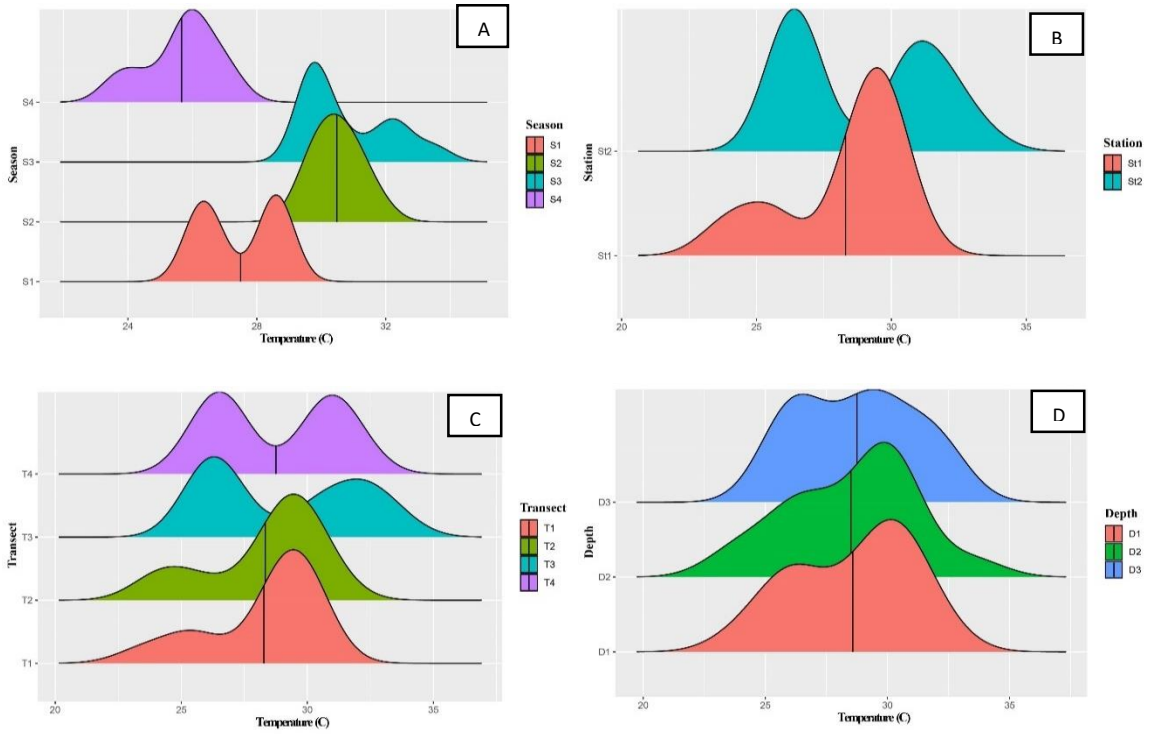

Figure 17: Water temperature fluctuation in northeastern BoB, A) Seasonal variation, B) Station-wise variation, C) Transect-wise variation, D) Depth-wise variation and black line indicate mean value.

4.3.2 Water salinity

During this study period, the water salinity of the study area varied between 6 to 31 psu (Table-5). The highest water salinity value (31 psu) was observed in the winter season (S1) of Cox's Bazar Station (St1), transect-1 (T1), 5m depth (D2). Whereas lowest value of water salinity (6 psu) was recorded during monsoon season (S3) at transect-4 (T4), 0m depth (D1) of Kutubdia station (St2) (Fig. 18). The seasonal average of water salinity noted higher in the winter season (S1) (29.29 psu) and decreased in the monsoon season (S3) (15.17 psu) (Fig. 18A), while Kutubdia station (St2) (21.40 psu) was lower water salinity than Cox's Bazar station (St1) (27.15) (Fig. 18B). In case of transect points variation, transect point-3 of Kutubdia was lower water salinity (21.2 psu) than other transect points (Fig. 18C). And the water salinity was increased from surface (D1) to deep water (D3) (Fig. 18D). A two-way ANOVA showed that variations in salinity among four seasons [$F(1, 3) = 33.357$, $p<0.05$] (Table-1), two stations [$F(1, 1) = 10.359$, $p<0.05$ (Table-2)] and four transects [$F(1, 3) = 3.32$, $p<0.05$ (Table-3)] were significant.

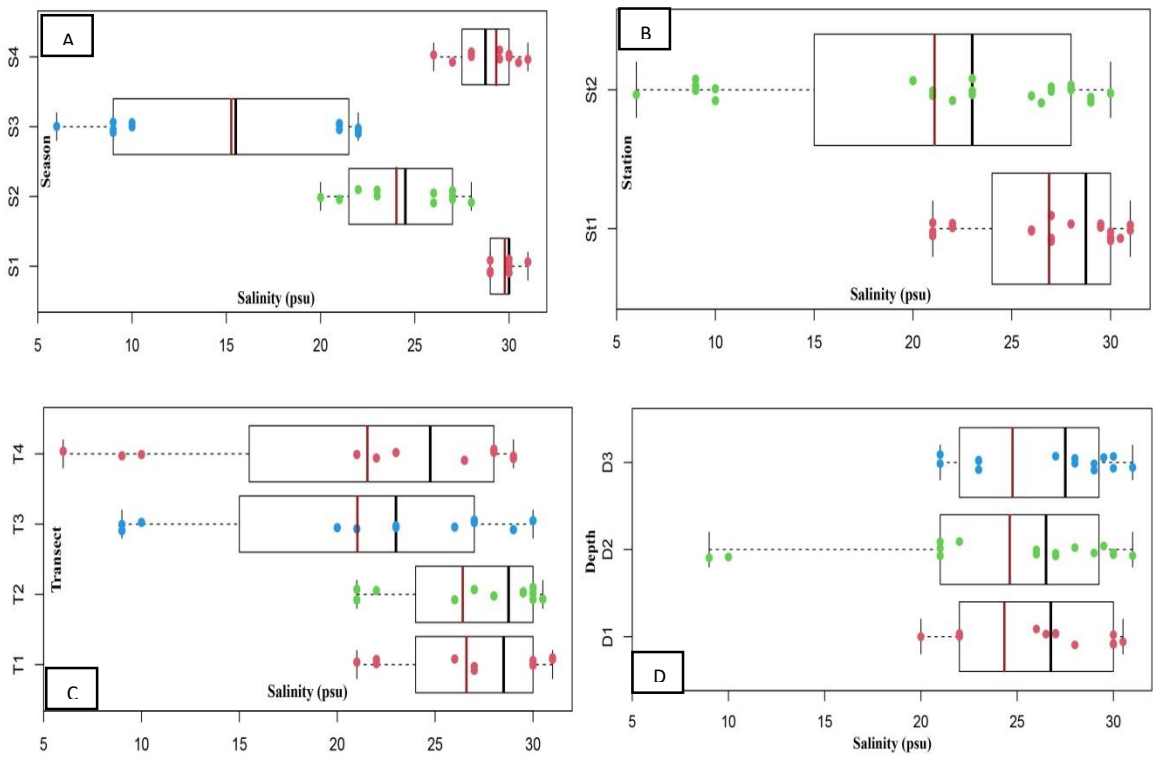

Figure 18: Water salinity fluctuation in northeastern BoB, A) Seasonal variation, B) Station-wise variation, C) Transect-wise variation, D) Depth-wise variation and black line indicate median value and red line indicate the mean value.

4.3.3 Sodium chloride percentage (NaCl %)

The water Sodium chloride percentage (NaCl %) of the study area varied between 63.0 to 143.1% (Table-5). The highest NaCl% (143.1%) was observed in the winter season (S1) of Cox's Bazar Station (St1), transect-2 (T2), 5m depth (D2), oppositely lowest value of NaCl% (63.0%) was recorded in the monsoon season (S3) at transect-4 (T4), 0m depth (D1) of Kutubdia station (St2) (Fig. 19). The seasonal average NaCl% highest in winter season (S1) (138.52%) than decreased winter (S1) to monsoon (S3) (91.68%) and again increased in post-monsoon season (S4) (125.5%) (Fig. 19A). In (Fig. 19B) showed that, Cox's Bazar station (St1) (125.35%) had the higher NaCl% than the Kutubdia station (St2) (111.52%). NaCl% continuously decreased from transect point-1 (T1) (124.3%) to transect point-4 (T4) (110.2%) (Fig. 19C), whereas surface water (D1) consisted the lower NaCl% (116.9%) than others depth (Fig. 19D). A two-way ANOVA showed that variations in NaCl % among four seasons [F (1, 3) = 30.441, p<0.05] (Table-1), two stations [F (1, 1) = 5.529, p<0.05 (Table-2)] were significant.

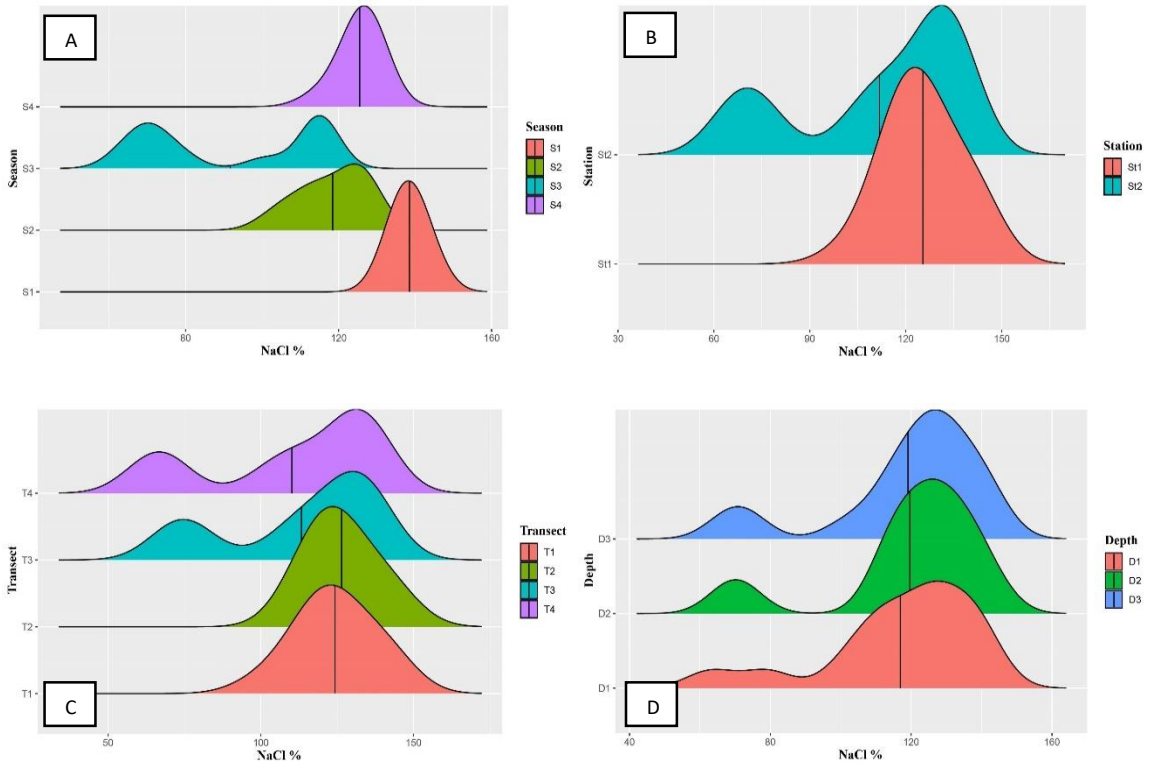

Figure 19: Sodium chloride (NaCl %) a fluctuation in northeastern BoB, A) Seasonal variation, B) Station-wise variation, C) Transect-wise variation, D) Depth-wise variation and black line indicate mean value.

4.3.4 Water pH

The water pH of the study area varied from 6.3 to 8.4 (Table-5). The highest water pH (8.4) was observed in the pre-monsoon season (S2) at transect-3 (T3), 10m depths (D3) of Kutubdia station (St2), oppositely lowest value of water pH (6.3) was recorded in the winter season (S1) at transect-1 (T1), 5m depth (D2) of Cox's Bazar station (St1) (Fig. 20). The seasonal average pH was higher in the post-monsoon season (S4) (8.11) and decreased in the winter season (S1) (6.44) (Fig. 20A), whereas Cox's Bazar station (St1) (7.52) consisted of a lower pH than the Kutubdia station (St2) (7.77) (Fig. 20B). On the other hand, transect-3 (T3) and transect-4 (T4) of Kutubdia had an equal level of pH (7.8) (Fig. 20C), and surface water (D1) was more acidic than other depths (Fig. 20D). A two-way ANOVA showed that variations in pH among four seasons [$F(1, 3) = 175.867$, $p<0.05$] (Table-1) were significant.

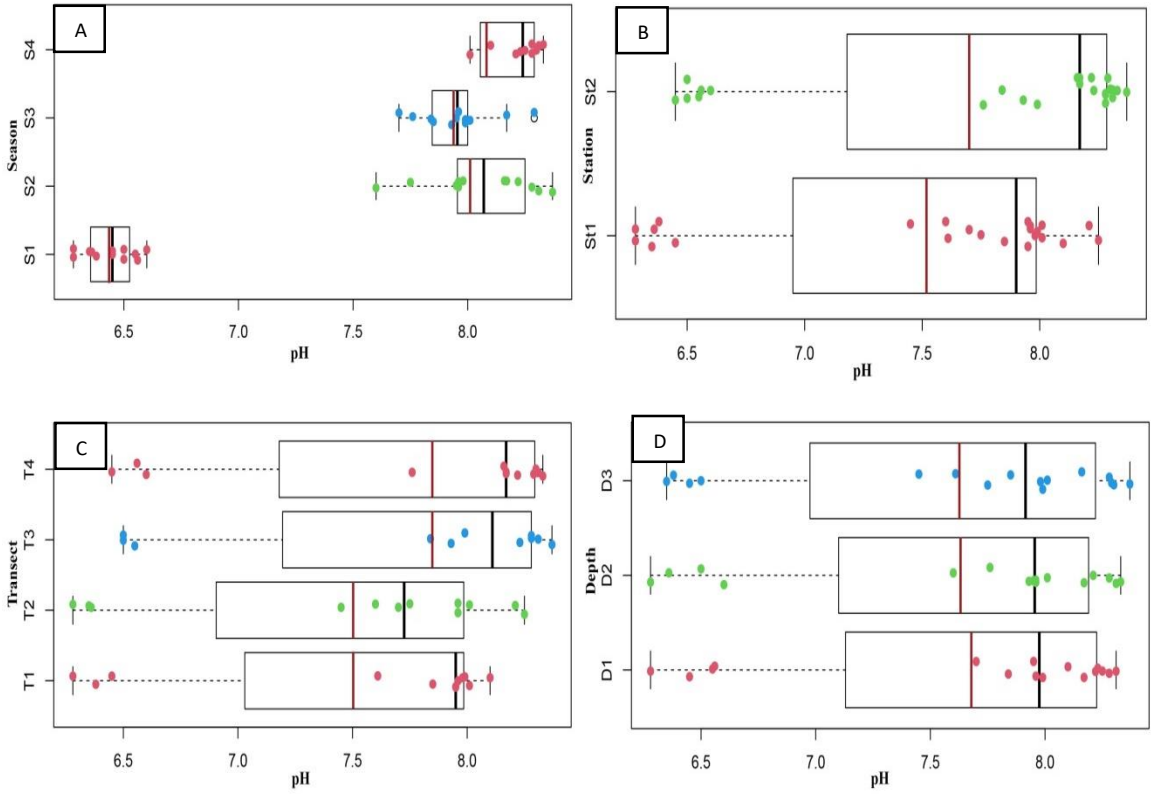

Figure 20: Water pH fluctuation in northeastern BoB, A) Seasonal variation, B) Station-wise variation, C) Transect-wise variation, D) Depth-wise variation and black line indicate median value and red line indicate the mean value.

4.3.5 Dissolved Oxygen (DO)

The water Dissolved Oxygen **(**DO) contents vary between 4.6 to 7.9 mg/l in the study period (Table-5). The maximum concentration of DO (7.9 mg/l) was observed in pre-monsoon season (S2) of Cox's Bazar station (St1) at transect-1 (T1), 10m depth (D3), and minimum DO found in monsoon season (S3) of Kutubdia station (St2) at transect- 4 (T4), 0m depth (D1) (Fig. 21). In Cox's Bazar station (St1), average DO (6.31 mg/l) was higher than Kutubdia station (St2) (5.81 mg/l) (Fig. 21B), while Winter (S1) and pre-monsoon (S2) season both had an equal concentration of DO (6.2 mg/l) throughout the study period (Fig. 21A). in case of transect points, transect point-4 (T4) of Kutubdia had the lower DO concentration than other transect (Fig. 21C). On the other hand, surface water (D1) DO concentration found lower than 5m (D2) and 10m (D3) depths (Fig. 21D). A two-way ANOVA showed that variations in dissolved oxygen among two stations [$F(1, 1) = 5.171$, $p<0.05$ (Table-2)] were significant.

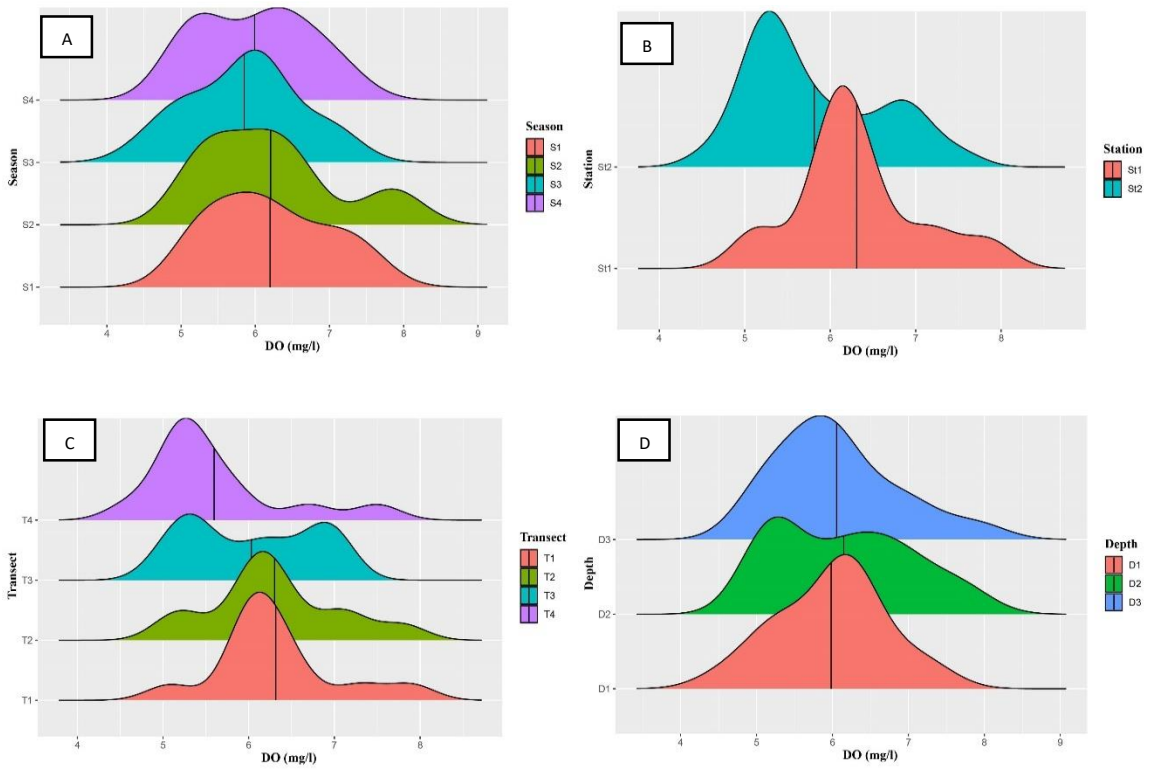

Figure 21: Dissolved Oxygen (DO) fluctuation in northeastern BoB, A) Seasonal variation, B) Station-wise variation, C) Transect-wise variation, D) Depth-wise variation and black line indicate mean value.

4.3.6 Total dissolved solids (TDS)

The total dissolved solids (TDS) concentration ranged from 16.2 to 36.4 g/l during the study period (Table-5). The maximum concentration (36.4 g/l) of TDS was measured in the winter season (S1) of Cox's Bazar Station (St1) at transect-2 (T2), 5m depth (D2). The lowest value (16.2 g/l) was observed in the monsoon season (S3) at transect-4 (T4), 0m depth (D1) of Kutubdia station (St2) (Fig. 22). During study period, winter season (S1) had the higher TDS concentration (35.38 g/l) and this concentration decreased from winter (S1) to monsoon season (S3) (23.27 g/l) and then again increased in post-monsoon season (S4) (32.08 g/l) (Fig. 22A), while Cox's Bazar Station (St1) contained maximum TDS (32.06 g/l) than Kutubdia station (St2) (28.47 g/l) (Fig. 22B).On the other hand in transect points, transect point-4 (T4) of Kutubdia had the lower TDS concentration (28.2 g/l) and transect point-2 (T2) of Cox's Bazar had higher concentration (32.3 g/l) of TDS (Fig. 22C). Surface water (D1) consisted lower TDS (29.9 g/l) throughout the study period and higher TDS found in 5m depth (D2) (Fig. 22D). A two-way ANOVA showed that variations in TDS among four seasons [$F(1, 3) = 30.245$, $p<0.05$] (Table-1), two stations [$F(1, 1) = 5.711$, $p<0.05$ (Table-2)] were significant.

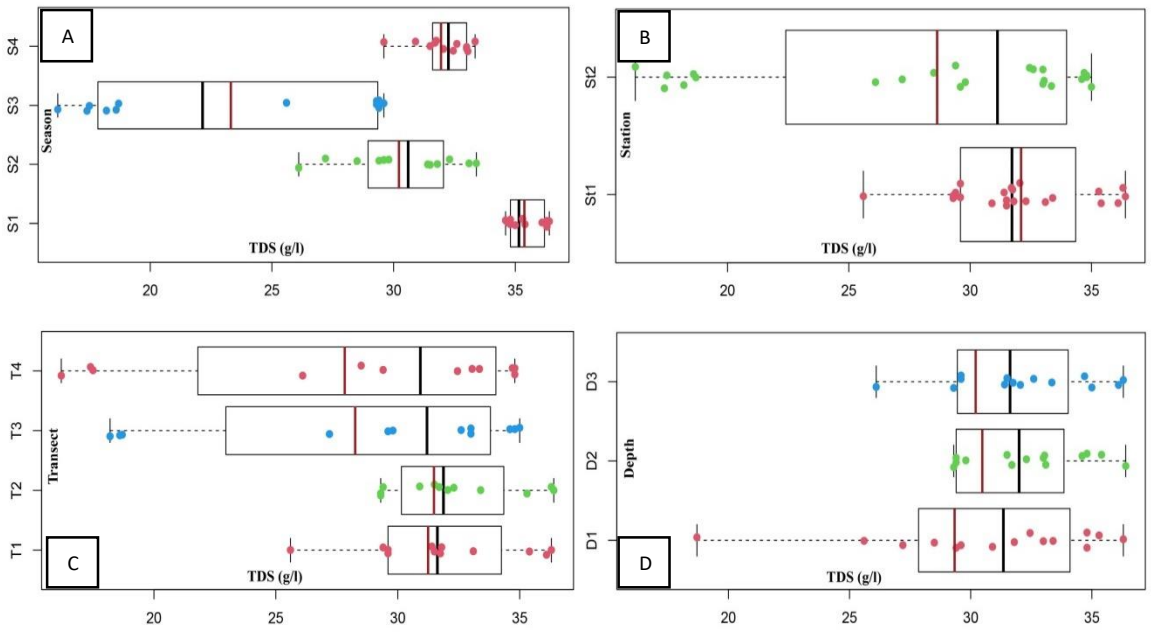

Figure 22: Total dissolved solids fluctuation in northeastern BoB, A) Seasonal variation, B) Station-wise variation, C) Transect-wise variation, D) Depth-wise variation and black line indicate median value and red line indicate the mean value.

4.3.7 Total suspended solids (TSS)

In the study periods, the maximum total suspended solids (TSS) (4.69 g/l) was observed in the winter (S1) of Cox's Bazar (St1) station at transect-1 (T1), and 5m depth (D2) while the lowest TSS (0.65 g/l) was found at same point in the winter season (S1) (Fig. 23). During the post-monsoon (S4), average TSS decreased to 1.27 g/l whereas, in winter (S1) it fluctuated to (2.6 g/l) (Fig. 23A) and Cox's Bazar station (St1) had a higher TSS (1.98 g/l) than Kutubdia (St2) (1.56g/l) (Fig. 23B). Transect point-1 (T1) of Cox's Bazar consisted of more TSS concentration (2.1 g/l) (Fig. 23C) and this was higher at 5m depth (D2) (1.9 g/l) (Fig. 23D). A two-way ANOVA showed that variations in TSS among four seasons [F (1, 3) = 15.364, $p<0.05$] (Table-1), two stations [F (1, 1) = 4.348, $p<0.05$ (Table-2)] were significant.

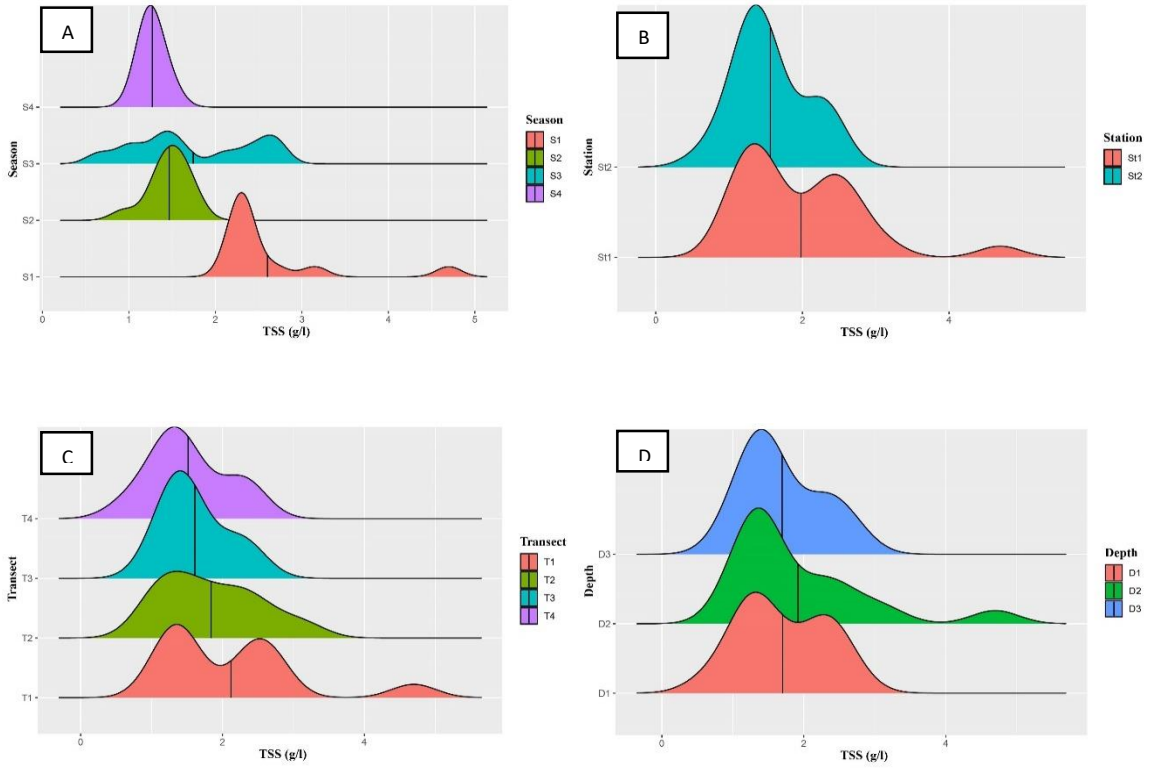

Figure 23: Total suspended solids fluctuation in northeastern BoB, A) Seasonal variation, B) Station-wise variation, C) Transect-wise variation, D) Depth-wise variation and black line indicate mean value.

4.3.8 Turbidity (Turb)

The water turbidity varied from 0.53 to 116.75 NTU during the study period (Table-5). The maximum value (116.75 NTU) turbidity was observed in the pre-monsoon season (S2) of Kutubdia station (St2) at transect-3 (T3), 5m depth (D2), while minimum value (0.53 NTU) was noted in the post-monsoon season (S4) at transect-2 (T2), 0m depth (D1) of Cox's Bazar station (St1) (Fig. 24). Turbidity consisted the highest average value in pre-monsoon (S2) (52.36 NTU) and lowest in the winter season (S1) (10.79 NTU) (Fig. 24A), on the other hand, Kutubdia (St2) was more turbid (45.09 NTU) than Cox's Bazar station (St1) (14.07 NTU) (Fig. 24B). In case of transect variation, transect-3 (T3) of Kutubdia was the more turbid than other transects (Fig. 24C), and 5m depth (D2) have higher turbidity than other depths (Fig. 24D). A two-way ANOVA showed that variations in turbidity among four seasons [$F(1, 3) = 6.530$, $p<0.05$] (Table-1), two stations [$F(1, 1) = 15.245$, $p<0.05$ (Table-2)] and four transects [$F(1, 3) = 5.98$, $p<0.05$ (Table-3)] were significant.

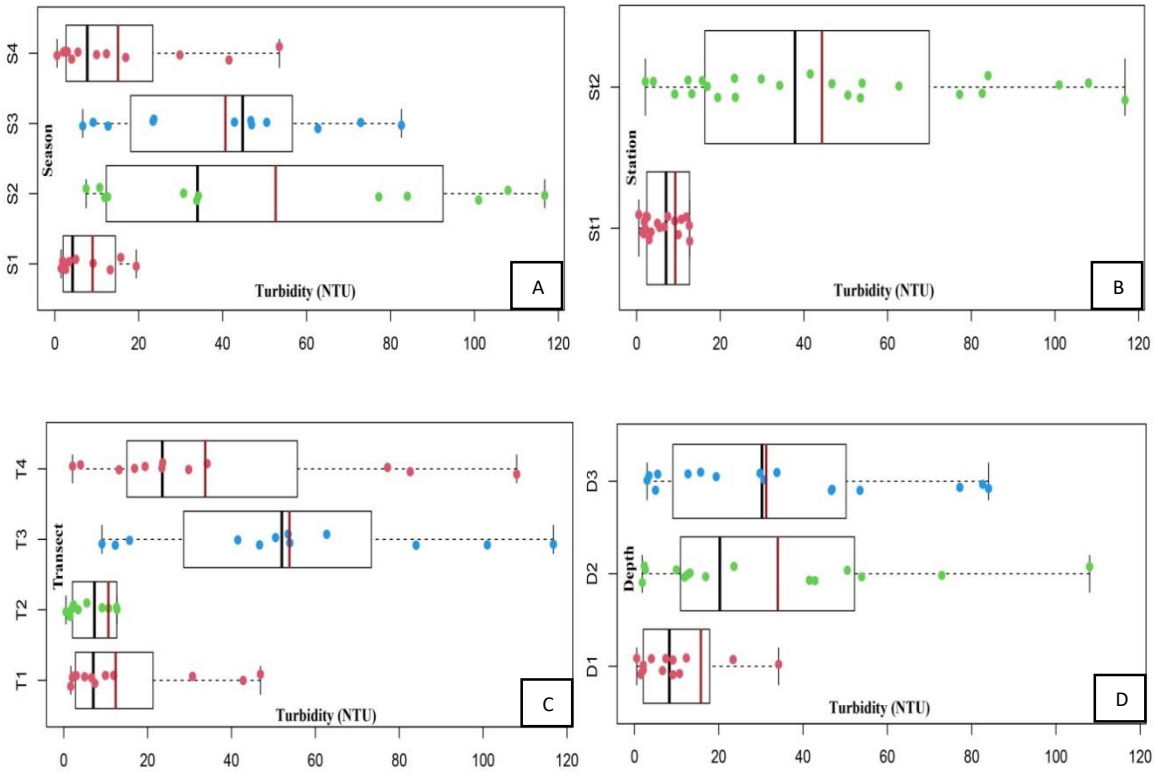

Figure 24: Water turbidity fluctuation in northeastern BoB, A) Seasonal variation, B) Station-wise variation, C) Transect-wise variation, D) Depth-wise variation and black line indicate median value and red line indicate the mean value.

4.3.9 Electric conductivity (EC)

The Electric conductivity (EC) of the study area ranged from 32.2 to 72.9 mS/cm (Table-5). The maximum value (36.4 g/l) of EC was measured in the winter season (S1) of Cox's Bazar Station (St1), transect-2 (T2), 5m depth (D2), whereas lowest EC (16.2 g/l) was noted in the monsoon season (S3) at transect-4 (T4), 0m depth (D1) of Kutubdia station (St1) (Fig. 25). Water conductivity gradually decreased from winter (S1) (70.75 mS/cm) to monsoon (S3) (46.57 mS/cm) and then a sharp increase in the post-monsoon season (S4) (64.12 mS/cm) (Fig. 25A). Whereas Cox's Bazar (St1) consisted the higher conductivity (63.8764.12 mS/cm) than Kutubdia station (St1) (56.9864.12 mS/cm) (Fig. 25B). In case of transect variation, transect-1 (T1) of Cox's Bazar had a higher conductivity than ther transect (Fig. 25C), and 5m depth (D2) had a higher concentration of EC than others depth (Fig. 25D). A two-way ANOVA showed that variations in conductivity among four seasons [F (1, 3) = 30.31, $p<0.05$] (Table-1), two stations [F (1, 1) = 5.25, $p<0.05$ (Table-2)] were significant.

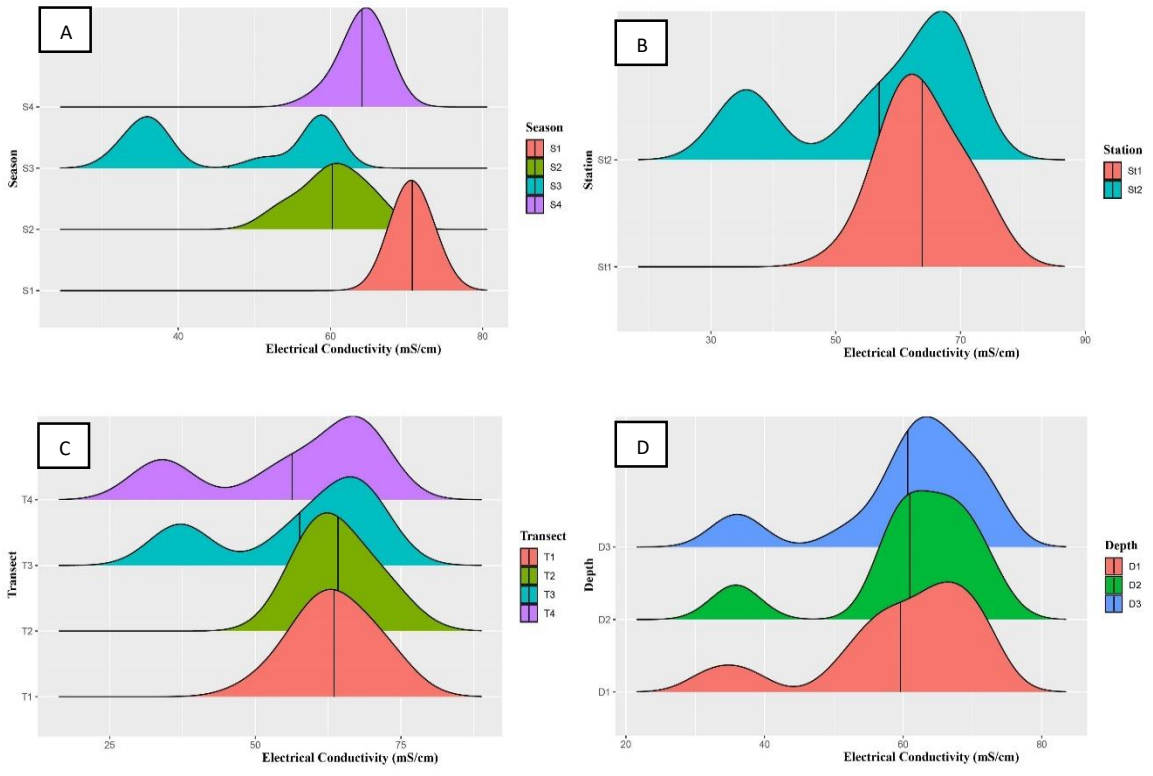

Figure 25: Electric conductivity fluctuation in northeastern BoB, A) Seasonal variation, B) Station-wise variation, C) Transect-wise variation, D) Depth-wise variation and black line indicate mean value.

Table 1: Comparison of water quality parameters in four seasons using two-way ANOVA

Season	Winter	Pre-monsoon	Monsoon	Post-monsoon	F	Sign.
Temperature (° C)	27.49 ± 1.18[b]	30.48 ± 0.70[a]	30.80 ± 1.37 [a]	25.67 ± 1.13[c]	(1,3) = 57.97	0.000
Salinity (psu)	29.29 ± 1.32[a]	24.25 ± 2.8[b]	15.17 ± 6.70[c]	28.38 ± 2.26[a]	(1,3) = 33.36	0.000
NaCl %	138.5 ± 2.87[a]	118.46 ± 8.6[b]	91.68 ± 22.59[c]	125.50 ± 4.66[b]	(1,3) = 30.44	0.000
pH	6.44 ± 0.11[b]	8.06 ± 0.23[a]	7.95 ± 0.16[a]	8.11 ± 0.29[a]	(1,3) = 175.87	0.000
DO (mg/l)	6.20 ± 0.79[a]	6.20 ± 0.91[a]	5.85 ± 0.74[a]	5.99 ± 0.74[a]	(1,3) = 0.56	0.644
TDS (g/l)	35.3 ± 0.71[a]	30.34 ± 2.30[b]	23.27 ± 5.87[c]	32.08 ± 1.08[b]	(1,3) = 30.24	0.000
EC (mS/cm)	70.75 ± 1.47[a]	60.25 ± 4.34[b]	46.57 ± 11.75[c]	64.12 ± 2.39[b]	(1,3) = 30.31	0.000
Turbidity (NTU)	10.7 ± 14.9[b]	52.3 ± 41.93[a]	40.05 ± 25.19[a]	15.11 ± 17.41[a]	(1,3) = 6.53	0.001
SiO_3-Si (µg/l)	200.2 ± 152.79[a]	16.71 ± 8.34[b]	62.68 ± 23.61[b]	11.64 ± 4.98[b]	(1,3) = 15.5	0.000
PO_4-P (µg/l)	1.31 ± 1.20[a]	0.09 ± 0.05[b]	0.37 ± 0.17[b]	0.13 ± 0.05[b]	(1,3) = 10.56	0.000
NO_2-N (µg/l)	1.08 ± 0.52[a]	0.05 ± 0.03[c]	0.49 ± 0.21[b]	0.46 ± 0.19[b]	(1,3) = 25.05	0.000
NO_3-N (mg/l)	7.96 ± 0.78[a]	6.56 ± 1.01[b]	6.22 ± 0.93[b]	6.48 ± 0.84[b]	(1,3) = 9.21	0.000
TSS (g/l)	2.60 ± 0.71[a]	1.47 ± 0.22[bc]	1.74 ± 0.71[b]	1.27 ± 0.11[c]	(1,3) = 15.36	0.000
Plankton Density (Cell/l)	52916.67 ± 13727.60[ab]	46666.67 ± 14354.8[b]	59583.33 ± 11571.58[a]	59583.33 ± 13221.60[a]	(1,3) = 2.63	0.062
Chlorophyll-a (µg/l)	0.17 ± 0.09[b]	0.23 ± 0.21[b]	0.15± 0.12[b]	0.61 ± 0.39[a]	(1,3) = 10.34	0.000
PSR (m day^{-1})	0.57 ± 0.52[a]	0.30 ± 0.16[a]	0.47 ± 0.38[a]	0.35 ± 0.09[a]	(1,3) = 1.61	0.201
TC (mg m^{-3})	3.66 ± 1.62[b]	4.92 ± 2.71[ab]	5.48 ± 1.50[a]	4.47 ± 2.09[ab]	(1,3) = 1.73	0.176
CF (mg C m^{-2} day^{-1})	2.03 ± 1.73[a]	1.65 ± 1.56[a]	2.52 ± 2.33[a]	1.56 ± 0.86[a]	(1,3) = 0.79	0.508

Table 2: Comparison of water quality parameters in two stations using two-way ANOVA

Station	Cox's Bazar	Kutubdia	F	Sign.
Temperature (° C)	28.30 ± 2.16[a]	28.92 ± 2.65[a]	(1,1) = 0.77	0.385
Salinity (psu)	27.15 ± 3.64[a]	21.40 ± 7.96[b]	(1,1) = 10.36	0.002
NaCl %	125.35 ± 11.01[a]	111.72 ± 26.18[b]	(1,1) = 5.53	0.023
pH	7.52 ± 0.71[a]	7.77 ± 0.75[a]	(1,1) = 1.40	0.242
DO (mg/l)	6.31 ± 0.72[a]	5.81 ± 0.79[b]	(1,1) = 5.17	0.028
TDS (g/l)	32.06 ± 2.81[a]	28.47 ± 6.79[b]	(1,1) = 5.71	0.021
EC (mS/cm)	63.87 ± 5.71[a]	56.98 ± 13.58[b]	(1,1) = 5.25	0.027
Turbidity (NTU)	14.07 ± 18.23[b]	45.09 ± 34.39[a]	(1,1) = 15.24	0.000
SiO_3-Si (µg/l)	38.14 ± 29.57[b]	107.53 ± 142.18[a]	(1,1) = 5.48	0.024

PO_4-P (µg/l)	0.21 ± 0.18[b]	0.74 ± 1.02[a]	(1,1) = 6.13	0.017
NO_2-N (µg/l)	0.48 ± 0.46[a]	0.56 ± 0.48[a]	(1,1) = 0.32	0.572
NO_3-N (mg/l)	6.90 ± 0.97[a]	6.70 ± 1.23[a]	(1,1) = 0.39	0.536
TSS (g/l)	1.98 ± 0.86[a]	1.56 ± 0.48[b]	(1,1) = 4.35	0.043
Plankton Density (Cell/l)	60416.67 ± 12240.05[a]	48958.33 ± 13349.74[b]	(1,1) = 9.61	0.003
Chlorophyll-a (µg/l)	0.41 ± 0.36[a]	0.18 ± 0.16[b]	(1,1) = 8.29	0.006
PSR (m day^{-1})	0.39 ± 1.20[a]	0.45 ± 0.41[a]	(1,1) = 0.42	0.520
TC (mg m^{-3})	4.34 ± 1.20[a]	4.93 ± 2.31[a]	(1,1) = 0.96	0.332
CF (mg C m^{-2} day^{-1})	1.67 ± 1.20[a]	2.21 ± 2.06 [a]	(1,1) = 1.23	0.273

Table 3: Comparison of water quality parameters in four transects using two-way ANOVA

Transect	**T1**	**T2**	**T3**	**T4**	**F**	**Sign.**
Temperature (° C)	28.3 ± 2.2[a]	28.3 ± 2.2[a]	29.1 ± 3.0[a]	28.8 ± 2.4[a]	(1,3) = 0.28	0.840
Salinity (psu)	27.3 ± 3.7[a]	27.0 ± 3.7[a]	21.2 ± 7.7[b]	21.6 ± 8.5[b]	(1,3) = 3.32	0.028
NaCl %	124.3 ± 12.2 [a]	126.4 ± 10.1[a]	113.3 ± 25.0[a]	110.2 ± 28.3[a]	(1,3) = 1.84	0.154
pH	7.5 ± 0.7[a]	7.5 ± 0.7[a]	7.8 ± 0.8[a]	7.8 ± 0.8[a]	(1,3) = 0.46	0.712
DO (mg/l)	6.3 ± 0.7[a]	6.3 ± 0.8[a]	6.0 ± 0.8[a]	5.6 ± 0.8[a]	(1,3) = 2.39	0.081
TDS (g/l)	31.8 ± 3.1[a]	32.3 ± 2.6[a]	28.8 ± 6.6[a]	28.2 ± 7.3[a]	(1,3) = 1.87	0.149
EC (mS/cm)	63.5 ± 6.3[a]	64.2 ± 5.3[a]	57.6 ± 13.2[a]	56.3 ± 14.5[a]	(1,3) = 1.72	0.177
Turbidity (NTU)	14.2 ± 16.3[b]	13.9 ± 20.7[b]	54.0 ± 33.8[a]	36.2 ± 34.0[ab]	(1,3) = 5.98	0.002
SiO_3-Si (µg/l)	37.8 ± 32.2[a]	38.5 ± 28.2[a]	102.2 ± 142.4[a]	112.8 ± 148.1[a]	(1,3) = 1.77	0.167
PO_4-P (µg/l)	0.2 ± 0.2[a]	0.2 ± 0.2[a]	0.7 ± 1.0[a]	0.7 ± 1.1[a]	(1,3) = 1.96	0.134
NO_2-N (µg/l)	0.6 ± 0.6[a]	0.4 ± 0.3[a]	0.6 ± 0.5[a]	0.5 ± 0.5[a]	(1,3) = 0.44	0.725
NO_3-N (mg/l)	6.9 ± 0.8[a]	7.0 ± 1.2[a]	6.5 ± 1.4[a]	6.9 ± 1.1[a]	(1,3) = 0.38	0.767
TSS (g/l)	2.1 ± 2.1[a]	2.1 ± 2.1[a]	2.1 ± 2.1[a]	2.1 ± 2.1[a]	(1,3) = 1.77	0.166
Plankton Density (Cell/l)	60000.0 ± 10871.1[a]	60833.3 ± 13953.4[a]	50000.0 ± 14301.9[ab]	47916.7 ± 12873.2[b]	(1,3) = 3.13	0.035
Chlorophyll-*a* (µg/l)	0.5 ± 0.4[a]	0.4 ± 0.3[ab]	0.2 ± 0.2[b]	0.2 ± 0.1[b]	(1,3) = 3.05	0.038
PSR (m day^{-1})	0.3 ± 0.2[a]	0.5 ± 0.3[a]	0.4 ± 0.4[a]	0.5 ± 0.5[a]	(1,3) = 0.56	0.642
TC (mg m^{-3})	3.8 ± 2.0[a]	4.9 ± 1.6[a]	4.8 ± 1.3[a]	5.0 ± 3.1[a]	(1,3) =0.84	0.479
CF (mg C m^{-2} day^{-1})	1.3 ± 1.2[a]	2.0± 1.2[a]	2.3 ± 2.4[a]	2.1 ± 1.7[a]	(1,3) = 0.84	0.479

Table 4: Comparison of water quality parameters in three depths using two-way ANOVA

Depth	0m	5m	10m	F	Sign.
Temperature (º C)	28.6 ± 2.4[a]	28.5 ± 2.6[a]	28.8 ± 2.3[a]	(1,2) = 0.04	0.959
Salinity (psu)	24.1 ± 7.3[a]	24.2 ± 2.6[a]	24.5 ± 6.7[a]	(1,2) =0.01	0.990
NaCl %	116.9 ± 21.6[a]	119.6 ± 2.6[a]	119.1 ± 21.5[a]	(1,2) =0.07	0.931
pH	7.7 ± 0.7[a]	7.6 ± 0.7[a]	7.6 ± 0.8[a]	(1,2) =0.04	0.965
DO (mg/l)	6.0 ± 0.7[a]	6.1 ± 0.9[a]	6.1 ± 0.8[a]	(1,2) =0.17	0.841
TDS (g/l)	29.9 ± 5.7[a]	30.6 ± 5.4[a]	30.3 ± 5.5[a]	(1,2) =0.07	0.934
EC (mS/cm)	59.6 ± 11.5[a]	61.0 ± 10.8[a]	60.7 ± 11.0[a]	(1,2) =0.07	0.935
Turbidity (NTU)	18.0 ± 27.3[a]	36.3 ± 36.5[a]	34.4 ± 28.3[a]	(1,2) =1.68	0.197
SiO_3-Si (µg/l)	75.0 ± 109.3[a]	74.7 ± 109.2[a]	68.8 ± 110.9[a]	(1,2) =0.02	0.984
PO_4-P (µg/l)	0.5 ± 0.8[a]	0.5 ± 0.8[a]	0.5 ± 0.8[a]	(1,2) =0.06	0.995
NO_2-N (µg/l)	0.5 ± 0.4[a]	0.6 ± 0.6[a]	0.4 ± 0.3[a]	(1,2) =1.02	0.370
NO_3-N (mg/l)	6.9 ± 1.3[a]	6.8 ± 0.8[a]	6.8 ± 1.2[a]	(1,2) =0.08	0.926
TSS (g/l)	1.7 ± 0.6[a]	1.9 ± 1.0[a]	1.7 ± 0.5[a]	(1,2) =0.49	0.616
Plankton Density (Cell/l)	55312.5 ± 15542.3[a]	59062.5 ± 12277.2 [a]	49687.5 ± 12970.3 [a]	(1,2) =1.91	0.160
Chlorophyll-*a* (µg/l)	0.3 ± 0.2[ab]	0.4± 0.4[a]	0.2 ± 0.2[b]	(1,2) =2.30	0.112
PSR (m day^{-1})	0.4 ± 0.3[b]	0.3 ± 0.2[b]	0.6 ± 0.4[a]	(1,2) =5.11	0.010
TC (mg m^{-3})	4.4 ± 1.7[a]	4.4 ± 2.3[a]	5.1 ± 2.2[a]	(1,2) =0.58	0.565
CF (mg C m^{-2} day^{-1})	1.9 ± 2.1[ab]	1.2 ± 1.2[b]	2.7 ± 1.4[a]	(1,2) =3.81	0.030

Table 5: Maximum and minimum value range of physico-chemical parameters

Depth	Minimum	Maximum
Temperature (º C)	23.55	33.50
Salinity (psu)	6.0	31.0
NaCl %	63.00	143.10
pH	6.28	8.37
DO (mg/l)	4.600	7.900
TDS (g/l)	16.20	36.40
EC (mS/cm)	32.20	72.90
Turbidity (NTU)	0.53	116.75
SiO3-Si (µg/l)	5.37	365.33

PO4-P (µg/l)	0.03	2.63
NO2-N (µg/l)	0.01	2.23
NO3-N (mg/l)	4.5	9.2
TSS (g/l)	0.65	4.7
Plankton Density (Cell/l)	25000	80000
Chlorophyll-a (µg/l)	0.03	1.64
PSR (m day^{-1})	0.04	1.86
TC (mg m^{-3})	0.43	10.61
CF (mg C m^{-2} day^{-1})	0.10	8.60

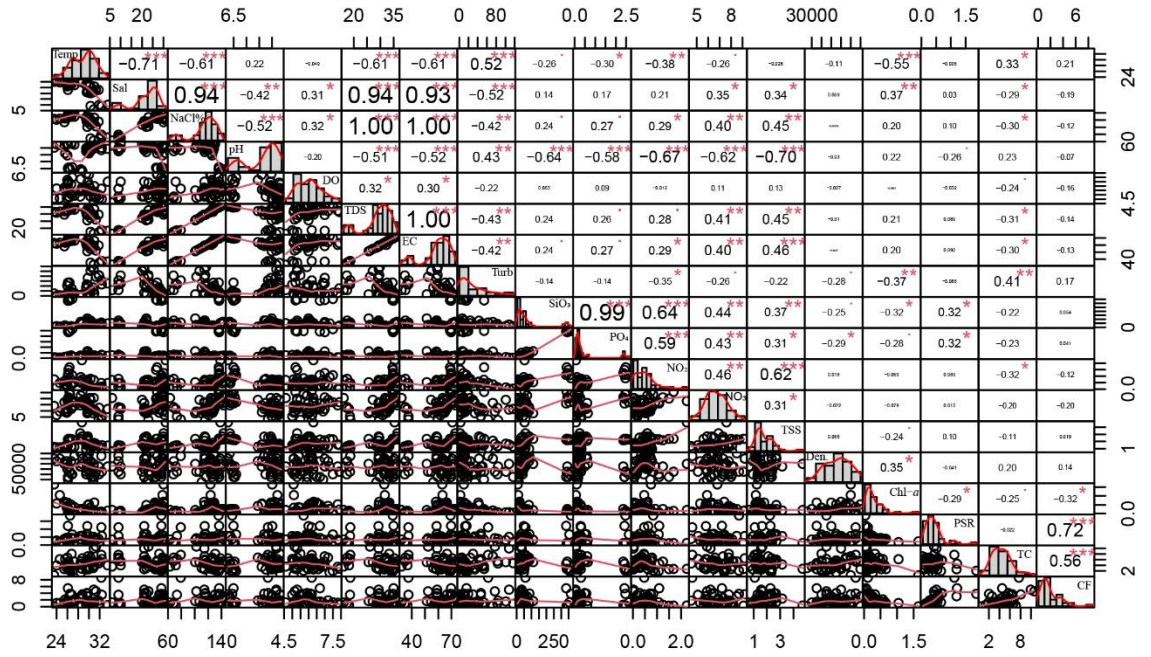

Figure 26: Correlation among physico-chemical parameters

4.4 Principal components analysis (PCA)

A principal components analysis (PCA) was run on 18 water quality parameters for the measured desired relationship between season, station, transect, and depth. The suitability of PCA was assessed before analysis. Inspection of the correlation (Fig. 26) showed that all variables had at least one correlation coefficient greater than 0.3. The overall Kaiser-Meyer-Olkin (KMO) measure was 0.686, with individual KMO measures all greater than 0.6 (Table. 05), classifications of 'mediocre' according to Kaiser (1974). Bartlett's test of sphericity was statistically significant ($p < 0.000$), indicating that the data was likely factorizable. PCA revealed six components that had eigenvalues greater than one and which explained 36.1%, 17.6%, 10.5%, 8.1%, 7.1%, and 5.6% of the total variance,

respectively (Table. 06). Visual inspection of the scree plot (Fig. 27) indicated that four components should be retained (Cattell, 1966). In addition, a four-component solution met the interpretability criterion. As such, four components were retained. The four-component solution explained 72.3% of the total variance.

Table 6: Kaiser-Meyer-Olkin Measure and Bartlett's Test of Sphericity

KMO and Bartlett's Test		
Kaiser-Meyer-Olkin Measure of Sampling Adequacy.		.668
Bartlett's Test of Sphericity	Approx. Chi-Square	1144.882
	df	153
	Sig.	0.000

Table 7: Component variation in Principal Component Analysis (PCA)

Total Variance Explained			
Component	Initial Eigenvalues		
	Total	% of Variance	Cumulative %
1	6.498	36.100	36.100
2	3.166	17.591	53.691
3	1.888	10.489	64.180
4	1.451	8.061	72.241
5	1.288	7.153	79.395
6	1.011	5.615	85.010

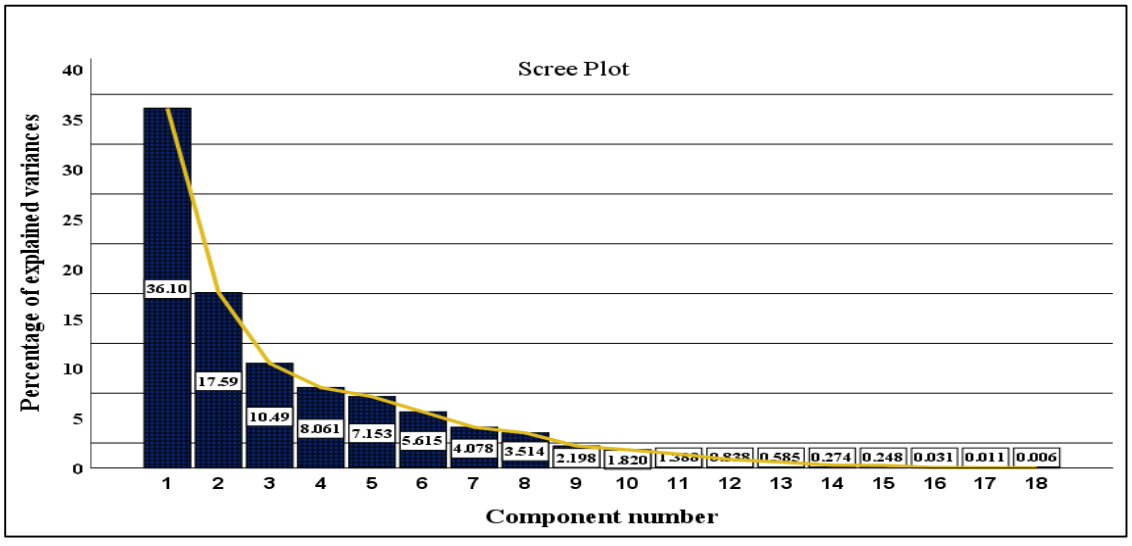

Figure 27: Scree plot of Principal Component Analysis (PCA)

4.4.1 Season-wise Principle Component Analysis of Physico-chemical parameters

Principle componant-1 (PC-1) and principle component-2 (PC-2) combined accounted for 53.7% of the total variance, where NaCl, TDS, and EC showed a highly positive correlation and formed a cluster during the winter season. Plankton density and chlorophyll-*a* showed a correlation in the post-monsoon season. Pre-monsoon season overlapped with the winter and monsoon season. Plankton density was also correlated with pre-monsoon season. Total carbon, turbidity, and water temperature correlated with the monsoon season, and the temperature had a higher value than the other two. Carbon flux, phytoplankton sinking rate, silicate-silicon, phosphate-phosphorus, nitrite-nitrogen, total suspended solids, pH, DO, salinity, and nitrate-nitrogen are not correlated with any season, but they are related to each other.

Plankton density, pH, total carbon, turbidity, temperature, and carbon flux was positively correlated with PC-1. On the other hand, Chlorophyll-*a*, Salinity, DO, NaCl %, EC, TDS, NO_3-N, TSS, NO_2-N, PO_4-P, SiO_3-Si, and PSR are negatively correlated with PC-1. Water Salinity, DO, NaCl %, EC, TDS, Chlorophyll-*a*, and pH are negatively correlated with PC-2 and NO_3-N, TSS, NO_2-N, PO_4-P, SiO_3-Si, PSR, CF, total carbon, turbidity, temperature are positively correlated with PC-2 (Fig. 28a). Principle componant-3 (PC-3) and Principle componant-4 (PC-4) combined accounted for 18.6% of the total variance.

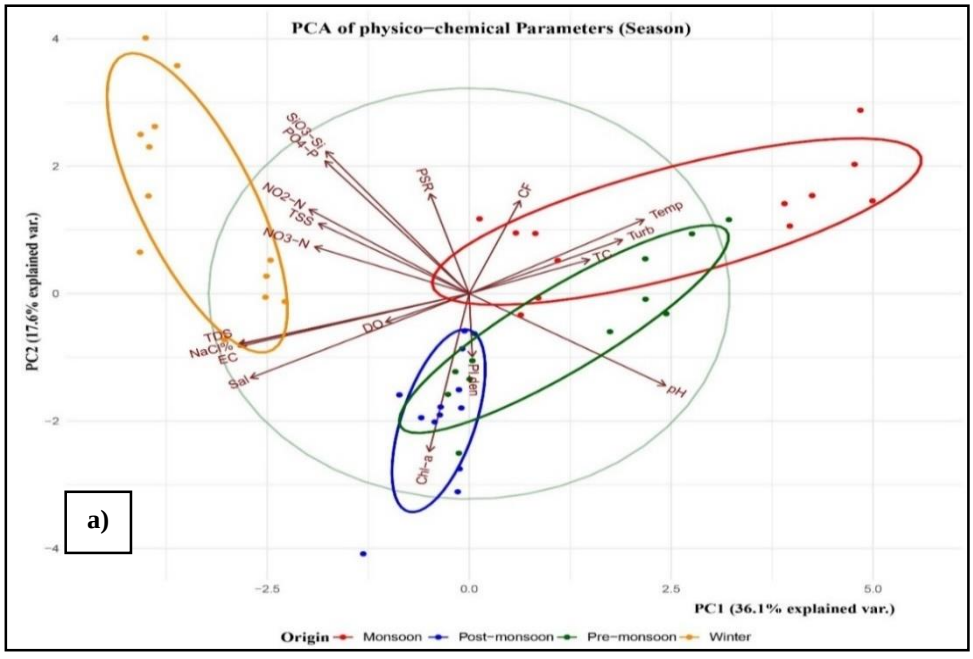

PC-3 and PC-4 explain a small percentage of the total variation. All the parameters have small variations; among them, carbon flux has a higher value, and TSS has a lower value. The winter, monsoon, and post-monsoon showed higher similarities, and the pre-monsoon season showed slight variation (Fig. 28b).

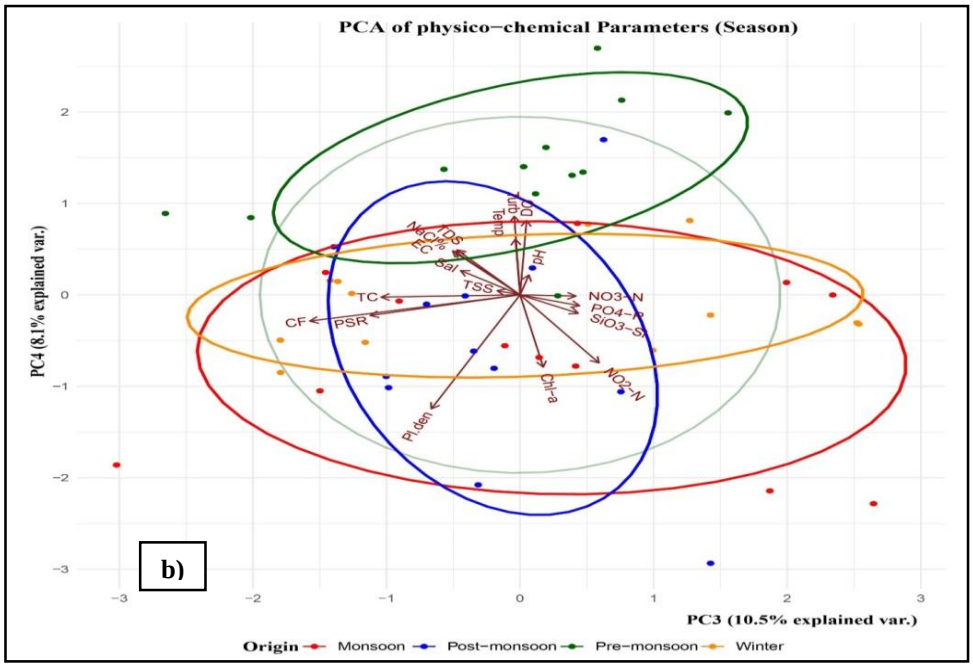

Figure 28: PCA biplot describing the season-wise correlation

a) PC1 and PC2, **b)** PC3 and PC4

4.4.2 Station-wise principle component analysis (PCA) of Physico-chemical parameters

Principle componant-1 (PC-1) contained 36.1% variance and principle component-2 (PC-2) contained 17.6% variance. Most of the parameters are correlated with station-2 (Kutubdia). In station-1, NaCl%, TDS, and EC made a cluster and showed a high correlation. Water salinity and chlorophyll-*a* also correlated with station-1 (Cox's Bazar). Plankton density, DO, NO_3-N, and TSS were correlated to both station-1 and station-2. The rest of the parameters are correlated with station-2. Plankton density, pH, total carbon, turbidity, temperature, and carbon flux positively correlate with PC-1, and pH has a higher value. Phytoplankton sinking rate, SiO_3-Si, PO_4-P, NO_3-N, TSS, NO_3-N, NaCl%, TDS, EC, salinity, DO, and chlorophyll-*a* are negatively correlated with PC-1. For PC-2, total

carbon, turbidity, temperature, carbon flux, phytoplankton sinking rate, SiO_3-Si, PO_4-P, NO_3-N, TSS, and NO_3-N are positively correlated with PC-2. On the other hand, NaCl%, TDS, EC, salinity, DO, chlorophyll, plankton density, and pH are negatively correlated with PC-2 (Fig. 29a). Principle componant-3 (PC-3) and Principle componant-4 (PC-4) combined accounted for 18.6% of the total variance. Most of the parameters have a close correlation and a small amount of variation. Carbon flux and plankton density had a higher variation than other parameters (Fig. 29b).

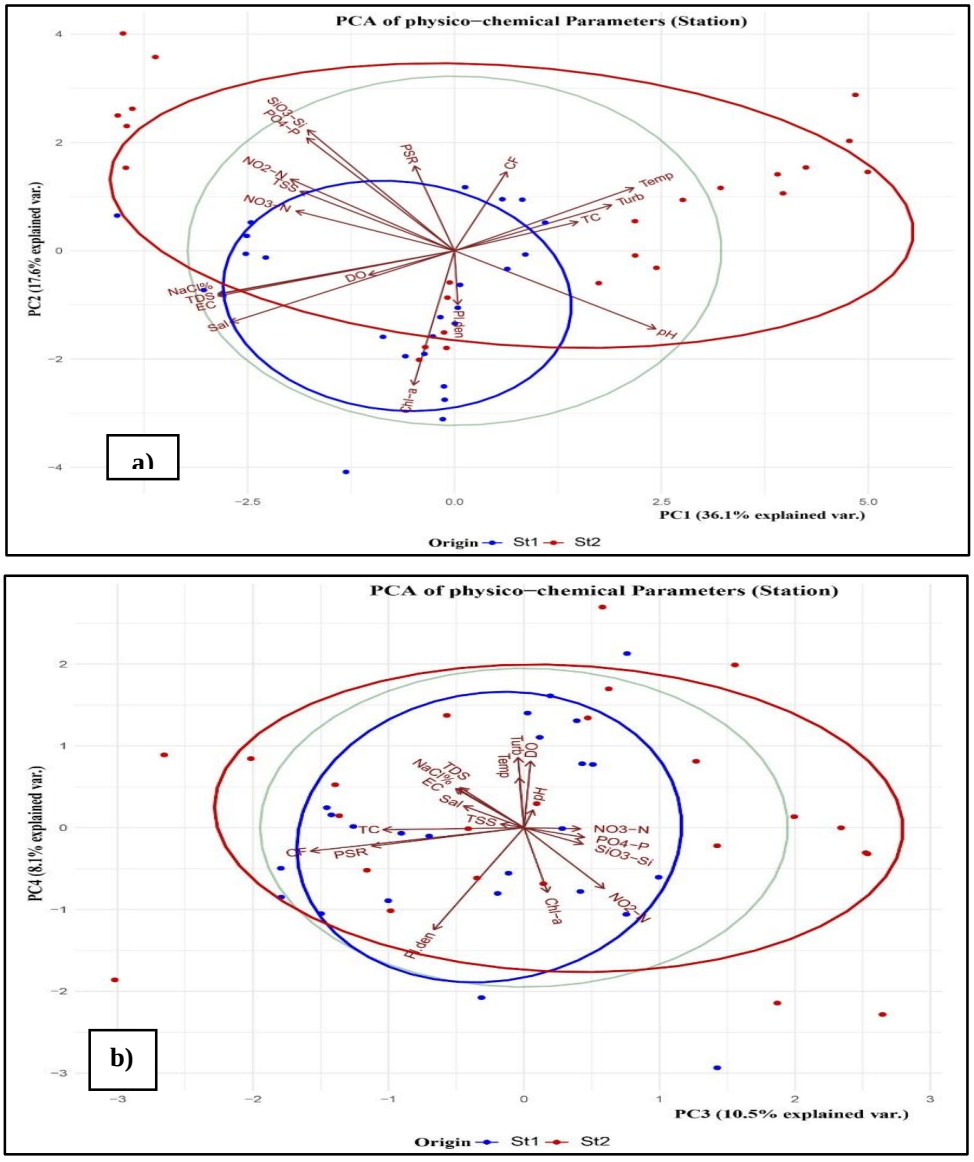

Figure 29: PCA biplot describing the station-wise correlation

a) PC1 and PC2, **b)** PC3 and PC4

4.4.3 Transect-wise principle component analysis (PCA) of Physico-chemical parameters

Principle componant-1 (PC-1) and principle component-2 (PC-2) for transect combined accounted for 53.7% of the total variance. Transect-1, Transect-2, and Transect-3 Transect-4 showed higher similarities among them. TDS, NaCl%, EC, and Salinity make a cluster and are highly correlated with transect-1 and transect-3. Chlorophyll-*a*, plankton density, DO, NO_3-N, and TSS are correlated with transect-2. All the other parameters are correlated with transect-3 and transect-4. Plankton density, pH, total carbon, turbidity, temperature, and carbon flux are positively correlated with PC-1, and others are negatively correlated. Total carbon, turbidity, temperature, carbon flux, PSR, NO_2-N, PO_4-P, SO3-Si, TSS, and NO_3-N are positively correlated, and other parameters are negatively correlated with PC-2 (Fig. 30a).

Principle componant-3 (PC-3) and Principle componant-4 (PC-4) contain a small amount of variation. PC-3 contained 10.5% of the variance and PC-4 contained 8.1% of the variance. All the parameters showed small variation. Carbon flux and plankton density have higher values and showed higher variance than other parameters. Carbon flux, PSR, and Total carbon made a cluster and showed a highly correlated relationship (Fig. 30b).

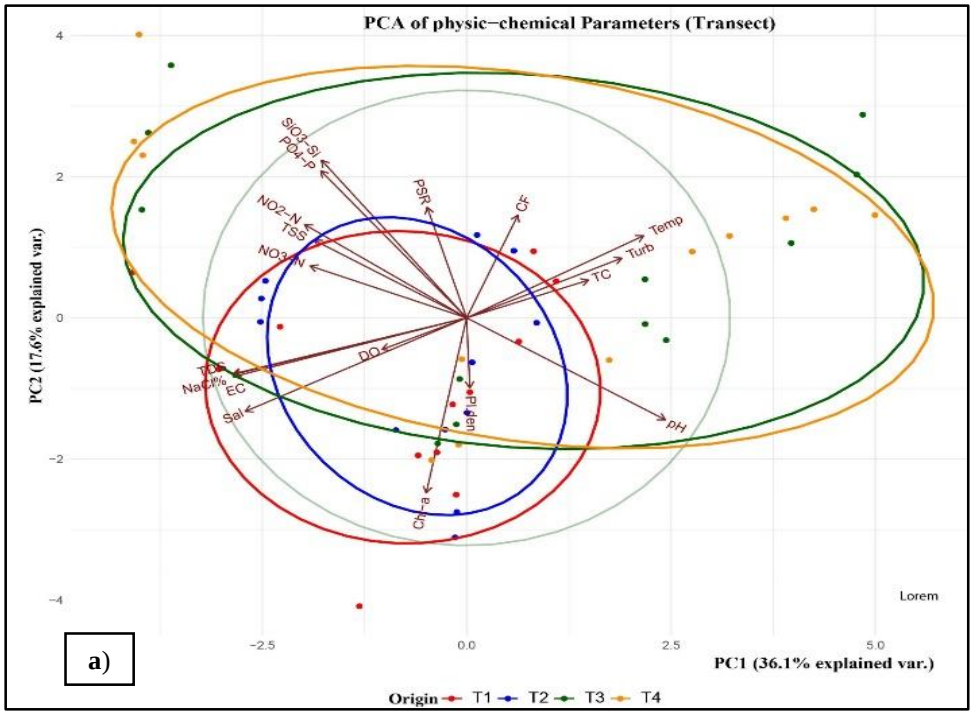

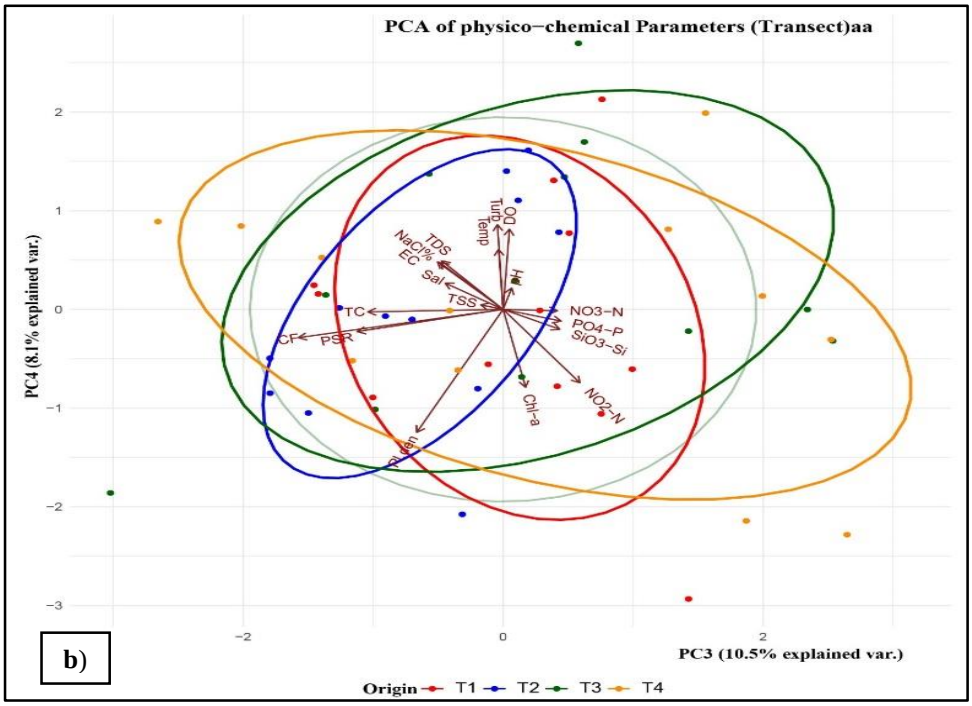

Figure 30: PCA biplot describing the transect-wise correlation

a) PC1 and PC2, **b)** PC3 and PC4

4.4.4 Depth-wise principle component analysis (PCA) of Physico-chemical parameters

Principle componant-1 (PC-1) and principle component-2 (PC-2) combined accounted for 53.7% of the total variance, where temperature, turbidity, plankton density, and total carbon were correlated with 5m depth. There was10m depth overlapped with 5m depth and correlated with plankton density and chlorophyll-*a*. Depth 0m partially overlapped with 5m and 10m depth and correlated with dissolved oxygen, NO_3-N, total suspended solids, and NO_2-N. Other physical parameters were distinct and not correlated with depth but were correlated among them. Carbon flux, temperature, turbidity, total carbon, pH, and plankton density were positively correlated with PC-1, and other components were negatively correlated with PC-1. NO_3-N, TSS, NO_2-N, PO_4-P, SO3-Si, PSR, temperature, turbidity, and total carbon were positively correlated with PC-2, and other components are negatively correlated (Fig. 31a). Principle componant-3 (PC-3) contained 10.5% of the variance, and principle componant-4 (PC-4) contained 8.1% of the variance. They accounted small

percentage (18.6%) of variation. Total carbon, PSR, and Carbon flux had a higher correlation and make a cluster. Total carbon, phytoplankton sinking rate, and carbon flux was closely correlate. Carbon flux and plankton density had a higher value than other parameters (Fig. 31b).

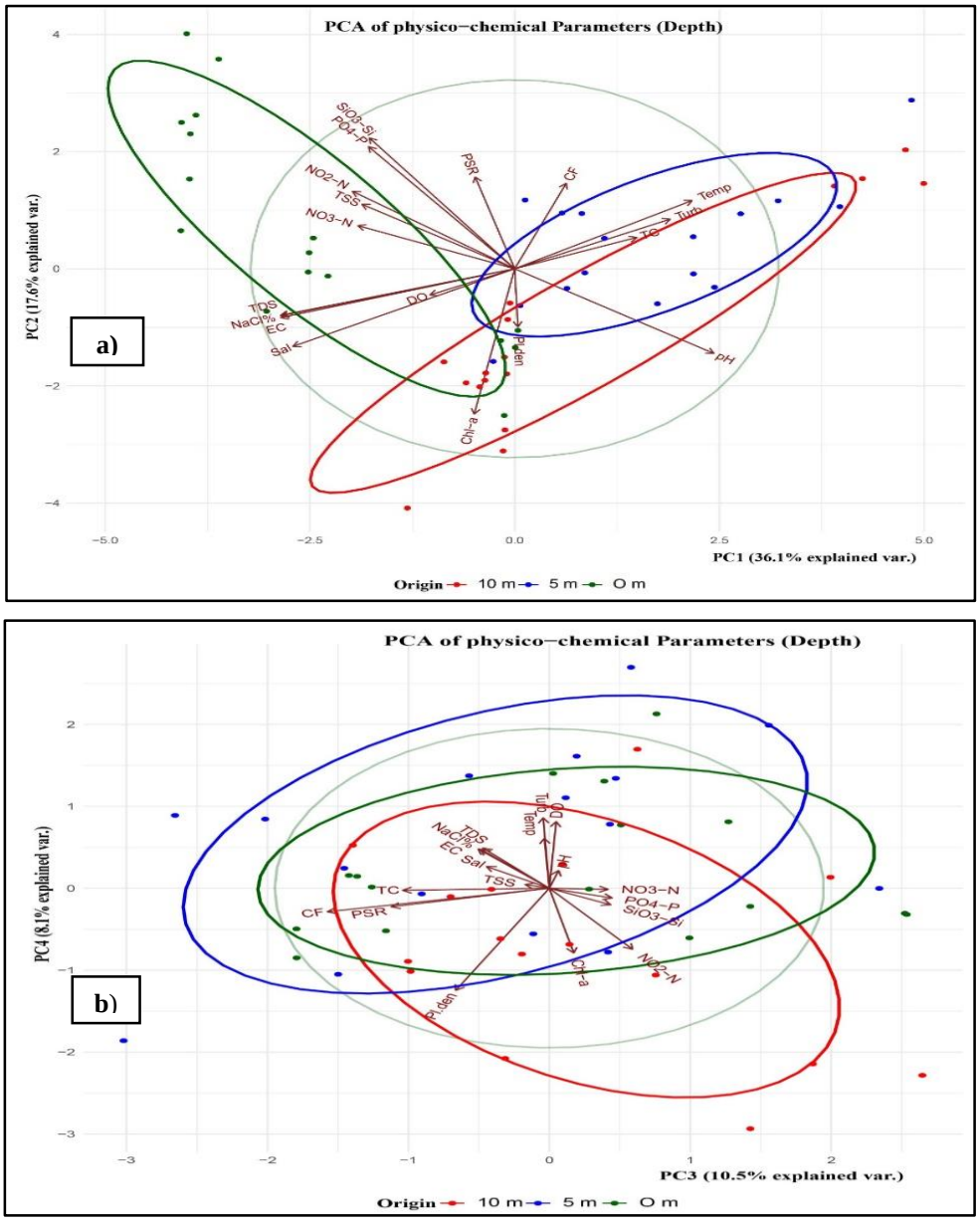

Figure 31: PCA biplot describing the depth-wise correlation

a) PC1 and PC2, **b)** PC3 and PC4

CHAPTER FIVE

DISCUSSION

5.1 Ocean and coastal productivity

Chlorophyll-*a* is the pigment found in all phytoplankton species. It is a good indicator of the tropic status (Anzecc, 2000). In this research, Chlorophyll-*a* concentration was mainly used for determining the phytoplankton sinking rate. Chlorophyll-*a* concentration significantly varies between the season and station during this study. Chlorophyll-*a* concentration correlated with salinity, pH, TDS, EC, and Plankton density. The higher concentration of Chlorophyll-*a* was observed in the post-monsoon season and lowered in the monsoon season. Cox's Bazar station was more concentrated than Kutubdia station. A study by Baliarsingh et al (2015) determine Chlorophyll-*a* concentration range between 0.12- 10.055 mg/m^{-3} in the northwestern Bay of Bengal. This finding is similar to the present research. A study by Dey and Singh (2003) found that maximum Chlorophyll-*a* concentration was in the northeast monsoon season and lower in pre and post-monsoon. These data are not comparable to ours because of the data collection method. According to Dey and Singh (2003) phytoplankton sample was collected by horizontally towing and in present study phytoplankton sample was collected by filtration method. First, collect the water vertically then it was filtrated with a phytoplankton net (45-micron mesh).

Phytoplankton sinking rate was determined by SETCOL method during the study time. SETCOL is a homogenous method that is suitable for all types of the phytoplankton community. The phytoplankton sinking rate was significantly different among depths. The average lowest PSR was found in the monsoon season, and the highest level was observed in the pre-monsoon season. According to Wang et al. (2022) the phytoplankton sinking rate range was −0.291 to 2.188 md^{-1}, with an average of 0.420 ± 0.646 md−1 in the Eastern Indian Ocean. And it was changed with nutrients and plankton density. The sinking rate was increased in higher depth and lower in surface area. Pearson correlation showed that sinking rate correlated with nutrients and negatively correlated with the temperature and Chlorophyll-*a*. The present study agreed with this statement. It was found that nutrient contents were highly correlated with PSR throughout the study, and the sinking rate

increased with depth. The higher PSR was found in 10m depth during the study. Phytoplankton sinking rate was measured in Changjiang estuary, and data showed that the summer season was a higher singing rate than spring (Guo et al., 2016). In this research sinking rate also changed with the season.

Phytoplankton is the key component of carbon flux. Phytoplankton is the main primary producer and takes up carbon into the deep ocean. Phytoplankton density significantly differed with station throughout the study and was correlated with salinity, TSS, NO_2-N, and EC. Peak average density was observed in Cox's Bazar, and a lower amount was found in Kutubdia station. Findings indicate that Cox's Bazar was more productive than Kutubdia station because of Cox's Bazar station had a higher nutrient availability than Kutubdia station. Among seasons, higher plankton is found in the monsoon season because in monsoon season, large amounts of land and river water mix with the ocean that boosting phytoplankton production. The peak phytoplankton production was observed in post-monsoon (578.0×10^5 cells/L) and the lowest in monsoon (37.5×10^5 cells/L) in the maheshkhali of Bay of Bengal (Jewel et al., 2002). In this research, the phytoplankton sample was collected by horizontal towing, and in our study research, data were collected by the vertical method.

Total carbon content is dependent on phytoplankton density. Phytoplankton cells consist of organic carbon, which is exchanged with the carbon system. This carbon sinks into the deep ocean through the biological pump. Carbon content was not statistically different with seasons, stations, transects, and depths. Carbon content correlated with plankton density, water temperature, turbidity, and pH. During the study period, the highest carbon was in the monsoon season and lowered in the winter season, and Kutubdia station contributed higher carbon than Cox's Bazar station. Carbon contents are lower in the Bay of Bengal because of the inability of the low-speed winds to break the stratification throughout the year (Gauns et al., 2005).

Carbon flux is the primary concern of this study. Carbon flux was significantly varied with depth change. During the study, Carbon flux ranged from 0.10 to 8.60 mg C m^{-2} day^{-1}. The maximum average carbon flux was observed in the monsoon season, and the minimum was found in the post-monsoon season. Kutubdia station is the major contributor, and Cox's

Bazar station is a minor contributor to carbon flux. At 10m depth, the higher amount of carbon flux was found, and it changed with depth level. Carbon flux correlated with temperature, turbidity, SiO_3-Si, PO_4-P, Total suspended solids, plankton density, Phytoplankton sinking rate, and total carbon content. Temperature, plankton density, Phytoplankton sinking rate, and total carbon content correlate with carbon flux. Carbon flux was higher in the Kutubdia because this station also had a higher phytoplankton sinking rate and total carbon. A study was conducted in Changjiang estuary by (Guo et al., 2016). Studies showed that carbon flux was higher in the summer season than in spring and the carbon flux range was 11.90 mg C m^{-2} day−1 to 129.69 mg C m^{-2} day^{-1} (average = 63.13 ± 48.16 mg C m^{-2} day^{-1}) in summer and 9.29 mg C m^{-2} day^{-1} to 82.44 mg C m^{-2} day^{-1} (average = 26.10 ± 26.25 mg C m^{-2} day^{-1}) in the spring season. Temperature and nutrient content regulated the carbon flux (Guo et al., 2016). This research data range was higher and is not similar to the present study because this research was conducted in when phytoplankton bloom occurred sampling site. In the present study, there was no phytoplankton bloom found, but present studies showed that flux correlated with temperature and nutrient content. Another study (Honda et al., 2017) showed that the annual mean of carbon flux of two stations in the western Pacific varied from 27.3 to 46.7 mg-C m^{-2} day^{-1}. This data was higher than in the present study. In the western Pacific, the variation is caused by the production of Sub-Tropical Mode Water (STMW) and the transport of large amounts of surface water CO_2 to the ocean interior. At the same time, the western Pacific had higher phytoplankton density and nutrients than the present study. As a result, carbon flux is concentrated higher in the western Pacific than in the Northeastern Bay of Bengal.

5.2 Nutrient components

For aquatic organisms, nitrate nitrogen is a crucial nutritional component. During this study, the season-average concentration varied between 6.22 µg/l to 7.96 µg/l. NO_3-N significantly differs with the season change. The highest concentration of NO_3-N was found in the winter season and lowered in the monsoon season. On the western coast of the Bay of Bengal, NO_3-N concentration was found (6.4–7.1 µg/l) (Carmichael et al., 2003). That's a concentration similar to our study finding. Cox's Bazar station had a higher concentration

than Kutubdia. It should be highlighted that transportation, livestock, biomass burning, and agricultural practices (Sharma et al., 2010a, b) may all contribute to releasing significant volumes of NH_3 (Sutton et al., 1995; Sutton et al., 2000).

The concentration of Nitrite-Nitrogen ranged from 0.01 µg/l to 2.23 µg/l throughout the study period. NO_2-N concentration significantly varied with season. The peak means concentration was observed in the winter season and the lowest in the pre-monsoon season. The average concentration observed on the southeastern coast of the Bay of Bengal was 0.126 to1.198 µg/l (Noori 1999). But this research had a higher concentration of nitrite. Various factors affect the NO_2-N concentration, such as river runoff, organic wastage, industrial wastage, etc.

The average concentration of Phosphate-phosphorus significantly differs with the season. The peak average PO_4-P concentration was found in the winter season and lowered in the pre-monsoon season. Kutubdia station had higher PO_4-P than Cox's Bazar. Noori (1999) found that the average value of PO_4-P on the southeastern coast of the Bay of Bengal was (0.410 to 2.330 µg/l). The value of PO_4-P is similar to our study's findings. The concentration of PO_4-P is changed by river runoff, organic waste, and industrial waste.

Siliceous organisms produce biogenic silica in seawater. Maximum average Silicate was observed in the winter season and minimum in the post-monsoon season. During the study, Silicate concentration significantly varies with season and station. The Kutubdia station contributes more Silicate than Cox's Bazar station. The Silicate was at a lower value in the post-monsoon season due to Silicates being taken up by phytoplankton for their biological function (Prasanna et al., 2007). The higher concentration in winter is because silicate leached out from rocks and exchanged the water within the coastal system (Mukhopadhyay al., 2006).

5.3 Water physicochemical parameters

Water temperature is one of the most critical physiological factors that affect all life activity in the water system. Water temperature variation is one of the factors in the estuaries system which may influence the physicochemical characteristics (Soundarapandian et al., 2009). During this study, water temperature ranged from 23.6 to 33.5^{o}C. The range of observed

water temperature was similar to the finding of Zafar (1992). The temperature significantly varies with the season fluctuation. The observed temperature was higher in the monsoon season and lowered during the post-monsoon season. According to Holmgren (1994), water temperature values were significant to the season, and temperature changes with the influence of the southeastern and southwestern wind pattern prevailing on the Bay of Bengal coast.

Water salinity is one of the important factors that influence the abundance and distribution of organisms in the estuarine environment and inshore water. A wide range of water salinity (6 to 31 psu) was found during the study period. The highest water salinity was in the winter season, and it decreased in the monsoon season. This salinity significantly varies with the season and stations. The higher salinity during the winter season results from the higher evaporation rate and temperature (Balasubramanian and Kannan, 2005). Lower salinity in the monsoon season is the cause of higher rainfall and land runoff (Balasubramanian and Kannan, 2005). In the Kutubdia station, water salinity was found lower because of surrounding land runoff and higher rainfall. During the sampling time, Cox's Bazar station represented higher water salinity because of high temperature evaporated the water and increased the salt concentration (Saxby, 2002).

The water NaCl% was observed higher in the winter season and lower in the monsoon season. Water NaCl% significantly differs with the season change and station change. The result of higher NaCl% is the result of high water evaporation and less rain. On the other hand, a lower level of NaCl% is the result of higher rainfall and neritic water inclusion. Kutubdia station has less NaCl% because of land runoff and higher rainfall, and Cox's Bazar station has higher NaCl% result of higher heat and evaporation. The most rainfall is found in the monsoon season in the southeastern part, with the next maximum in the northeastern part and the lowest rainfall found in the winter season (December-January) (Ahasan et al., 2010). Cox's Bazar station was a higher salinity concentration than the Kutubdia station.

Organic effluents from land are known to be the main factor in reducing the pH level in marine environments (Tavakoly Sany et al., 2004). The suitable water pH range for supporting aquatic life is pH 6.5-8.2 (Murdoch et al., 2001). During the study period, water

pH values ranged from 6.3 to 8.4. Water pH value significantly correlated with the season. Water pH was highest in the post-monsoon season and decreased in the winter season. The higher pH found in the post-monsoon season causes of inclusion of freshwater influx, seawater dilution, low temperature, and organic decomposition.

Dissolved Oxygen concentration varied significantly with the station. Cox's Bazar station had a higher concentration of DO than Kutubdia. DO concentration also changes with the season. During this study, a higher amount of DO concentration was seen in winter season and pre-monsoon season. The water DO concentration changed because of the combined effect of higher wind speed joined with heavy rainfall and the result of freshwater mixing (Das et al., 1997).

Total dissolved solids (TDS) contain all of the distanced electrolytes that contribute to salinity values along with other substances such as dissolved organic material. The land activity increases the total dissolved solids concentration in the saltwater (Islam et al., 2018). The average water TDS concentration was maximum during the winter season and lowest in the monsoon season. Cox's Bazar station had maximum TDS than Kutubdia. The TDS concentration differs with season and station. TDS concentration is affected by variations in pH. Some solutes will precipitate due to pH changes, and the solubility of the suspended materials will also be impacted. The lower value of TDS concluded that the land runoff is the only contributor to its dilution in the monsoon season (Izonfuo and Bariweni, 2001)

Total suspended solids are the materials that affect the water transparency or light scattering of the water. As well as TDS, TSS is also influenced by pH. TSS typically consists the fine particles, plankton, or organic compounds. During the study period, the maximum TSS was found in the winter season and the minimum in the post-monsoon season. The TSS contents also significantly varied with the station. TSS concentration changed with the land runoff, rainfall, presence of organics particles, inorganics particles, and other microorganisms (Prabu et al., 1983).

Water turbidity has defined the loss of water clarity. Water turbidity is lost by dissolved particles, suspended particles, and organic inorganics particles. Turbidity is an essential

parameter that regulates the fish and other organisms movements (Amesbury, 1981; Fabricius et al., 2005; Mallela et al., 2007). During the study period, water turbidity ranged from 0.53 to 116.75 NTU. The highest turbid water was found in the pre-monsoon season and the lowest in the winter season. Water turbidity significantly varied with seasons and stations. Kutubdia station was more turbid than Cox's Bazar station. Turbidity is higher in the pre-monsoon season because of rainfall and surface runoff; however, the winter season has small rainfall and surface runoff (Khan and Rajshekhar, 2020).

The capacity of water to carry an electrical current is called electric conductivity. It is mainly dependent on water's dissolved solids. Also, depending on the number of ions present in water. During the study period, electric conductivity significantly varied with the season and station. Water EC was maximum during the winter season and lowest in the monsoon season. At the same time, EC was in Cox's Bazar station and lowered in Kutubdia station. The current study supports prior findings published by (Surana R. et al., 2013). High conductivity during winter might be linked to the low mixing of freshwater input from rivers. The low value during the monsoon season was related to rain and the combining of more water from rivers and land (Islam et al., 2018).

5.4 Principal Component Analysis (PCA) discussion among season, station, transect, and depth

Principal Component Analysis revealed that the first four principle components accounted for 72.3% of the variance. PCA analysis measured the correlation among season, station, transects, and depths. Season-wise PCA showed that in the winter season, TDS, NaCl%, and EC made a cluster and presented a highly positive correlation. Nutrient content remains closely but not correlated with any of the seasons. Temperature, turbidity, and carbon content correlated with the post-monsoon season. Phytoplankton sinking rate and carbon flux are not correlated with any season but are correlated with each other. Station-wise biplot showed that the stations had a similar correlation. Most of the parameters are correlated with the Kutubdia station. TDS, NaCl%, EC, salinity, and chlorophyll-*a* are correlated with Cox's Bazar station. Phytoplankton sinking rate and carbon flux correlated with the Kutubdia station. In transect, most of the parameters are correlated with Kutubdia transects. Only salinity and chlorophyll-*a* correlated with Cox's Bazar transect.

Phytoplankton sinking rate, carbon content, and carbon flux were correlated with transect-3 of Kutubdia. In depths, PCA showed that 10m depth overlapped with the other two depths. NO_2-N, NO_3-N, DO, and TSS correlated with the 0m depth. Temperature, turbidity, and total carbon correlated with 5m depth. Phytoplankton sinking rate and carbon flux were positively correlated with 10m depth.

CHAPTER SIX
CONCLUSION

Phytoplankton have a profound influence on the oceanic carbon cycle. Carbon dioxide that absorbed by phytoplankton and then taken to the deep ocean from the surface by biological pump. This storage of carbon be secured in the deep ocean for thousands of years. In addition, increases in ocean carbon dioxide also affect the fisheries community. Increasing atmospheric CO_2 will likely result in a proportional rise in ocean water acidity by decreasing pH units. An increase in acidification mostly affects the shellfish resource. It also decreases the shell formation ability of different invertebrate communities.

From this study, it is found that a significant amount of carbon sink in northeastern Bay of Bengal. The highest amount of carbon flux was observed in the monsoon season, which changed with depth variation. Carbon flux is significantly influenced by plankton density and the amount of carbon contents, and these both are found higher in the monsoon period. The correlation matrix showed that carbon flux also correlated with various factors such as turbidity, total suspended solids, phytoplankton sinking rate, etc. From the findings of this study, it is also said that Kutubdia station contributes more carbon flux than Cox's Bazar station. For carbon flux estimation, this research is the pioneering research in the county. This study's methods and data are helpful for further study in another coastal system for estimating carbon flux. Finally, these studies will give information about carbon sequestration in coastal system and will be beneficial for the management of our fisheries stock and mitigate the climate change effect.

CHAPTER SEVEN

RECOMMENDATION AND FUTURE PERSPECTIVES

This research work help to know how much carbon is exchanged between our northeastern coastal systems. As this research is still the pioneer research work in our northeastern coastal systems, it can be done in other parts of our coastal systems that would benefit our country. This work is mainly ocean-based and challenging; a well-decorated vessel with a laboratory facility should be more beneficial for getting accurate data and ensuring safety. Updated methods could be adjusted to expand this research. Hopefully, this research can be used as a source of secondary data that will help future researchers and also help the national and international levels make laws for environmental issues regarding ocean carbon.

REFERENCES

Ahasan MN, Chowdhary MA, Quadir DA. 2010. Variability and trends of summer monsoon rainfall over Bangladesh. Journal of Hydrology and Meteorology, 7(1): 1-17.

Ahmad H. 2019a. A field assessment on Karnafully estuarine ecology. International Journal of Fisheries and Aquatic Studies, 7(1): 35-38.

Ahmad H. 2019b. Bangladesh coastal zone management status and future trends. Journal of Coastal Zone Management, 22(1): 1-7.

Al MA, Akhtar A, Hassan ML, Rahman MF, Warren A. 2019. An approach to analyzing environmental drivers of phytoplankton community patterns in coastal waters in the northern Bay of Bengal, Bangladesh. Regional Studies in Marine Science, 29, 100642.

Alam MK. 2014. Ocean/blue economy for Bangladesh. In Proceedings of international workshop on blue economy. Dhaka: Ministry of Foreign Affairs. pp. 28–49.

Ali A. 1999. Climate change impacts and adaptation assessment in Bangladesh. Climate research, 12(2-3): 109-116.

Amesbury SS. 1981. Effects of turbidity on shallow-water reef fish assemblages in Truk, Eastern Caroline Islands. Proc 4th Int Coral Reef Symp, Manila 1: 155−159.

Anzecc A. 2000. Australian and New Zealand guideline for fresh and marine water quality. Australian and New Zealand Environment and Conservation Council and Agriculture and Resource Management Council of Australia and New Zealand. Canberra, Australia.

Apha A. 1995. WPCF, Standard methods for the examination of water and wastewater. American Public Health Association/American Water Works Association/Water Environment Federation, Washington DC, USA.

Aricò S, Wanninkhof R, Sabine C. 2021. Integrated ocean carbon research: A summary of ocean carbon research, and vision of coordinated ocean carbon research and observations for the next decade. Paris: UNESCO-IOC.

Balasubramanian R, Kannan L. 2005. Physicochemical characteristics of the coral reef environment of the Gulf of Mannar Biosphere Reserve, India, Int. j. Ecol. Environ. Sci., vol. 31, pp. 265-27.

Baliarsingh SK, Lotliker AA, Sahu KC, Sinivasa Kumar T. 2015. Spatio-temporal distribution of chlorophyll-*a* in relation to physico-chemical parameters in coastal waters of the northwestern Bay of Bengal. Environmental monitoring and assessment, 187(7): 1-14.

Basu S, Mackey KR. 2018. Phytoplankton as key mediators of the biological carbon pump: Their responses to a changing climate. Sustainability, 10(3): 869.

Bauer JE, Cai WJ, Raymond PA, Bianchi TS, Hopkinson CS, Regnier PA. 2013. The changing carbon cycle of the coastal ocean. Nature, 504(7478), 61-70.

Baumert HZ, Petzoldt T. 2008. The role of temperature, cellular quota, and nutrient concentrations for photosynthesis, growth, and light-dark acclimation in phytoplankton. Limnologica. 38: 313–326.

Bendschneider K, Robinson RJ. 1952. A new spectrophotometric method for the determination of nitrite in sea water.

Bienfang P, Laws E, Johnson W. 1977. Phytoplankton sinking rate determination: technical and theoretical aspects, an improved methodology. Journal of Experimental Marine Biology and Ecology, 30(3): 283-300.

Bienfang PK. 1981. SETCOL—a technologically simple and reliable method for measuring phytoplankton sinking rates. Canadian Journal of Fisheries and Aquatic Sciences, 38(10), 1289-1294.

Bishop JKB.2009. Autonomous observations of the ocean biological carbon pump. Oceanography, 22, 182–193. blooms. Aquat. Microb. Ecol. 27, 57–102.

Boyd PW, Newton PP. 1999. Does planktonic community structure determine downward particulate organic carbon flux in different oceanic provinces? Deep-Sea Res. I46: 63–91.

Boyd PW, Stevens CL. 2002. Modeling particle transformations and the downward organic carbon flux in the NE Atlantic Ocean. Prog. Oceanogr. 52, 129. DOI: 10. 1016/ S0079-6611 (02) 00020-4.

Boyd PW, Trull TW. 2007. Understanding the export of biogenic particles in oceanic waters: Is there consensus?. Progress in Oceanography, 72(4): 276-312.

Boyd PW. 2015. Toward quantifying the response of the oceans' biological pump to climate change. Front. Mar. Sci. 2.

Cai WJ. 2011. Estuarine and coastal ocean carbon paradox: CO_2 sinks or sites of terrestrial Carbon incineration? Ann. Rev. Mar. Sci. 3: 123–145.

Carlson CA, Ducklow HW, Michaels AF. 1994. Annual flux of dissolved organic-carbon from the euphotic zone in the northwestern Sargasso Sea. Nature, 371, 405–408.

Carmichael GR, Ferm M, Thongboonchoo N, Woo JH, Chan LY, Murano K, Viet PH, Mossberg C, Bala R, Boonjawat J, Upatum P, Mohan M, Adhikary SP, Shrestha AB, Pinaar J J, Brunke EB, Chen T, Jie T, Guoan D, Peng LC, Dhiharto S, Harjanto H, Jose AM, Kimani W, Kirouane A, Lacaus JP, Richard S, Barturen O, Cerda JC, Athayde A, Tavares T, Cotrina JS, Bilici E. 2003. Measurements of sulfur dioxide, ozone and ammonia concentration in Asia, Africa and South America using passive samplers, Atmos. Environ., 37: 1293–1308.

Cattell RB. 1966. The scree test for the number of factors. Multivariate Behavioral Research, 1, 245-276

Chisholm SW. 1995. The iron hypothesis: Basic research meets environmental policy. Rev. Geophys. 33: 1277–1286.

Cooley SR, Kite-Powell HL, Doney SC. 2009. Ocean acidification's potential to alter globalmarine ecosystem services. Oceanography. 22:172–81

Das J, Das SN, Sahoo RK. 1997. Semidiurnal variation of some physico-chemical parameters in the Mahanadi estuary, east coast of India.

Dey S, Singh RP. 2003. Comparison of chlorophyll distributions in the northeastern Arabian Sea and southern Bay of Bengal using IRS-P4 Ocean Color Monitor data. Remote Sensing of Environment, 85(4): 424-428.

Fabricius K, De'ath G, McCook L, Turak E. and Williams DM. 2005. Changes in algal, coral and fish assemblages along water quality gradients on the inshore Great Barrier Reef. Mar Pollut Bull 51: 384−398.

Falkowski P, Scholes RJ, Boyle E, Canadell J, Canfield D, Elser J, Gruber N, Hibbard K, Hogberg P, Linder S, et al. 2000. The global carbon cycle: A test of our knowledge of earth as a system. Science, 290, 291–296.

Friedlingstein P, O'Sullivan M, Jones MW, Andrew RM, Hauck J et al. 2020. Global carbon budget 2020. Earth Syst. Sci. Data 12: 3269–340

Gauns M, Madhupratap M, Ramaiah N, Jyothibabu R, Fernandes V, Paul JT, Prasanna Kumar S. 2003. A comparative estimate of carbon flux in the Arabian Sea and the Bay of Bengal. Deep-Sea Research II, 52.

Gauns M, Madhupratap M, Ramaiah N, Jyothibabu R, Fernandes V, Paul JT, Kumar SP. 2005. Comparative accounts of biological productivity characteristics and estimates of carbon fluxes in the Arabian Sea and the Bay of Bengal. Deep Sea Research Part II: Topical Studies in Oceanography: 1;52(14-15):2003-17.

Guo S, Sun J, Zhao Q, Feng Y, Huang D, Liu S. 2016. Sinking rates of phytoplankton in the Changjiang (Yangtze River) estuary: A comparative study between Prorocentrum dentatum and Skeletonema dorhnii bloom. Journal of Marine Systems, 154, 5-14.

Hader DP, Villafane VE, Helbling EW. 2014. Productivity of aquatic primary producers under global climate change. Photochem. Photobiol. Sci. 13: 1370–1392.

Hansell DA, Carlson CA, Repeta DJ, Schlitzer R. 2009. Dissolved organic matter in the ocean a controversy stimulates new insights. Oceanography, 22, 202–211.

Holmgren S. 1994. An environmental assessment of the Bay of Bengal region.

Honda MC, Wakita M, Matsumoto K, Fujiki T, Siswanto E, Sasaoka K, Saino T. 2017. Comparison of carbon cycle between the western Pacific subarctic and subtropical time-series stations: highlights of the K2S1 project. Journal of Oceanography, 73(5): 647-667.

Hulse D, Arndt S, Wilson JD, Munhoven G, Ridgwell A. 2017. Understanding the causes and consequences of past marine carbon cycling variability through models. Earth-Sci. Rev. 171: 349–382.

Hussain MG, Failler, Pierre Al Karim, Ahmad, Khurshed Alam Md. 2018. Major opportunities of blue economy development in Bangladesh. Journal of the Indian Ocean Region. 14. 88-99. 10.1080/19480881.2017.1368250.

Iftekhar MS. 2006. Conservation and management of the Bangladesh coastal ecosystem: overview of an integrated approach. In Natural resources forum (Vol. 30, No. 3, pp. 230-237). Oxford, UK: Blackwell Publishing Ltd.

Islam MS. 2003. Perspectives of the coastal and marine fisheries of the Bay of Bengal, Bangladesh. Ocean & Coastal Management, 46(8), 763-796.

Islam MT, Sharif A, Mahbub-E-Kibria M, Emon SB, Biswas S. 2018. Seasonal Variation of Physico-Chemical Characteristics in the South Eastern Coastal Waters of Cox's Bazar, Bangladesh. Bangladesh Oceanographic Research Institute (BORI), Cox's Bazar-4730, Bangladesh, Bangladesh International Journal of Science and Research (IJSR)

Izonfuo WA, L Bariweni. 2001. The effect of urban runoff water and human activities on some physicochemical parameters of the Epie creek in the Niger Delta.J. Appl. Sci. &Enviro.Mgt, 5(1): 4755.

Jeffrey ST, Humphrey GF. 1975. New spectrophotometric equations for determining chlorophylls a, b, c1 and c2 in higher plants, algae and natural phytoplankton. Biochemie und physiologie der pflanzen, 167(2), 191-194.

Jewel MAS, Haque MM, Haq MS, Khan S. 2002. Seasonal dynamics of phytoplankton in relation to environmental factors in the Maheshkhali channel, Cox's Bazar, Bangladesh.

Kaiser HF. 1974. An index of factorial simplicity. psychometrika, 39(1): 31-36.

Khan MZH, Rajshekhar A. 2020. Short Communication on Variation of Turbidity and TSS in Seawater around Moheshkhali area of the Bay of Bengal, Bangladesh. Bangladesh journal of environmental research, 11: 116-123.

Kim JM, Lee K, Shin K, Yang EJ, Engel A, Karl DM, Kim HC. 2011. Shifts in biogenic carbon flow from particulate to dissolved forms under high carbon dioxide and Warm Ocean conditions. Geophys. Res. Lett. 38.

Lacroix F, Ilyina T, Laruelle GG, Regnier P. 2021. Reconstructing the preindustrial coastal carbon cycle through a global ocean circulation model: Was the global continental shelf already both autotrophic and a CO_2 sink? Glob. Biogeochem. Cycles. 35: e2020GB006603.

Lam MK, Lee KT, Mohamed AR. 2012. Current status and challenges on microalgae-based carbon capture. Int. J. Greenh. Gas Control. 10: 456–469.

Li W, Gao KS, Beardall J. 2012. Interactive effects of ocean acidification and nitrogen-limitation on the diatom phaeodactylum tricornutum. PLoS ONE. 7: e51590.

Li Zhao, Song Shuqun, Li Caiwen, Yu Zhiming. 2018. The sinking of the phytoplankton community and its contribution to seasonal hypoxia in the Changjiang (Yangtze

River) estuary and its adjacent waters. Estuarine, Coastal and Shelf Science. 208: 170-179. DOI: 10.1016/j.ecss.2018.05.007.

Mallela J, Roberts C, Harrod C, Goldspink CR. 2007. Distributional patterns and community structure of Caribbean coral reef fishes within a river-impacted bay. J Fish Biol 70: 523−537.

Mélières MA, Maréchal C. 2015. The carbon cycle prior to the industrial era. Climate Change: Past, Present and Future. John Wiley & Sons. pp. 298-301.

Mehedi Iqbal M, Masum Billah M, Nurul Haider M, Shafiqul Islam M, Rajib Payel H, Khurshid Alam Bhuiyan M, Dawood MA. 2017. Seasonal distribution of phytoplankton community in a subtropical estuary of the south-eastern coast of Bangladesh. Zoology and Ecology: 2;27(3-4):304-10.

Minar MH, Hossain MB, Shamsuddin MD. 2013. Climate change and coastal zone of Bangladesh: vulnerability, resilience, and adaptability. Middle-East Journal of Scientific Research, 13(1): 114-120.

MoFA. 2014, July 8. Press release: Press statement of the Hon'ble Foreign Minister on the verdict of the arbitral tribunal/PCA. Dhaka: Ministry of Foreign Affairs. Retrieved from.http://www.mofa.gov.bd/PressRelease/PRDetails.php?txtUserId=&PRid=854

Mukhopadhyay SK, Biswas H, De TK, Jana TK. 2006. Fluxes of nutrients from the tropical river Hooghly at the land-ocean boundary of Sundarbans. NE coast of Bay of Bengal. India. J. Mar. Syst, 6: 9-21.

Mullin J, Riley JP. 1955. The colorimetric determination of silicate with special reference to sea and natural waters. Analytica chimica acta, 12, 162-176.

Murdoch T, Cheo M, O-Laughlin K. 2001. Streamkeeper's Field Guide: Watershed Inventory and Stream Monitoring Methods. Adopt-A-Stream Foundation, Everett, WA. pp. 297.

Murphy JAMES, Riley JP. 1962. A modified single solution method for the determination of phosphate in natural waters. Analytica chimica acta, 27, 31-36.

Nair NB, Azis PK, Dharmaraj K, Arunachalam M, Kumar KK, Balasubramanian NK. 1983. Ecology of Indian Estuaries: part 1-physico-chemical features of water and sediment nutrients of Ashtamudi Estuary.

Napiórkowska-Krzebietke, A, Kobos J. 2016. Assessment of the cell biovolume of phytoplankton widespread in coastal and inland water bodies. Water Research, 104, 532-546.

Noori M. 1999. An investigation on seasonal variation of micronutrients and standing crop of phytoplankton in neritic waters of the southeast coast of Bangladesh. Current Sciences, 20: 45-65.

Olenina I. 2006. Biovolumes and size-classes of phytoplankton in the Baltic Sea.

Passow U, Carlson CA. 2012. The biological pump in a high CO_2 world. Mar. Ecol. Prog. Ser. 470, 249–271.

Paul JT, Ramaiah N, Sardessai S. 2008. Nutrient regimes and their effect on distribution of phytoplankton in the Bay of Bengal. Marine Environmental Research: 66(3):337-44

Petrou K, Kranz SA, Trimborn S, Hassler CS, Ameijeiras SB, Sackett O, Ralph PJ, Davidson AT. 2016. Southern ocean phytoplankton physiology in a changing climate. J. Plant Physiol. 203: 135–150.

Pitcher GC, Walker DR, Mitchel-Innes BA. 1989. Phytoplankton sinking rate dynamics in the southern Benguela upwelling system. Marine ecology progress series. Oldendorf, 55(2), 261-269.

Pörtner H-O, Roberts DC, Masson-Delmotte V, Zhai P, Tignor M, et al. 2019. The IPCC Special Report on the Ocean and Cryosphere in a Changing Climate. Geneva: IPCC

Prabu VA, Rajkumar M, Perumal P. 1983. Seasonal variations in physico-chemical characteristics of Pichavaram mangroves, southeast coast of India. Journal of Environmental Biology, 29(6): 945-950.

Prasanna KS, Sardesai S, Ramaiah N, Bhosle NB, Ramaswamy V, Ramesh R et al. 2007. Bay of Bengal process studies (BoBPS) Final Report. Final Report Submitted to the Department of Ocean Development New Delhi, 142. http://drs.nio.org/drs/handle/2264/535

Roshan S, DeVries T. 2017. Efficient dissolved organic carbon production and export in the oligotrophic ocean. Nat. Commun. 8: 2036.

Sanders R, Henson SA, Koski M, De la Rocha CL, Painter SC, Poulton AJ, Riley J, Salihoglu B, Visser A, Yool A et al. 2014. The biological carbon pump in the north Atlantic. Prog. Oceanogr. 129: 200–218.

Saxby SA. 2002. Sea water characteristics at coastal culture sites in temperate and warm temperate regions of the world.

Sharma SK, Datta A, Saud T, Mandal TK, Ahammed YN, Arya BC, Tiwari MK. 2010a. Study on concentration of ambient NH3 and interactions with some other ambient trace gases, Environ. Monit. Asses. 162: 225–235.

Sharma SK, Datta A, Saud T, Saxena M, Mandal TK, Ahammed YN, Arya BC. 2010b. Seasonal variability of ambient NH3, NO, NO_2 and SO2 over Delhi, J. Environ. Sci., 22: 1023–1028.

Smayda TJ. 1970. The suspension and sinking of phytoplankton in the sea. Oceanogr. Mar. Biol. Ann. Rev. 8: 353– 414.

Soundarapandian P, Premkumar T, Dinakaran GK. 2009. Studies on the physico-chemical characteristic and nutrients in the Uppanar estuary of Cuddalore, South east coast of India. Curr. Res. J. Biol. Sci, 1(3): 102-105.

Steinberg DK, Van Mooy BA, Buesseler KO, Boyd PW, Kobarin T, Karl DM. 2008. Bacterial vs. zooplankton control of sinking particle flux in the ocean's twilight zone. Limnology and Oceanography, 53(4): 1327-1338.

Stirling HP. 1985. Chemical and Biological Methods of Water Analysis for Aquaculturists. 1st Edn., Institute of Aquaculture, University of Striling, Scotland. 1985, 119

Surana R, Gadhia M, Ansari E. 2013. Seasonal variations in physico-chemical characteristics of Tapi Estuary in Hazira Industrial Area".Our Nature-March, 10:249-257.

Sutton MA, Dragostis U, Tang YS, Flower D. 2000. Ammonia emissions from nonagricultural sources in the UK, Atmos. Environ., 34: 855–869, 2000.

Sutton MA, Place CJ, Eagar M, Fowler D, Smith RL.1995. Assessment of the magnitude of ammonia emissions in the United Kingdom, Atmos. Environ., 29, 1393–1411, 1995.

Tavakoly Sany SB, Hashim R, Rezayi M, Salleh A, Safari O. 2014. A review of strategies to monitor water and sediment quality for a sustainability assessment of

Turner JT. 2002. Zooplankton fecal pellets, marine snow and sinking phytoplankton

Turner JT. 2015. Zooplankton fecal pellets, marine snow, phytodetritus and the ocean's biological pump. Prog. Oceanogr. 130, 205–248.

Wang X, Sun J, Wei Y, Wu X. 2022. Response of the Phytoplankton Sinking Rate to Community Structure and Environmental Factors in the Eastern Indian Ocean. Plants, 11(12): 1534.

Zafar M. 1992. Study on some hydrobiological aspects of the southeastern part of Bangladesh coastal waters in the Bay of Bengal.

APPENDICES

APPENDIX- A

A book used for cell biovolume measurement

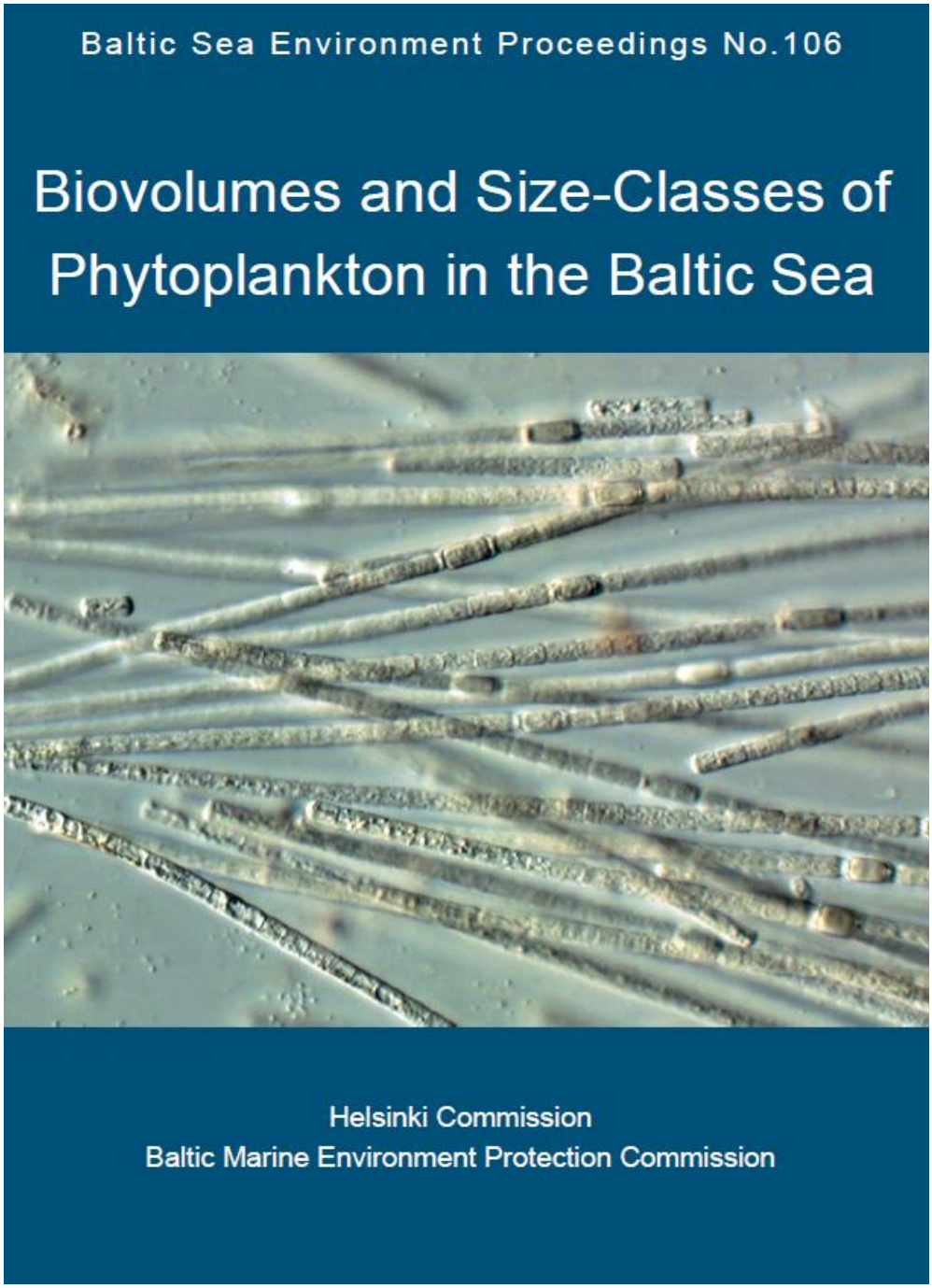

APPENDIX- B

Observed phytoplankton community during the study period.

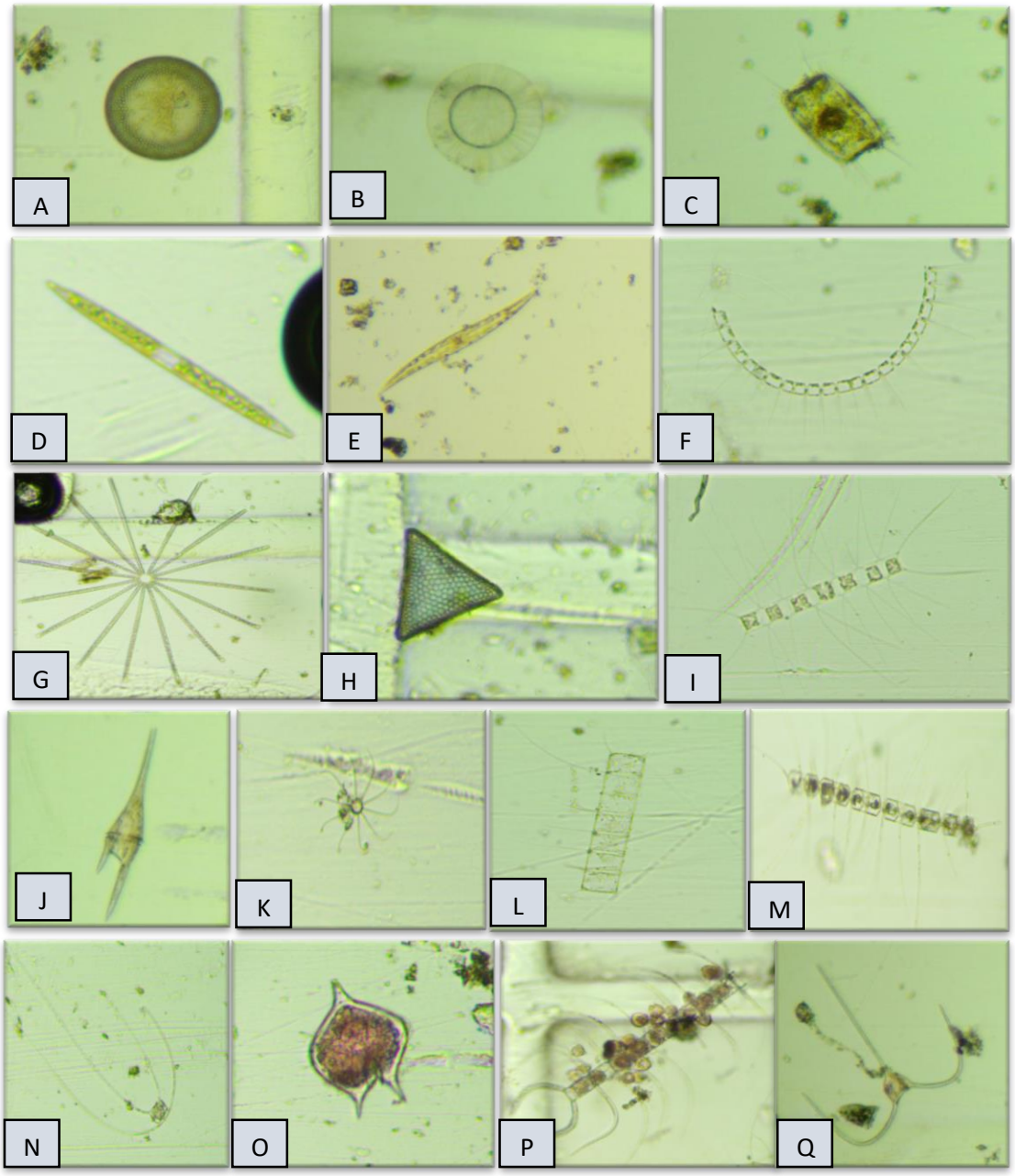

Phytoplankton diversity: A) *Coscinodiscus sp.* B) *Cyclotella sp.* C) *Odontella sp.* D) *Nitzschia sp.* E) *Pleurosigma sp.* F) *Chaetoceros curvisetus.* G) *Thalassiothrix sp.* H) *Triceratium sp.* I) *Chaetoceros sp.* J) *Ceratium furca.* K) *Chaetoceros sp.* L) *Chaetoceros sp.* M) *Chaetoceros sp.* N) *Chaetoceros sp.* O) *Protoperidinium sp.* P) *Chaetoceros sp.* Q) *Ceratium sp.*